UNIVERSIDAD COMPLUTENSE DE MADRID

FACULTAD DE CIENCIAS FÍSICAS
Departamento de Física de la Tierra, Astronomía y Astrofísica I
(Geofísica y Meteorología) (Astronomía y Geodesia)

TESIS DOCTORAL

Desarrollos de parametrizaciones urbanas y optimización del acoplamiento ciudad-atmósfera

Urban parameterizations development and city-atmosphere coupling optimization

MEMORIA PARA OPTAR AL GRADO DE DOCTOR

PRESENTADA POR

Andrés Simón Moral

Director
Alberto Martilli

Madrid, 2016

DESARROLLO DE PARAMETRIZACIONES URBANAS Y OPTIMIZACIÓN DEL ACOPLAMIENTO CIUDAD - ATMÓSFERA

URBAN PARAMETERIZATIONS DEVELOPMENT AND CITY-ATMOSPHERE COUPLING OPTIMIZATION

Tesis Doctoral presentada por:
Andrés Simón Moral

Director: **Alberto Martilli (CIEMAT)**
Tutor (UCM)**: Carlos Yagüe Anguís**

Departamento de Física de la Tierra, Astronomía y Astrofísica I
(Geofísica y Meteorología)

Facultad de Ciencias Físicas
Universidad Complutense de Madrid
Noviembre 2015

AGRADECIMIENTOS

Quisiera dar las gracias de corazón a las siguientes personas que me han ayudado durante la realización de esta tesis.

- Al Dr. Alberto Martilli por haberme dado la oportunidad de realizar este trabajo con él, por haberme transmitido parte de su conocimiento y por haberme apoyado en los momentos duros.
- Al Dr. Jose Luis Santiago por la aportación de los datos necesarios, la obtención de las parametrizaciones, la ayuda en el análisis y, como no, por los muy buenos momentos compartidos.
- Al Dr. Fernando Martín por haberme acogido en el grupo de modelización de la contaminación atmósferica del CIEMAT, que él dirige, y a los compañeros del mismo, con los que he compartido muchas comidas y conversaciones. Gracias a Juan Luis Garrido, Beatriz Sanchez, David Manrique (y los que me pueda dejar) y, gracias también a Elvira Tejedor por su gran trabajo y su gran ayuda siempre que la he necesitado.
- Al Dr. Carlos Yagüe por su gran ayuda en la universidad.
- Al Dr. Scott Krayenhoff por su ayuda y colaboración durante el trabajo.
- Al Dr. Francisco Salamanca por sus consejos y conversaciones cuando las he necesitado.
- Al Dr. Juan Angel Acero y la Dr. Julia Hidalgo, por sus consejos y direcciones desde el principio del trabajo.
- Al CIEMAT por la financiación de parte de este trabajo, a traves tanto de un contrato como de la financiación de viajes y congresos.
- A mis ex-compañeros de TECNALIA, con los que compartí el principio del viaje.
- Por último pero no por eso, ni muchísimo menos, menos importante (sino todo lo contrario), quiero dar las gracias de todo corazón a mis padres y hermanos, asi como a mis amigos. Sin ellos esto jamás podría haber salido adelante. Quisiera hacer una mención especial a Carmen, su apoyo en todos los sentidos ha sido enorme, como tambien lo ha sido la inmensa paciencia, comprensión, consejos y compañía en todos los momentos en que la he necesitado, de verdad, ¡¡muchisimas gracias!!

Table of contents

RESUMEN

Introducción y Objetivos

Las ciudades interaccionan con la atmósfera, produciéndose un aumento de la temperatura con respecto al medio rural circundante (Isla de calor) y una disminución de la velocidad del viento. Estos fenómenos pueden llegar a ocasionar problemas para la salud de la población, que cada vez mas, esta en aumento, en detrimento de la población que habita las zonas rurales. Con la idea de mejorar las condiciones de vida en las ciudades, la comprensión y caracterización del clima urbano, mediante la modelización atmósferica, se ha convertido en una herramienta necesaria. Con este propósito se han desarrollado las denominadas parametrizaciones urbanas, que representan, de forma promediada, el comportamiento de las variables meteorologicas dentro de la ciudad.

Los objetivos de esta tesis son la mejora de la parametrización urbana BEP (Building Effect Parameterization, Martilli et al. 2002) implementada en el modelo de mesoescala WRF (Weather Research and Forecast model, Skamarock et al. 2008), y la optimizacion del acoplamiento de dichas parametrizaciones y el modelo atmosférico, con la finalidad de aumentar su resolución sin generar un coste computacional.

En la primera parte de la tesis, se utilizan modelos numéricos de microescala para extraer la física para la parametrización urbana. Por un lado, se propone una parametrización para el coeficiente de arrastre, definido para calcular la fuerza de arrastre de los edificios sobre el viento, en función de las distancias entre edificios, en las direcciones paralela y perpendicular al viento, para configuraciones alineadas de edificios. Además, se extiende la fórmula presentada en Santiago y Martilli (2010) para las longitudes de escala involucradas en el transporte turbulento y en la disipación de la turbulencia, para dichas configuraciones de edificios. Ambas fórmulas son extraídas para condiciones de estratificación térmica neutra.

Por otro lado, se proponen formulas para el cálculo de los parametros anteriores en el caso de una estratificación térmica inestable. Además, se estudia el flujo dispersivo, parametrizandolo, junto al flujo turbulento, mediante una extensión de la teoría K de Monin – Obukhov.

En la segunda parte se presenta una nueva técnica para el acoplamiento del modelo de mesoescala y la parametrización urbana que permite un aumento de la resolución dentro de la subcapa rugosa, permitiendo una disminución de la resolucion vertical del modelo atmosférico y, por lo tanto, una disminución del tiempo de computación.

Metodología

El desarrollo de las parametrizaciones ha sido llevado a cabo mediante la metodología presentada en Santiago et al. (2008) y Santiago y Martilli (2010). Esta metodología se basa en el uso de modelos de microescala para extraer las propiedades promedio del flujo para su parametrización. Los resultados de alta resolucion obtenidos de simulaciones de microescala son promediados espacial y temporalmente de forma que pueden ser considerados el estado estacionario del fluido en una región equivalente a la de una celda mesoescalar. El comportamiento promedio del flujo es parametrizado e incluido en una versión unidimensional de la parametrización urbana. Posteriormente, la parametrización es comparada con los resultados promediados del modelo de microescala.

Una vez que el modelo unidimensional produce buenos resultados, las parametrizaciones desarrolladas son introducidas en una versión tridimensional del mismo.

Resultados

En el caso de una atmosfera con estratificación térmica neutra, el coeficiente de arrastre muestra una dependencia con la distancia entre edificios en las direcciones paralela y perpendicular a la dirección del viento. Esta parametrización permite la diferenciación entre tipos de barrio en cuanto a su interacción con el viento. Un buena caracterización de este coeficiente muestra una mejora en la estimación del viento en la subcapa inercial de la capa límite.

Las longitudes de escala turbulentas, muestran una dependencia con la densidad de edificios, sin ser afectadas por su configuración dentro del dominio.

En el caso en que la estratificación térmica sea inestable, se observa un aumento tanto del coeficiente de arrastre como de las longitudes de escala turbulentas. En este estudio se presentan sendas funciones que caracterizan dichas variaciones en función de la razón entre las fuerzas de flotabilidad y las fuerzas inerciales, permitiendo la distinción del comportamiento del flujo en función de la hora del día.

La existencia de flujos de calor desde las superficies urbanas produce un aumento de los flujos dispersivos de calor y momento, que muestran valores equivalentes a los flujos turbulentos. La suma de ambos flujos es parametrizada mediante una extensión de la teoría K, variando el valor del coeficiente de difusión, que, dentro del cañón urbano, muestra valores diferentes para el momento y

el calor.

Se presenta una nueva técnica para acoplar la parametrización urbana en el modelo meteorológico. Esta técnica permite un aumento de la resolución en la subcapa rugosa, independientemente de la resolución de la malla vertical del modelo meteorológico, lo cual permite disminuir el número de niveles y por lo tanto el tiempo de computación.

Además, se introducen las parametrizaciones de la primera parte del trabajo, generando valores más altos de temperatura y mas bajos para el viento. Estos resultados reducen el bias de BEP, observado en Salamanca et al. (2011).

Conclusiones

Se demuestra una dependencia de la fuerza de arrastre con la configuración de edificios y con la razón entre las fuerzas de flotabilidad y de inercia. Se ha observado como una buena estimación del coeficiente que caracteriza esta fuerza es clave para la estimación del la velocidad del viento en la subcapa rugosa.

Las longitudes de escala para el transporte turbulento y la disipación de la turbulencia dependen de la densidad de edificios, independientemente de su configuración. Así mismo, se ha observado un incremento de estos parámetros con la razón entre las fuerzas de flotabilidad y de inercia.

Se ha demostrado la importancia de los flujos dispersivos en la mezcla vertical, cuando la estratificación térmica es inestable.

Una buena estimación de los parámetros previamente descritos tiene una gran importancia en la estimación de la dispersión de contaminantes y del confort térmico de las ciudades.

Se ha presentado una técnica de acoplamiento del esquema urbano BEP en el modelo de mesoscala WRF, aumentando la resolución en la subcapa inercial, permitiendo una reducción de la resolución del modelo meteorológico y por lo tanto del tiempo de computación. Las parametrizaciones del coeficiente de arrastre, las longitudes de escala turbulentas y los flujos dispersivos han mejorado los resultados del modelo urbano.

SUMMARY

Cities interact with the atmosphere, generating an increase of temperature respect to the rural sourrounding area (Urban heat Island) and a decrease of the wind speed. This phenomena can produce health problems on the population, which is increasig, due to the decrease of the rural population. In order to improve the quality of living inside the cities, the understanding and characterization of the urban climate, by means of atmospheric modeling has become necessary. For this purpose, the so called urban canopy parameterizations have been developed, which represent, in an averaged way, the behaviour of the meteorological variables within the city.

The objectives of this thesis are the improvement of the urban parameterization BEP (Building Effect Parameterization, Martilli et al. 2002) implemented in the WRF mesoscale model (Weather Research and Forecast model, Skamarock et al. 2008), and the optimization of the urban parameterization and the atmospheric model coupling, in order to increase its resolution without computational cost.

In the first part of the thesis, microscale numerical models are used in order to extract the physiscs for the urban parameterization. From one side, a parameterization for the drag coefficient is proposed, defined in order to calculate the drag force on the wind speed produced by the buildings, by means of the distance between them, in the direction parallel and perpendicular to the flow, for aligned configurations. In addition, the parameterization of the length scales for turbulent transport and turbulence dissipation presented in Santiago and Martilli (2010) is extended. Both parameterizations are extracted for neutral thermal conditions.

On the other side, parameterizations of the previous parameters are proposed, for unstable thermal conditions. In addition, the dispersive flux is studied and parameterized with the turbulent flux, by an extension of the Monin – Obukhov K- theory.

In the second part of the thesis, a new technique to couple the mesoscale model and the urban parameterization is presented, which allows an increase of the resolution within the roughness sublayer, allowing a decrease of the vertical resolution of the atmospheric model, and thus, a decrease of the computational time.

Methodology

For the development of the parameterizations, the methodology presented in Santiago et al. (2008) and Santiago and Martilli (2010) has been used. This methodology is based in the use of microscale

models in order to extract the averaged properties of the flow for its parameterization. The high resolution results obtained from the microscale simulations are averaged in time and space, in order to be considered as the stationary state of the flow in a region equivalent to a mesoscale grid cell. The averaged behaviour is parameterized and implemented in a unidimensional version of the urban parameterization and compared with the averaged results of the microscale simulations.

Once the unidimensional model produce good results, the developed parameterizations are implemented in a three dimensional version of the urban model.

Results

In the case of an atmosphere with neutral thermal stratification, the drag coefficient shows a dependency with the distance between buildings in the directions parallel and perpendicular to the flow. This parameterization allows the differentiation between different neighborhoods, respect to its interaction with the wind field. A good estimation of this coefficient shows an improvement of the wind speed results in the roghness sublayer.

The turbulent length scales show a dependency with the density of buildings, not been affected by its configuration within the domain.

In the case of an atmosphere with a unestable thermal stratification, an increase of the drag coefficient and the turbulent length scales is observed. In this study, equations for the variations of both parameters with the ratio between the buoyancy and the inertial forces are presented, allowing the differentiation of the flow behaviour with the moment of the day.

The presence of heat fluxes from the urban surfaces produce an increase of the dispersive fluxes of heat and momentum, showing comparable values to the turbulent fluxes. The sum of both fluxes is parameterized by an extension of the K-theory, modifying the value of the diffusion coefficient, which, within the urban canopy, shows different values for heat and momentum.

A new technique to couple the urban scheme within the atmosphere model is presented. This technique allows an increase of the resolution in the roughness sublayer, independently of the vertical resolution of meteorological model, allowing a decrease of the number of the vertical levels and, thus, the computational time.

In addition, the parameterizations presented in the first part of the study are implemented in the urban canopy parameterization, producing higher values of temperature and lower values of the wind field. These results decrease the bias produced by the BEP model observed in Slamanca et al.

2011)

Conclusions

The dependency of the drag force with the configuration of buildings and the ratio between the buoyancy and inertial forces is showed. It is obsevred how a good estimation of the coefficient that characterizes this force is needed for the estimation of the wind speed within the roghness sublayer.

The length scales for the turbulent transport and turbulence dissipation depend on the buildings density, regardless of its configuration. In addition, an increase of these with the ratio of buoyancy and inertial forces is found.

The importance of the dispersive fluxes in vertical mixing when the thermal stratification in unstable is showed.

A good estimation of the previously described parameters is very important in the estimation of the pollutants dispersion and the thermal confort inside the cities.

A new technique for the coupling of the BEP urban scheme within the WRF mesoscale model is presented, increasing the resolution in the roughness sublayer and allowing a decrease of the meteorological model resolution and the computational time. The parameterizations of the drag coefficient, the turbulent length scales and the dispersive fluxes have improved the results of the urban model.

1. State of the art and objectives of the work

1.1. Introduction

Cities interact with the atmosphere modifying their climate and meteorology. Considering that more than half of the world population lives in urban areas (54%), that this percentage is increasing (UN report, 2014) and that the behaviour of the urban atmosphere has strong impact on citizens life, the study of the urban climate becomes necessary. One of the most common effects observed in urban areas is the increase of temperature compared to the surrounding rural areas, in particular during the night, effect known as the Urban Heat Island (UHI). In addition, a decrease of the wind speed and the ventilation in the city is often observed. These two effects are related with a worsening of the thermal comfort and an increase of the pollutants concentration. The former can be a serious problem, especially in cases of heat waves, for the vulnerable sectors of the population, and, at the same time, it is related to the energy consumption by means of air conditioning or heating devices. The latter is related with an enhancement of respiratory illnesses.

At the same time, the impact of the urban areas on the surroundings is also an important issue because the city acts as a source of pollutants and heat and is able to modify the local to regional meteorology, as is the case of the rural/urban breeze phenomenon.

Atmospheric numerical modeling has appeared to be an adequate tool for the study of the urban climate. Depending on the purpose and extension of the study, several types of models can be used, with different capabilities and resolutions. Models with very high resolution (of the order of meters), also called microscale models, are able to simulate the flow around the urban obstacles and can be useful for a neighborhood-scale study, but can not cover the whole city due to computational limitations. On the other hand, models with resolutions of several hundreds of meters (e. g. mesoscale models) are not able to simulate the flow around each building with a high degree of detail but can be used to cover the whole city. In order to fill the gap between the two scales, the buildings effects are parameterized in the mesoscale models by means of the so called Urban Canopy Parameterizations (hereafter UCP).

The aim of this thesis is to **improve** the capability of a UCP in mesoscale atmospheric models to reproduce the impact of the urban surfaces on the atmosphere, considering urban **morphological features**, and different **stability conditions**, **without increasing the computational time**, and so allowing the use of the models for **long periods** (months, years).

Taking into account the inhomogeneity of urban areas, building a data base of measurements that can be used to test and develop a UCP becomes very difficult. In order to solve this problem, high resolution simulation techniques and/or wind tunnel experiments can be used instead. Such type of data can be more easily used for the calculation of the averaged properties of the flow that are relevant for the UCP.

A detailed UCP, calibrated with the high resolution microscale simulations, can significantly improve the accuracy of the atmospheric model in urban areas. Such models can then be used more reliably for the definition of policies to reduce pollution, thermal stress, energy consumption or to improve the ventilation, making the cities a better place to live.

1.2. Urban boundary layer

The boundary layer over urban areas has different properties than the one existing over homogeneous terrain. The presence and configuration of obstacles as the buildings, the materials used and the human activities (industry, traffic, air conditioning/heating, etc.) produce thermal and mechanical impacts over the atmosphere. In the following sections, the physics of the urban induced boundary layer modifications are described, a scheme of those interactions is shown in Fig. 1.1.

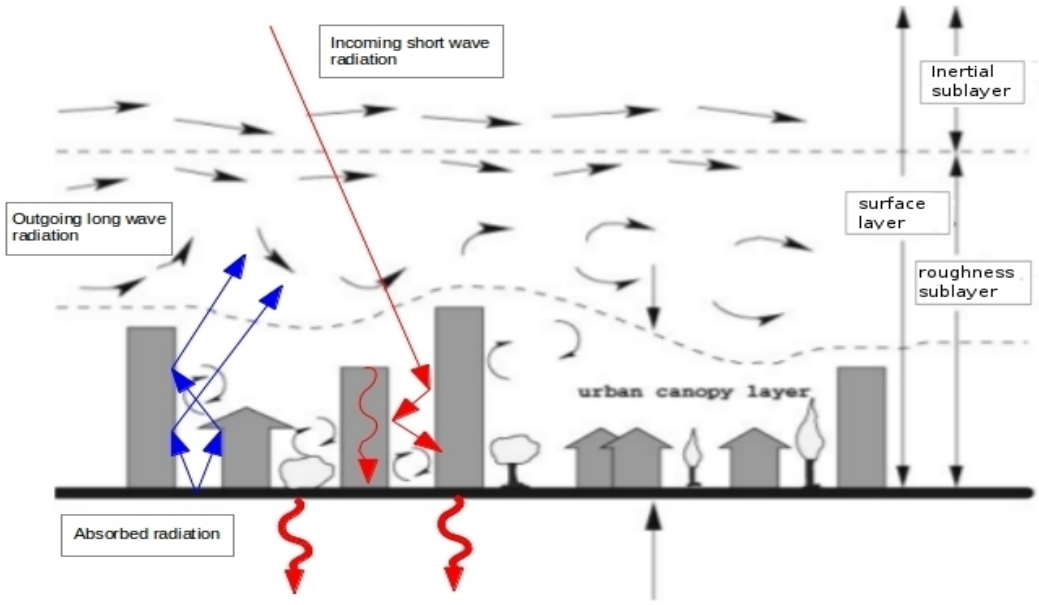

Figure 1.1: Scheme of the flow and radiation over an urban area. Adeapted from Grimmond and Oke (2002) and Britter and Hanna (2003).

1.2.1. Mechanical interaction

Urban areas are an arrangement of buildings acting as obstacles for the wind. At the top of the canopy a large shear stress is generated that converts mean kinetic energy into turbulent kinetic energy and increases the downward transport of momentum and temperature. Inside the canopy, when the wind impacts over these obstacles, a drag force is generated by the pressure differences across the individual roughness elements. This drag decreases the wind speed. In addition, the presence of the buildings also produce turbulent wake diffusion by eddies of the size of the obstacles, which disperse heat, momentum, moisture and other scalars (as pollutants).
The buildings, hence, act as a barrier for the wind, decreasing the entrance of air from the outside, thus decreasing the ventilation of the city.

1.2.2. Thermal interaction

The cities interact with the atmosphere from a thermal point of view due to the street structure, the materials used and the anthropogenic activities.
The buildings form structures known as street canyons (Fig. 1.2) that produce shadowing, and the so called radiation trapping effect, related to the multiple reflections on the walls and bottom of the canyon, and to the decrease of the sky-view factor. These phenomena increase the amount of short wave radiation absorbed during the day (compared to a flat surface with the same albedo), and decrease the nocturnal cooling (always compared to a flat surface with the same emissivity), because part of the energy emitted by one canyon element (wall or street) is absorbed by another element and not lost to the space. In addition, the materials used for buildings construction have larger thermal capacity compared to the dry soil, and this, together with the previous effect, increases the heat storage within the urban surfaces and thus increases the thermal inertia of the area. Concerning the human activities, some of them result in an emission of heat to the atmosphere (air conditioning/heating, traffic, etc.) that increases the temperature. As a consequence, a difference between rural and urban temperature is often observed, an effect called Urban Heat Island (UHI). The UHI intensity, defined as the difference between urban and rural temperature, is maximum during night, with typical values up to 5º for medium European cities, and minimum at the central hours of the day, when it can reach negative values for some cities surrounded by very dry areas,

like Madrid. The UHI effect is maximized in clear days with calm synoptic conditions (Arya 1988). The urban temperature increase, in addition to the higher mechanical turbulence generated by the higher roughness elements found in the city, often produces an increase of the planetary boundary layer (PBL) height, as compared with the one in the rural surroundings. Moreover, during the night, the slower cooling, due to the higher thermal inertia and the anthropogenic heat release can generate, under calm meteorological conditions, a neutral or even an unstable atmospheric layer over the city, few hundreds of meters deep, different from the stable layers observed on rural areas. The two modifications of the urban boundary layer structure described above, may affect citizens' life mainly in two ways:

Air quality

Urban areas are characterized by high emission levels of pollutants, mainly due to traffic, that induce high levels of pollution located where the population lives, resulting in a serious potential health problem. The way in which the buildings modify the flow and generate/suppress turbulence is clearly very important for the dispersion. It is the combination of these effects, and the height of PBL above the city, mainly controlled by the thermal factors, that determine the level of pollution in the city.

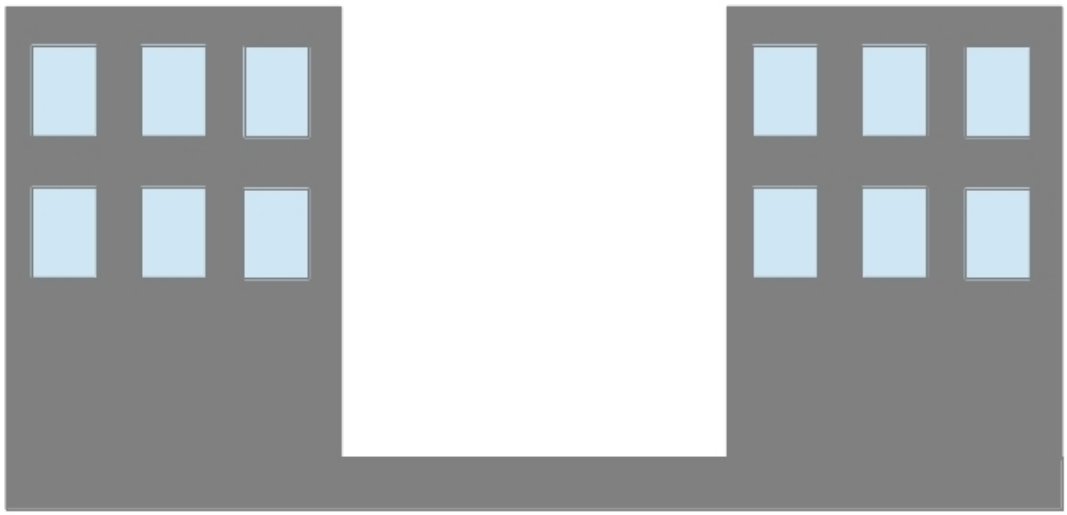

Figure 1.2: Street canyon formed by two buildings and the street between them

Thermal comfort

The higher temperatures found in urban areas can reach dangerous levels, especially during heat wave events. The decrease of the nocturnal cooling increases the amount of hours with thermal stress over the population, being especially problematic for the vulnerable sectors, as old people. At the same time an increase of the use of air conditioning devices increases the energy consumption.

1.3. Numerical modeling

In order to study and improve the quality of life inside the urban areas, the physical processes described above must be understood and characterized. In this context, atmospheric numerical modeling has appeared to be a good technique to reproduce the meteorology inside the city and to evaluate mitigation scenarios. The choice of the best numerical modeling approach to tackle this problem is necessarily the result of a trade-off between resolution and CPU time. The smaller the size of the grid cell, the higher the resolution and the smaller the detectable physical process. On the other hand, the smaller is the grid spacing, the larger is the number of grid points needed to cover a certain area, and so the larger is the computational time needed. Moreover, the spatial and temporal resolutions are related by the Courant–Friedrichs–Lewy condition, so that an increase of resolution (e. g. decrease of the grid spacing), often requires a decrease of the time step of integration, with consequent further increase of the CPU time. Although the computational resources have had a huge development in the last years, the conflict between the resolution of the simulation and the computational time is still there.

The reason that makes difficult the simulation of the urban canopy layer is related with the complexity of the surfaces and obstacles existing in a city. These obstacles, with typical sizes of a few tens of meters or less, have their own thermal and dynamical properties, creating flow structures of their spatial scale (Martilli 2007). At the same time, the urban canopy layer is highly influenced by meteorological structures of the order of several kilometers. As mentioned above, depending on the interest of the study, different kind of models, attending to its resolution and computational demand can be found:

- Microscale models: These models use a resolution of the order of 1 m in both the horizontal and the vertical, being able to detect the small scale interactions between the flow and the

urban obstacles. On the other hand, they can not be used to cover a whole city because of its high computational demand.

- Mesoscale models: This kind of models works with a resolution of the order of 10^{2-3} m in the horizontal and 10^{1} m in the vertical. This spatial scale is larger than the size of the buildings, not being able to solve the processes caused inside the street canyons. Nevertheless, due to the larger size of the cells, they can be used to model a whole city and the mesoscale meteorological processes.

Taking this into account, in order to simulate a whole city and its urban canopy layer, it is desirable to represent structures from the size of the buildings to the mesoscale. Microscale models cannot be used for meteorological simulation and mesoscale models are not accurate enough to detect the small structures inside the urban areas.

Therefore, we ask ourselves, how can we simulate the urban mechanisms and the meteorological structures responsible of the urban canopy layer? The answer lies on the definition of the so called Urban Canopy Parameterizations (UCP). These parameterizations try to overcome the lack of information in the mesoscale models, by averaging the impact of the phenomena produced by the processes spatially smaller than the size of the mesoscale grid cell. This kind of parameterizations has been considered as a good compromise between simplicity and accuracy and is the only way to include the microscale properties of the city in a lower resolution model, able to simulate a whole urban area and the meteorological structures.

1.3.1. Urban Canopy Parameterizations

Urban canopy parameterizations are defined to represent, in an averaged way, the subgrid effects caused by the presence of obstacles inside the urban areas.

Parameterizations with different degrees of complexity have been defined in recent years. The development of these parameterizations has been parallel to the development of the computational resources. The simplest use Monin–Obukhov similarity theory (MOST) and modify several parameters, such as the roughness length, the albedo and the thermal capacity and diffusivity, to represent the wind-speed reduction and the increased thermal admittance at the surface; an example of this approach is Liu et al. (2006). This kind of parametrization does not need a change in the model formulation, because they use the same formulation used for rural areas (Martilli 2007), not

increasing the computational cost. With the improvement of computation, the possibility of simulating with more complex parameterizations allows a better characterization of the city. Parameterizations with a single layer (Masson 2000; Kusaka et al. 2001; Kanda et al. 2005) are forced by the mesoscale model in a layer over the urban canopy, where the momentum and heat fluxes between the city and the atmosphere are exchanged. Multilayers schemes, with more than one vertical atmospheric layer inside the urban canopy (Uno et al. 1989; Brown and Williams 1998; Martilli et al. 2002; Coceal and Belcher 2004; Kondo et al. 2005; Hamdi and Masson 2008; Di Sabatino et al. 2008; Masson and Seity 2009) allow the representation of the city as a porous medium, being able to consider the vertical heterogeneity of the urban canopy and thus its impact on the airflow. This kind of UCPs can be forced by the mesoscale model in the top or in the whole vertical.

1.3.2. Dynamics of the UCP

1.3.2.1. Drag force

The dynamical interaction between the urban obstacles and the atmosphere is represented as a sink of momentum and a sink and a source of turbulent kinetic energy, both included in the respective equations.

The sink of momentum is usually parameterized by a drag force acting over the wind field, represented as a constant of proportionality, called sectional drag coefficient (C_d), multiplied by the square of the mean wind speed (or the mean wind speed orthogonal to the street, as in the case of Martilli et al. 2002).

$$Drag = -\rho C_d \alpha U_i \left|\vec{U}\right| \qquad (1.1)$$

This parameterization is based on those defined for forest canopies (Martilli 2007). The sectional drag coefficient has been taken as a constant, and different values have been proposed ranging from 0.1 (Uno et al. 1989) to 1 (Coceal and Belcher 2004). Nevertheless, it has been shown that this parameter depends on the city configuration (Santiago et al. 2008; Santiago and Martilli 2010; Simón-Moral et al. 2014). This behaviour is linked to the differences between the vegetation and urban canopies. For vegetation, leafs are small, occupy only a small volume of air, and weakly interact one with the other. On the other hand, buildings occupy a large volume, strongly modify the

flow, and consequently the pressure field which is the responsible of the drag. The way in which this field is modified depends on the building arrangements.

1.3.2.2. Turbulent transport

Concerning the turbulent transport, a prognostic equation is calculated for the turbulent kinetic energy, where a source term accounting for the production due to drag is introduced, proportional to the cube of the wind speed multiplied by the sectional drag coefficient, in order to represent the conversion from the mean to the turbulent kinetic energy (Martilli 2007). Uno et al. (1989), uses a *k*-epsilon scheme, where the equation for the dissipation of the turbulence is modified by the introduction of a source term. In the case of Martilli et al. (2002), a *k* - *l* scheme is used, where a modification on the length scale is introduced, in order to take into account the presence of buildings on the dissipation and turbulent vertical diffusion coefficients. It has been shown that this length scale is dependent on the characteristics of the city (Santiago and Martilli 2010; Simón-Moral et al. 2014).

1.3.3. Thermal of the UCP

In an UCP, the thermal influence of the city over the atmosphere can be represented by two approximations. A semi-empirical procedure, relating the urban net heat storage with the net radiation on the surfaces (Taha 1999) and a second technique, where the physics of the problem are introduced in the energy equation.

The physical approximations range from the modification of the land surfaces thermal characteristics to the definition of an intermediate layer where fluxes are exchanged between the city and the atmosphere (Best 1998) or the resolution of the energy balance equation in every natural and urban surfaces (gardens, ground, roofs or walls), calculating the averaged fluxes in each cell.

Several schemes have also included the shadowing and radiation trapping effect explained in the urban canopy layer section (Masson 2000; Kusaka et al. 2001; Martilli et al. 2002). These schemes take into account the sky view factor of every surface and the reflected and re-emitted radiation from the surrounding surfaces. It has been applied in single or multilayer schemes.

1.3.4. Development of UCPs

Great improvements have been done in mesoscale urban modeling. Now the shape of the vertical profiles of mean and turbulent variables over urban areas (Martilli et al. 2002), the heat island effect (Lemonsu and Masson 2005) and the dispersion of pollutants (Chin et al. 2005) are qualitatively well reproduced (Martilli 2007). Nevertheless, from the quantitative point of view there are still several features to improve.

Two research directions are currently followed concerning urban canopy layer modeling development. From one side, in order to simulate the behaviour of the urban canopy layer, input data are needed, e. g. thermal properties of the buildings materials or urban morphology. In this field, research must be done to determine which are the data that define the cities. In addition, these data have to be collected and stored in a global data base for the scientific community use.

On the other hand, the increase of computational power allows an increase of the number of vertical layers inside the urban canopy layer, allowing a better representation of the urban micrometeorology. For this task, there is a scarcity of microscale urban flow experimental data. Although some campaigns are found in the literature (ESCOMPTE In Marseille, Mestayer et al. 2005; BUBBLE in Basel, Rotach et al. 2005; URBAN 2000 in Salt lake city, Allwine et al. 2002; Joint URBAN 2003 in Oklahoma City, Allwine et al. 2004, CAPITOUL in Toulousse, Pigeon et al. 2006), the urban morphology defining the interactions with the flow, completely changes from one city to another existing also a high dependency on the weather conditions. Therefore, these data bases are not enough to extract a general behaviour of urban areas.

In addition to the standard data bases, computational fluid dynamics (CFD) models can be used to improve the understanding of the microscale processes occurring inside the urban canyons (Santiago et al. 2007 and Santiago and Martilli 2010). This methodology consists on performing simulations with Reynolds-Averaged Navier-Stokes (RANS) or Large Eddy Simulation (LES) models over different regular configurations of buildings. Taking into account the different resolution of the CFD and the mesoscale models, the microscale results are averaged in a region equivalent to a mesoscale grid, in order to extract the general average properties of the sub grid structures that the mesoscale resolution is not able to reproduce. The aim of this methodology is to define a parameterization for these subgrid processes.

1.4. Scientific questions and objectives

The research questions addressed during this thesis are three, consisting in:

1. Are the drag coefficient or the length scales properly parameterized to correctly characterize the spatially-averaged behaviour of the airflow within the urban canopy or are more parameters required to unequivocally represent them?

   The methodology applied in Santiago et al. (2008) and Santiago and Martilli (2010) has been used for the study of the dynamical properties of different aligned configurations of buildings with different densities and arrangements. The study has demonstrated that dynamical parameters as the drag coefficient or the length scales for turbulent transport and turbulence dissipation are not constant or independent of the city considered showing a dependency with the distance between the obstacles and its density, respectively. These processes are better parameterized for its implementation in a UCP.

2. Does the thermal stratification modifies the behaviour of the dynamical parameters (drag coefficients, and turbulent lengths scales) of the UCPs?

   The influence of realistic heat flux from the buildings and street surfaces on the drag generated on the wind and on the vertical transport of momentum, heat or other scalars presented in Santiago et al. (2014) has been parameterized and included in a UCP. The importance of the dispersive fluxes has also been highlighted for the vertical transport of meteorological variables. This process has been neglected by some authors (Cheng and Castro 2002; Santiago and Martilli 2010) although its importance have also been detected by others (Coceal et al. 2006; Santiago and Martilli 2010).

3. How can we increase the resolution of the UCP in order to take the advantage of the microscale improvements without increasing the computational time?

   One important drawback of multilayer UCP is the computational cost derived from the increase of the number of vertical levels needed to better represent the vertical heterogeneity of the urban areas or to take advantage of the developments obtained from microscale simulations. Although the improvement of the computers allows a better representation of the cities, it remains unfordable to include the UCPs in an operational weather prediction model, in a warning alert system or in climate modeling. In this thesis a new technique to couple the UCP within the mesoscale model and to calculate the meteorological variables is presented. This new model allows an increase of the vertical urban resolution without an

increase of the computational time.

These features are included in a BEP (Martilli et al. 2002) based UCP, implemented in the WRF (Weather Research and Forecast model, Skamarock et al. 2008) mesoscale model. The first two points produce an increase of the accuracy of the results while the third point allows the possibility of the introduction of the urban signal within global or climate models.

2. Methodology and models description

The increase of computational power allows an increase of the resolution of mesoscale models. In order to take advantage of it, the UCPs have to be improved to be able to represent higher resolution processes. In addition, an increase of the model resolution allows a better characterization of the city in terms of morphological parameters. This idea puts on the table the debate on which parameters are the best to unequivocally represent the urban interaction with the air flow.

Concerning the dynamical interaction of the buildings with the atmosphere, a drag force, parameterized by means of a drag coefficient multiplied by the square of the wind speed, and a modification of the length scales for turbulent transport and turbulence dissipation are considered. Traditionally, the drag coefficient has been considered as a constant value, regardless of the buildings configuration within the city, and the length scales have been parameterized in each vertical level by a relation between the distance to the ground and the height of the buildings (Martilli et al. 2002). Nevertheless, recent studies (Macdonald 2000; Kanda et al. 2004; Cheng et al. 2007; Santiago et al. 2008, Santiago and Martilli 2010) have shown a dependency of the drag coefficient and the length scales with the plan area density λ_p and the frontal area density λ_f (defined as in Grimmond and Oke 1999) , although not accounting for their configuration beyond aligned vs. staggered layouts. With this in mind, the following question arises: *are these parameters (λ_p and λ_f) enough to correctly characterize the spatially-averaged behaviour of the airflow within the urban canopy or are more parameters required to unequivocally represent it?*

Moreover, all the studies mentioned above, have been performed for neutral conditions, but, *to what extent the thermal stratification modifies the behaviour of the dynamical parameters (drag coefficients, and turbulent lengths scales) of the UCPs?*

These two questions are the motivation for the work presented in chapter 2 and published in Simón-Moral et al. (2014), and in chapter 3 (and included in Simón-Moral et al. 2015, in preparation).

Given that the variables involved in UCPs are representative of spatial averages over mesoscale cells (more than hundreds of meters of size), and that the meteorological fields are very heterogeneous in urban areas, it is not possible to use experimental data that are point measurements, representative of a limited (and smaller) area. For this reason, the methodology proposed by Martilli (2007), Martilli and Santiago (2007), Santiago et al. (2008) and Santiago and Martilli (2010), is adopted in this thesis. This technique consists in the use of Reynolds Averaged Navier – Stokes (RANS) computational fluid dynamics (CFD) models, able to resolve the turbulent flow around the obstacles, and to calculate the interactions of the urban medium with the air flow

within. The CFD results are, then, spatially averaged in an area equivalent to a typical mesoscale unit cell, in order to parameterize the flow behaviour for a lower resolution model.
Given the importance of this technique in the context of this thesis, a detailed description of it is presented below.

2.1. Methodology

As explained previously, in this study, the methodology presented in Martilli (2007), Martilli and Santiago (2007) and Santiago et al. (2008) and continued in Santiago and Martilli (2010) is used. This methodology consists in the use of microscale CFD models, able to resolve the flow between the obstacles, in order to extract averaged properties of the flow for the UCPs development. The results are spatially averaged and the parameterization of the average signal is implemented in a UCP. The parameterization is then tested in a one-dimensional version of the urban scheme for the implementation in a full 3D mesoscale model. An scheme of the methodology is shown in Fig. 2.1.
In this section, the conceptual (averaging procedure) and numerical tools (1D column UCP, and the 3D CFD models) used in the methodology are described.

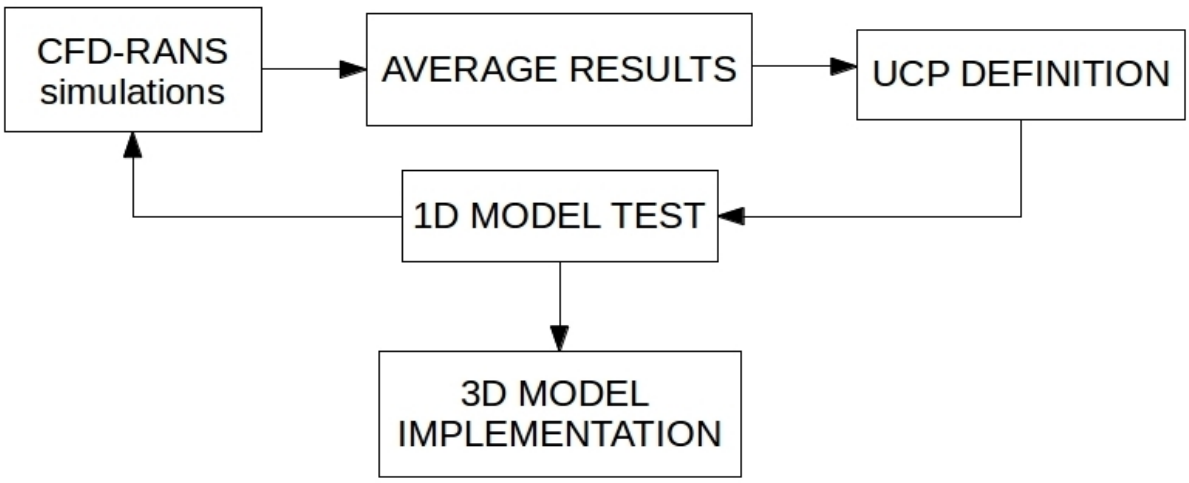

Figure 2.1: Scheme of the methodology used for the UCP development.

2.2. UCP model

The urban canopy parameterization used in this part of the study is a one dimensional version of the the BEP scheme (Martilli et al. 2002) implemented in the Weather Research and Forecast (WRF) mesoscale model (Skamarock et al. 2008). The urban scheme calculates the subgrid interactions between the city and the atmosphere, as the fluxes of heat, momentum and turbulent kinetic energy from the urban surfaces. This model takes into account the drag force of the buildings over the flow and the shadowing and radiation trapping effect within the street canyons.

Following Martilli and Santiago (2007), a mesoscale model over an urban area, due to its resolution, solves the Navier Stokes momentum and energy equations averaged in time (ensemble average) and space over the grid cell, which is too coarse to resolve the buildings, e. g. its dimension is such that there are several buildings and streets within one grid cell.

The space average of the time averaged fields (Raupach and Shaw 1982; Finnigan 2000) are calculated by the following expression:

$$\langle \overline{\psi} \rangle = \frac{1}{T} \frac{1}{V_{air}} \int_{T} \int_{V_{air}} \psi(\vec{x}, t)\, d\vec{x}\, dt \qquad (2.1)$$

where the brackets and the overbar represent the spatial and time averages, respectively. Ψ is a generic variable, T is the time considered for the average, much larger than the characteristic time scale of the turbulence, so that it can considered similar to an ensemble average, and V_{air} is the volume of air without the building volume, over which the average is done. In order to average the fluxes, two kinds of fluctuating variables must be distinguished. The deviation from the time averaged value of the instantaneous value in a fixed point $\psi'(\vec{x}, t)$ and the deviation from the time and space average of the time average at a fixed point $\tilde{\psi}(\vec{x}, t)$. These fluctuations are defined as:

$$\psi'(\vec{x}, t) = \psi(\vec{x}, t) - \overline{\psi}(\vec{x}) \qquad (2.2)$$

$$\tilde{\psi}(\vec{x}) = \overline{\psi}(\vec{x}) - \langle \overline{\psi} \rangle \qquad (2.3)$$

Averaging over a fixed volume, in order to apply Reynolds averaging assumptions (Galmarini and Thunis 1999), the (in this case vertical) fluxes are written as:

$$\langle \overline{\psi w} \rangle = \langle \overline{w} \rangle \langle \overline{\psi} \rangle + \langle \overline{\psi' w'} \rangle + \langle \tilde{\psi}\, \tilde{w} \rangle \qquad (2.4)$$

where w represents the vertical component of momentum. The first term of the right hand side of the equation (hereafter r.h.s) is the flux due to the mean transport; this flux is produced by the mean structures larger than the averaging volume and can be explicitly resolved. The second term on the

r.h.s. represents the spatial average of the time averaged turbulent fluxes, and it is produced by the stochastic turbulent motions. The third term on the r.h.s of Eq. 2.4 is the so-called dispersive flux, and it is produced by the time averaged structures smaller than the grid cell, as they can be the vortices produced in a street canyon. Since they are predictable (by higher resolution models) they can not be considered part of the turbulent fluxes.

The dispersive flux has been traditionally neglected comparing with the turbulent one. This can be true for homogeneous surfaces, as in this kind of terrains upward and downward drafts can form randomly, implying that in a fixed point the spatial average equals the time average. However, in heterogeneous terrains as urban surfaces, coherent structures can be formed in fixed points, resulting in different values for the spatial and time averages. This implies that the dispersive fluxes can be different than zero.

When applying the time and spatial averages to the Navier-Stokes equation, the first (time or ensemble) averaging process filters out the turbulent features while the second (space) filters out the structures smaller than the grid cell. Both structures should be parameterized. After the two averaging processes and assuming horizontal homogeneity of the averaged mean (space and time) values, and zero averaged mean vertical velocity, the momentum equation for the *x* component of the wind, *u*, is:

$$\frac{\partial \rho \langle \bar{u} \rangle}{\partial t} = \frac{-\partial \rho \langle \overline{u' w'} \rangle}{\partial z} - \frac{\partial \rho \langle \tilde{u} \tilde{w} \rangle}{\partial z} - \left\langle \frac{\partial \bar{p}}{\partial x} \right\rangle + D_{u_i} \qquad (2.5)$$

where u' represents the turbulent fluctuation, $\tilde{u}$ the dispersive fluctuation and ρ is the density of the air. The first term on the r.h.s. accounts for the divergence of the spatially averaged turbulent flux of momentum, the second term is the divergence of the dispersive flux, which is neglected in the original version of the parameterization, and the third term is the spatially average of the horizontal mean pressure gradient. Within the canopy, this term can be written as:

$$\left\langle \frac{\partial \bar{p}}{\partial x} \right\rangle = \frac{\partial \langle \bar{p} \rangle}{\partial x} + \frac{1}{V_{air}} \sum_{i=1,N} \int_{S_i} \bar{p} \cdot ds \qquad (2.6)$$

where the pressure gradient due to external forces $\frac{\partial \langle \bar{p} \rangle}{\partial x}$ is considered zero inside this 1-D column version, and coming form the mesoscale model when the UCP is embedded in it. S_i is the vertical surface of the building *i* facing the wind in each layer and *N* is the number of buildings in the domain. The second term appears due to the discontinuity in the volume generated by the presence of buildings (Raupach and Shaw 1982). This term, assumed as the drag, or sink of momentum, due to the vertical surfaces of the buildings, is parameterized as (Martilli and Santiago

2007):

$$\sum_{i=1,N} \frac{1}{S_i} \int_{S_i} p \cdot n ds = Fu^v = -\rho C_d S \langle \overline{u(z)} \rangle \left| \langle \overline{u(z)} \rangle \right| \qquad (2.7)$$

where the Fu^v refers to the momentum flux due to the drag force produced by the vertical surfaces, S is the sum of all the building surfaces facing the flow in the layer, S_i, and C_d is the drag coefficient, which in the first version of the UCP is parameterized as a constant value equal to 0.4.

The fourth term in the r.h.s. of Eq. 2.5, D_{ui}, results from the viscous force in the original Navier-Stokes equation and represents a momentum flux from the horizontal and vertical solid surfaces. Taking into account the assumption of zero averaged mean vertical velocity, the contribution of the vertical surfaces comes from the interaction with the x and y components of the wind, resulting two orders of magnitude lower than the pressure drag force contribution (Claus et al. 2012b). Therefore, only the viscous interaction with horizontal surfaces is considered, parameterized following the classical formulas from Louis (1979), as:

$$Fu^H = -\rho \frac{k^2}{\left[\ln\left(\frac{\Delta z/2}{z_0} \right) \right]^2} f_m\left(\frac{\Delta z/2}{z_0}, Ri_B \right) \left| U^{hor} \right| \vec{U} S^H \qquad (2.8)$$

where U^{hor} is the horizontal component of the wind at the grid point closest to the surface, Δz is the thickness of the grid cell, z_0 is the roughness length of the surface, S^H its area of contact with the air, Ri_B is the Bulk Richardson number and f_m are expressions as defined in Louis (1979).

The turbulent flux of momentum from Eq. 2.5 is parameterized by means of the K-theory as:

$$\langle u' w' \rangle = -K_m \frac{\partial \langle \bar{u} \rangle}{\partial z} \qquad (2.9)$$

where K_m is the diffusion coefficient, calculated using a modified *k-l* scheme (Martilli et al. 2002 based on Bougeault and Lacarrere 1989) following the expression:

$$K_m = C_k l_k \langle k \rangle^{1/2} \qquad (2.10)$$

being C_k a model constant equal to 0.4, k the turbulent kinetic energy and l_k the turbulent length scale for vertical transport of momentum.

For the calculation of the turbulent kinetic energy k, a k - l scheme is used (Bougeault and Lacarrere 1989), where the urban surfaces fluxes are taken into account, as shown below. With the same considerations made for the momentum, the equation is the following:

$$\frac{\partial \rho k}{\partial t} = \frac{-\partial \rho \overline{k' w'}}{\partial z} + \rho K_m \left[\left(\frac{\partial U_x}{\partial z} \right)^2 + \left(\frac{\partial U_y}{\partial z} \right)^2 \right] - \frac{g}{\theta_0} \rho K_h \frac{\partial \theta}{\partial z} - \rho \varepsilon + \rho D_k \qquad (2.11)$$

where g is the gravity acceleration, θ_0 is the potential temperature of the reference hydrostatic state

and K_m and K_h, the diffusion coefficients for momentum and heat, respectively, calculated as in Eq. 2.10. The first term on the r.h.s. of Eq. 2.11 represents the turbulent transport of k, the second and third terms are the turbulence production terms due to the wind shear and buoyancy, respectively. The fourth term represents the dissipation, being ε the dissipation, calculated as:

$$\varepsilon = C_\varepsilon \frac{\langle k \rangle^{3/2}}{l_\varepsilon} \qquad (2.12)$$

where l_ε is the length scale for turbulence dissipation and C_ε is a model constant, equal to 0.71 (Martilli et al. 2002).

The last term in Eq. 2.11 accounts for the source/sink of k due to the interaction with the solid surfaces and is divided in the contributions of horizontal and vertical surfaces. Although the production of k from horizontal surfaces in each vertical layer is produced by shear and buoyant interaction, only the buoyant term is taken into account, since it is the dominant one, resulting in:

$$Pr^H = \frac{g}{\theta_0} \frac{F\theta^H}{\rho S^H} S^H \Delta z \rho \qquad (2.13)$$

The contribution of the vertical surfaces is represented by an enhancement of the conversion of mean kinetic energy into turbulent kinetic energy (Raupach and Saw 1982), parameterized in analogy of the momentum equation by:

$$Fk^V = C_{drag} |U|^3 S^V \qquad (2.14)$$

For the temperature field, after the spatial and time averages, and, according to the assumptions made for the momentum equation, the following equation is solved:

$$\frac{\partial \rho \langle \bar{\theta} \rangle}{\partial t} = \frac{-\partial \rho \langle w' \theta' \rangle}{\partial z} - \frac{\partial \rho \langle \tilde{\theta} \tilde{w} \rangle}{\partial z} + D_\theta \qquad (2.15)$$

The first term on the r.h.s. represents the turbulent flux and the second term the dispersive flux. As in the momentum equation, the turbulent flux of temperature is parameterized using a K-theory, as:

$$\langle \overline{u'\theta'} \rangle = - K_h \frac{\partial \langle \bar{\theta} \rangle}{\partial z} \qquad (2.16)$$

where K_h, originally equal to K_m, is calculated with Eq. 2.10. The dispersive flux (second term on *r.h.s*) is neglected in the original version of the model.

The last term on the r.h.s. of Eq. 2.15, D_θ, represents the heat fluxes coming from the solid obstacles through the vertical and horizontal surfaces. For the fluxes from vertical surfaces, $F\theta^v$, the formulation proposed by Clarke (1985) is used, where a sensible heat coefficient is used, calculated as a function of the canopy wind speed. For a north-south street canyon, we get:

$$F\theta^V = \frac{-\eta}{C_p}[(\theta_{air} - \theta^{west^{air}}) + (\theta_{air} - \theta^{east^{air}})]S^V \quad (2.17)$$

where $\theta^{west^{wall}}$ and $\theta^{east^{wall}}$ are the surface potential temperatures of the west and east walls, respectively, and

$$\eta = c_c\left(a_c + b_c\left(\frac{U^{h\vee}}{d_c}\right)\right) \quad (2.18)$$

being a_c, b_c, c_c and d_c empirical constants, equal to 1.09, 0.23, 5.678 and 0.3048, respectively.

As in the case of the momentum, the fluxes from horizontal surfaces are calculated using the formulation introduced by Louis (1979), applied in each layer where an horizontal surface is found as:

$$F\theta^h = -\rho\frac{k^2}{\left[\ln\left(\frac{\Delta z/2}{z_0}\right)\right]^2}|U^{hor}|\Delta\theta f_h\left(\frac{\Delta z/2}{z_0}, Ri_B\right)\vec{U}S^H \quad (2.19)$$

where $\Delta\theta$ is the difference between the air temperature and temperature of the ground or roofs and, as in the previous case, f_h refers to the expressions defined in Louis (1979).

For the fluxes calculation, the temperature of each of the surfaces is calculated using a diffusion equation in which the radiation trapping, the shadowing effects and the sky view factor are taken into account. The details of the calculation can be found in Martilli et al. (2002).

Urban Fluxes

The total contribution of the buildings surfaces in each variable, D_{ui}, D_θ and D_k are computed as the sum of the horizontal and vertical contributions divided by the volume of air of the grid cell, as:

$$D_A = \frac{Fa^H + Fa^V}{V^A} \quad (2.20)$$

where D_A is the total source/sink of each variable A, V^A is the volume of air in the grid cell and Fa^H and Fa^V are the contributions to the variable A from the horizontal and vertical surfaces, respectively.

2.3. RANS model

The RANS simulations for this study are performed with the CFD model STARCCM+ (CD-adapco 2012); with a standard *k*-*ε* turbulence closure scheme. This closure scheme solves one equation for turbulent kinetic energy (*k*) and another for its dissipation rate (*ε*). The governing equations for steady state (time derivatives equal to zero) are the following:

Continuity equation:

$$\frac{\partial u_j}{\partial x_j}=0 \qquad (2.21)$$

The Navier-Stokes equation:

$$u_j\left(\frac{\partial u_i}{\partial x_j}\right)=\frac{-1}{\rho}\frac{\partial p}{\partial x_i}+\frac{\mu}{\rho}\frac{\partial^2 u_i}{\partial x_i \partial x_j}-\frac{\partial}{\partial x_j}\left(\overline{u_i' u_j'}\right)+g_i \qquad (2.22)$$

The energy conservation equation:

$$u_i\frac{\partial \theta}{\partial x_i}=\frac{-\partial}{\partial x_i}\left(\overline{u_i' \theta_i'}\right) \qquad (2.23)$$

and the two turbulence closure scheme equations. A first one for turbulent kinetic energy and a second one for its dissipation:

$$u_i\frac{\partial k}{\partial x_j}=\frac{1}{\rho}\frac{\partial}{\partial x_j}\left[\left(\mu+\frac{\mu_t}{\sigma_k}\right)\frac{\partial k}{\partial x_j}\right]+\frac{G_k}{\rho}-\varepsilon \qquad (2.24)$$

$$u_j\frac{\partial \varepsilon}{\partial x_j}=\frac{1}{\rho}\frac{\partial}{\partial x_j}\left[\left(\mu+\frac{\mu_t}{\sigma_\varepsilon}\right)\frac{\partial \varepsilon}{\partial x_j}\right]+\frac{1}{\rho}G_{\varepsilon 1}G_k\frac{\varepsilon}{k}-C_{\varepsilon 2}\frac{\varepsilon^2}{k} \qquad (2.25)$$

being μ the dynamic viscosity and $g_i=-g\delta_{i3}$ is the gravitational body force. The Reynolds stress in Eq 2.22 in this case is calculated as:

$$-\overline{u_i' u_j'}=\frac{1}{\rho}\mu_t\left(\frac{\partial u_i}{\partial x_j}+\frac{\partial u_j}{\partial x_i}\right)-\frac{2}{3}k\,\delta_{ij} \qquad (2.26)$$

where μ_t is the turbulent viscosity, calculated as $\mu_t=\rho C_\mu\frac{k^2}{\varepsilon}$. G_k represents the turbulent kinetic energy production (or destruction) due to shear and buoyancy, σ_k (=1.0) and σ_ε (=1.3) are the turbulent Prandtl numbers for *k* and *ε*, respectively. C_μ, $C_{\varepsilon 1}$ and $C_{\varepsilon 2}$ are model constants, equal to 0.09, 1.44 and 1.92, respectively, used in various turbulent flows.

For the vertical transport of temperature in the conservation equation (Eq. 2.23), the following term is added:

$$\overline{u_i'\theta'} = -\frac{\mu_T}{\sigma_T}\frac{\partial \bar{\theta}}{\partial x_i} \qquad (2.27)$$

where σ_T is the turbulent Prandtl number for the temperature, equal to 0.9.

These set of equations are solved by finite volume methods to obtain a discrete version of the integral form of the continuum transport equations.

2.4. Averaging technique

The CFD model is applied for the simulation of different regular arrays of urban-like obstacles, formed by series of identical canyon units, consisting of a cubical building and a street canyon (Fig. 2.2). The microscale model gives the time-averaged (steady state) values of the meteorological variables (namely temperature, *x*, *y* and *z* components of momentum, turbulent kinetic energy, variances and covariances, etc) in every grid point. Assuming that the CFD results in each grid point are representative of the volume average over the grid cell of the CFD, averaging over all the points within a volume or plane, gives the spatial average, that can be assigned to mesoscale grid cell (Martilli and Santiago 2007).

As a typical unit cell of a mesoscale model contains several buildings and canyons, the domain for the averaging process must include more than one canyon unit. However, since periodic boundary conditions are considered, and all the canyon units are equal, averaging over one unit is equivalent than averaging over many units (Martilli and Santiago 2007).

Numerically, the averaged variables and fluxes are calculated by:

$$\langle \bar{\psi} \rangle_k = \frac{1}{M}\sum_i \sum_j \bar{\psi}_{i,j,k} \qquad (2.28)$$

$$\langle \overline{\psi' w'} \rangle_k = \frac{1}{M}\sum_i \sum_j \left(\overline{\psi' w'}\right)_{i,j,k} \qquad (2.29)$$

$$\langle \tilde{\psi}\tilde{w} \rangle_k = \frac{1}{M}\sum_i \sum_j \left(\tilde{w}_{i,j,k} - \langle \bar{w} \rangle_k\right)\left(\tilde{\psi}_{i,j,k} - \langle \bar{\psi} \rangle_k\right) \qquad (2.30)$$

where Ψ' is the perturbation to the time average and $\tilde{\psi}$ is the departure of the time average from the spatial average. The sum is performed over the *M* points in each horizontal layer *K*. The values of $\overline{\psi' w'}$ in each point are directly computed by the RANS model following the equations in the previous section.

The behaviour of the spatially averaged values will be used in the next chapters to determine the

best way to estimate the drag coefficient C_d and the length scales for turbulent transport and turbulence dissipation.

2.5. Validation and Justification for the use of RANS simulations

In this study, the results from RANS simulations are used to derive spatially-averaged fields over several arrays of cubes with different configurations. These spatially-averaged results are used for the estimation of variables such as the vertically-integrated sectional drag coefficient (Santiago and Martilli 2010), defined as:

$$C_{deq} = \frac{(\rho H)^{-1} \int_0^H \Delta \langle \overline{p(z)} \rangle \, dz}{H^{-1} \int_0^H \langle \overline{u(z)} \rangle \left| \langle \overline{u(z)} \rangle \right| dz} \qquad (2.31)$$

where $\Delta \langle \overline{p(z)} \rangle$ is the mean pressure deficit between the upwind and downwind faces of the cube at height z and H is the height of the buildings. This is a sectional drag coefficient since the drag force is computed using the horizontally-averaged wind speed at the same height as the pressure deficit within the canopy (and not at a reference height above).

Figure 2.2: Canyon unit formed by a building and the street canyon.

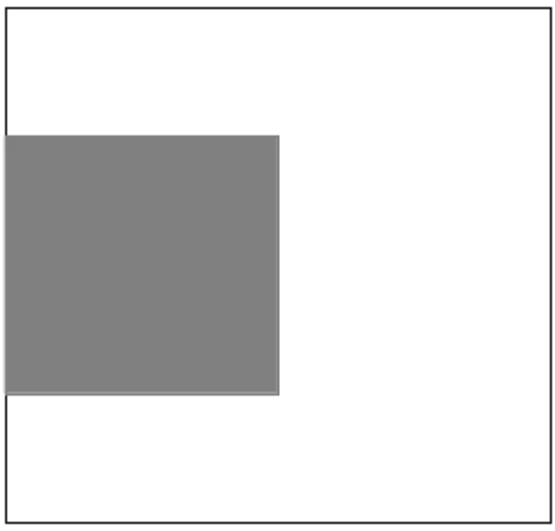

The direct validation of this approach with experimental values of C_{deq} as defined in Eq. 2.31 is not straightforward because direct measurements of C_{deq} are scarce. Instead, measurements of C_D, defined as a function of the wind speed at a certain height above the canopy, are available in the literature. For example, Hagishima et al. (2009) computed as $C_D = \frac{\tau_0}{0.5\,\rho\,U_{ref}}$ from wind-tunnel experiments for different regular arrays of cubes, with τ_0 the total surface shear stress per unit area and U_{ref} the reference mean speed at a reference height. Values for z_{ref} = 3.5H and 6H were considered, with the C_D values compared with those computed from RANS simulations for the same configurations (Fig. 2.3). RANS set-ups are described in Sect. 3.1. In these cases λ_p is calculated as:

$$\lambda_p = \frac{B_x B_y}{(B_x + W_x)(B_y + W_y)} \qquad (2.32)$$

where $W_{x(y)}$ is the distance between buildings in *x(y)* direction and $B_{x(y)}$ is the building width in *x(y)* direction (Fig. 2.3). Note that for the aligned configurations of cubic obstacles used here, B_x is equal to B_y and λ_p is equal to λ_f, being $\lambda_f = \frac{B_y H}{(B_x + W_x)(B_y + W_y)}$.

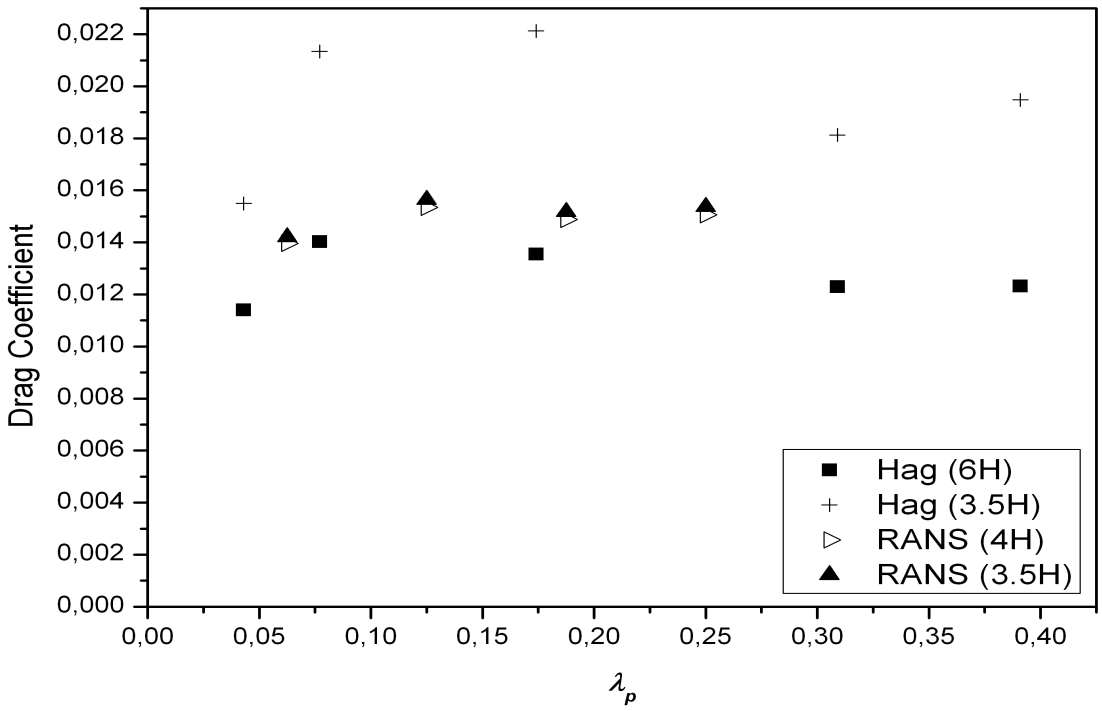

Figure 2.3: Comparison of C_D calculated from Hagishima et al. (2009) and the RANS model used in this study

In this case RANS results underestimate the value of the coefficient, however, the variation of C_D with λ_p is similar to the experimental data. In addition, the same comparison was performed for staggered arrays and similar results were obtained (not shown here). This tendency is in agreement with that measured by Cheng and Castro (2002), with a slightly different formulation

$C_D = \frac{\tau_0 A_C}{0.5 \rho U_{ref} A}$ where A_C is the unit plan area of the roughness surface ($4H^2$ since λ_p = 0.25) and A is the frontal area of the cube (H^2). Using the wind speed at 1.5H as a reference, the measured value of the coefficient was 0.18 while RANS results give 0.12.

Comparison with DNS results is another way to validate the simulations, because DNS are assumed to be more accurate, though significantly more expensive in computational time (about 2–3 orders of magnitude). The advantage is that with DNS the spatial averages of wind speed in the canopy and the pressure on the faces of the cubes can be computed, and consequently C_{deq} estimated. The DNS results of Coceal et al. (2006) yield C_{deq} = 0.4 for an aligned array with λ_p = 0.25 as compared to 0.73 as computed by RANS. However in DNS (Coceal et al. 2006) only 66 % of the imposed force is dissipated by pressure forces acting on the faces of the cube; the remainder is dissipated by viscous forces, while in RANS this ratio is close to 95 %. To understand these differences it is important to consider that the Reynolds number in DNS is 5,000, while that in RANS is 10^6 –10^7, close to the full scale values observed in cities. Whether it is more realistic to use DNS at low Reynolds number or RANS at high Reynolds number is not clear. Kanda et al. (2013) applied large-eddy simulations (LES) over realistic and idealized (staggered and aligned) configurations of buildings and found that the fraction of the imposed forces dissipated by the friction on the floor is less than 20 % for real configurations and regular staggered arrays, but is between 20 and 40 % for aligned arrays. However, Kanda et al. (2013) in their LES used a surface roughness length of 0.1 m corresponding to a much rougher surface than the smooth walls and floor used in the RANS and DNS of the present study. On the other hand, Claus et al. (2012a) suggested a possible dependence of the drag coefficients computed with DNS with Reynolds number. This is in agreement with the fact that when RANS is used with the same Reynolds number as DNS (5,000) over aligned arrays, the fraction of the total force dissipated by viscous forces is 70 % approximately, close to the DNS-based value. In addition, Claus et al. (2012b) using experimental data for different wind directions over a staggered array found that the proportion of viscous drag to the total drag is relatively small for all angles, and they showed that this does not agree completely with DNS data for corresponding channel flows.

For all these reasons it seems of interest to consider also the value of the drag coefficient obtained by using the total drag force (and not only that generated by the pressure on the cubes). Ideally we should use the total drag force to estimate the coefficient. In this case the value for DNS results rises to $C_{deq} = 0.6$.

These results indicate that RANS tends to overestimate the value of C_{deq} and underestimate the value of C_D (e. g. based on a velocity at a reference height). In order to evaluate the impact of this inaccuracy on the mean wind speed, which constitutes the main objective of this study, it should be considered that, for a given drag force D, $\langle \bar{u} \rangle \propto \frac{1}{\sqrt{C_{deq}}}$. The percentage inaccuracy in $\langle \bar{u} \rangle$ due to the inaccuracy in C_{deq} (based on differences between DNS and RANS) is

$$\frac{\frac{1}{\sqrt{C_{deq}(RANS)}} - \frac{1}{\sqrt{C_{deq}(DNS)}}}{\frac{1}{2}\left(\frac{1}{\sqrt{C_{deq}(RANS)}} + \frac{1}{\sqrt{C_{deq}(DNS)}}\right)} \times 100$$

for the values indicated above, i.e. -29.8 % with C_{deq} (DNS) = 0.4, and −9.8 % with C_{deq} (DNS) = 0.6. For the purposes of the present study this error is acceptable, considering that RANS permits far greater exploration of possible array arrangements than with DNS (or even with LES), because of the lower computational cost.

Moreover, as shown below, the variability in C_{deq} obtained from RANS simulations is significantly larger than this error. It is important to remember here that our aim is to show that C_{deq} depends on geometrical parameters beyond λ_p, and to provide a simple means of improving schemes that ignore this additional dependency (since all the UCP have a constant drag coefficient).

3. Streamwise versus spanwise spacing of obstacle arrays: parametrization of the effects on drag and turbulence [1]

The dynamical interaction between the urban obstacles and the wind is modeled within the urban schemes by a drag force proportional to a drag coefficient and the square of the wind, and a modification of the length scales involved in turbulent transport and turbulence dissipation. Previous approaches have proposed the drag coefficient as a constant value ranging from 0.1 (Uno et al. 1989) to 1 (Coceal and Belcher, 2004), while, recently, Santiago and Martilli (2010) proposed a parameterization of this coefficient as a function of the density of the obstacles based on CFD results. Concerning the turbulent length scales, they have been parameterized by a relation between the distance to the ground and the height of the buildings (Martilli et al. 2002), although, in Santiago and Martilli (2010), a parameterization by means of the density of the urban obstacles have been proposed.

Nevertheless, we ask ourselves, *are these parameters enough to unequivocally represent the dynamical behaviour of the flow?*

In order to answer this research question, in this chapter, a RANS-CFD model (STARCCM+, from CD-adapco) is used to investigate the evolution of the sectional drag force and the length scales for turbulent transport and turbulence dissipation with different layouts of aligned arrays of building-like cubes. Considering the sectional drag coefficient, the results analyzed in this chapter show a dependency with the non-dimensional streamwise distance (sheltering parameter), and the non-dimensional spanwise distance (channelling parameter) between obstacles.

The length scales have shown a similar behaviour comparing to results from staggered arrays of buildings Santiago and Martilli (2010), showing a dependency on the density of obstacles within the domain.

Analytical formulae are proposed for the sectional drag coefficients and the length scale for turbulent transport and turbulence dissipation and implemented in a one-dimensional UCP. This approach has demonstrated good skills in the prediction of vertical profiles of the spatially-averaged horizontal wind speed. These results have been published in an article in Boundary Layer Meterelogy (Simón-Moral et al. 2014).

1 This chapter is mainly based on Simón-Moral et al. 2014

3.1. Set up of the simulations

With the aim to search an answer to the research question highlited above, a set of simulations of aligned configurations of cubes with different plan area density values, λ_p (Eq. 2.32), and distances between building rows in both the streamwise (x) and spanwise (y) directions are analyzed Fig. 3.1. In addition to λ_p, each configuration is characterized by other two geometrical parameters: a sheltering parameter, λ_s, and a channelling parameter λ_{ch}, related with the width of the streets. These parameters are defined as :

$$\lambda_s = \frac{W_x}{H} \qquad (3.1)$$

$$\lambda_{ch} = \frac{W_y}{B_y} \qquad (3.2)$$

Where $B_{x(y)}$ and $W_{x(y)}$ are the length of the buildings and the width of the street in $x(y)$ directions, respectively (Fig. 3.1) and H, as seen in previous chapter, is the height of the buildings. The rationale of the study is to investigate if cases with the same value of λ_p, but different values of the other paramters, behave in the similar way in terms of equivalent drag coefficient and length scales, or not. The configurations studied, listed in Table 3.1, are named from the value of the sheltering and channelling factors as SXXCHYY, where XX and YY refer to the values of the sheltering and the channelling factors, respectively. For example, S1CH3 is the configuration with λ_s = 1 and λ_{ch} = 3.

The numerical domains for the RANS simulations have periodic boundary conditions and tests have demonstrated that larger domains provide identical results. The flow is driven by a height-independent horizontal pressure gradient in the x-direction, applied in every vertical layer, and the top boundary is fixed at $4H$ as in Coceal et al. (2006) and Santiago et al. (2008) where symmetric boundary conditions are used. The pressure gradient is related to a reference velocity by:

$$u_\tau = \sqrt{\left(\frac{\tau H_{domain}}{\rho}\right)} \qquad (3.3)$$

where τ is the horizontal pressure gradient and H_{domain} is the height of the domain. This reference velocity is used for the normalization of the wind speed or the k. Taking into account that the RANS results are stationary, u_τ corresponds to the total momentum flux lost at the urban surfaces.

Both the buildings and ground are modeled with standard smooth wall functions; H = 16 m is set and simulations with $Re = 5 \times 10^5$ (based on the velocity at the top of the domain) are performed.

The mesh is composed of cartesian grids and resolves each cube with 16 cells in each dimension (1 m resolution in every direction). For the λ_p = 0.25 case, a test of grid independence (using 32 cells to resolve each cube) showed that the previous resolution is acceptable. The domain of the column model is a vertical column of computational cells over an urban zone. The height of the canopy (e. g. building height) is 16 m and 16 vertical levels are used to resolve each building (similar *Re* and identical vertical resolution to those used in the RANS simulations).

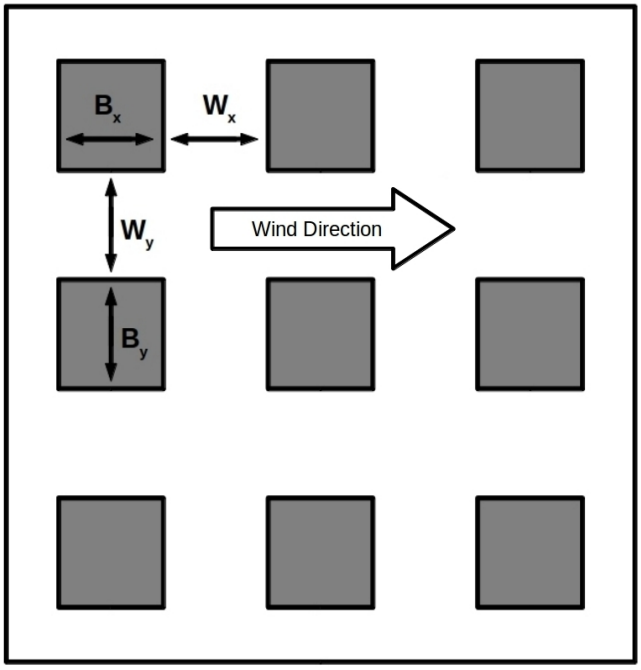

Figure 3.1: Plan view of the aligned configuration used in the RANS simulation

Table 3.1: Aligned configurations used for the CFD simulations; S refers to the sheltering factor value and CH to the channelling factor

	λ_s	λ_{ch}	λ_p	C_{deq}
S6CH2	6	2	0.048	1.230
S3CH3	3	3	0.0625	0.538
S6CH1	6	1	0.071	2.070
S3CH2	3	2	0.083	0.820
S4CH1	4	1	0.1	2.040
S1.83CH1.83	1.83	1.83	0.125	0.535
S3CH1	3	1	0.125	1.857
S1CH3	1	3	0.125	0.136
S2CH1	2	1	0.167	1.357
S1CH2	1	2	0.167	0.250
S1.31CH1.31	1.31	1.31	0.1875	0.536
S1CH1	1	1	0.25	0.728
S0.5CH1	0.5	1	0.33	0.360

3.2. Dependence of C_d on Novel Geometrical Parameters

The drag coefficient considered in this study, C_{deq} (defined in Sect. 2.5), is calculated from the spatially-averaged RANS results. As shown in Fig. 3.2, different configurations with the same λ_p (and λ_f, defined as $\frac{HB_y}{(B_x+W_x)(B_y+W_y)}$) have different values of the drag coefficient. This is an important result, because several formulations for the calculation of the drag coefficient as a function of λ_p or λ_f only have been proposed in the literature (Macdonald 2000; Kanda et al. 2004; Cheng et al. 2007; Santiago et al. 2008; Santiago and Martilli 2010). Clearly, there are other geometrical parameters that determine the value of C_{deq}. After analyzing the behaviour of the coefficient as a function of each parameter, the following expression is proposed (details of the calculation method are presented in Appendix 1):

$$C_{deq}=\left[\left(1-\exp\left(-a\left(\lambda_s\right)^b\right)\right)\right]\left(\frac{c}{\lambda_{ch}}\right)\left(\frac{f}{\lambda_s^i\lambda_{ch}^j}+1\right) \qquad (3.4)$$

with a = 0.24, b = 1.67, c = 2.07, f = 0.6, i = 1.4 and j = 4, values determined to minimize the differences between the relation (Eq. 3.5) and the drag coefficients derived from the RANS results. In Fig. 3.3, a comparison between the RANS values and the parameterized values of C_{deq} is shown. Clearly, the parameterization closely approximates the RANS results.

Figure 3.2: C_{deq} as function of λ_p for the configurations studied. Par refers to the parameterization results

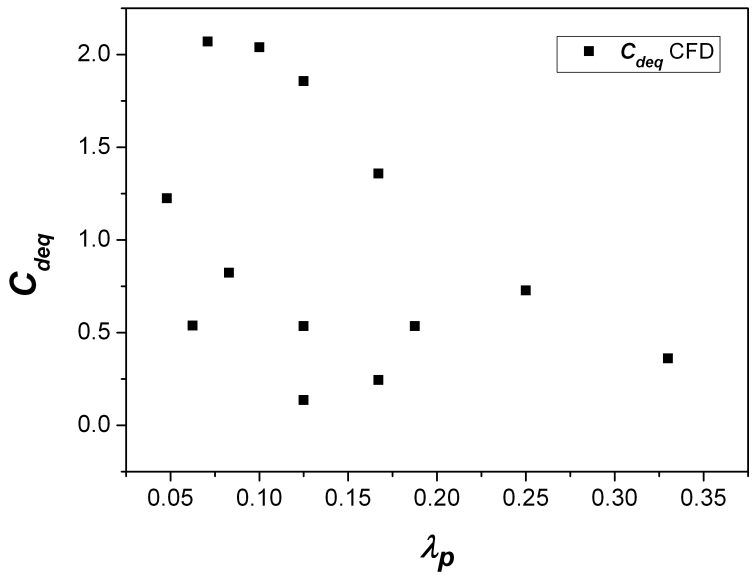

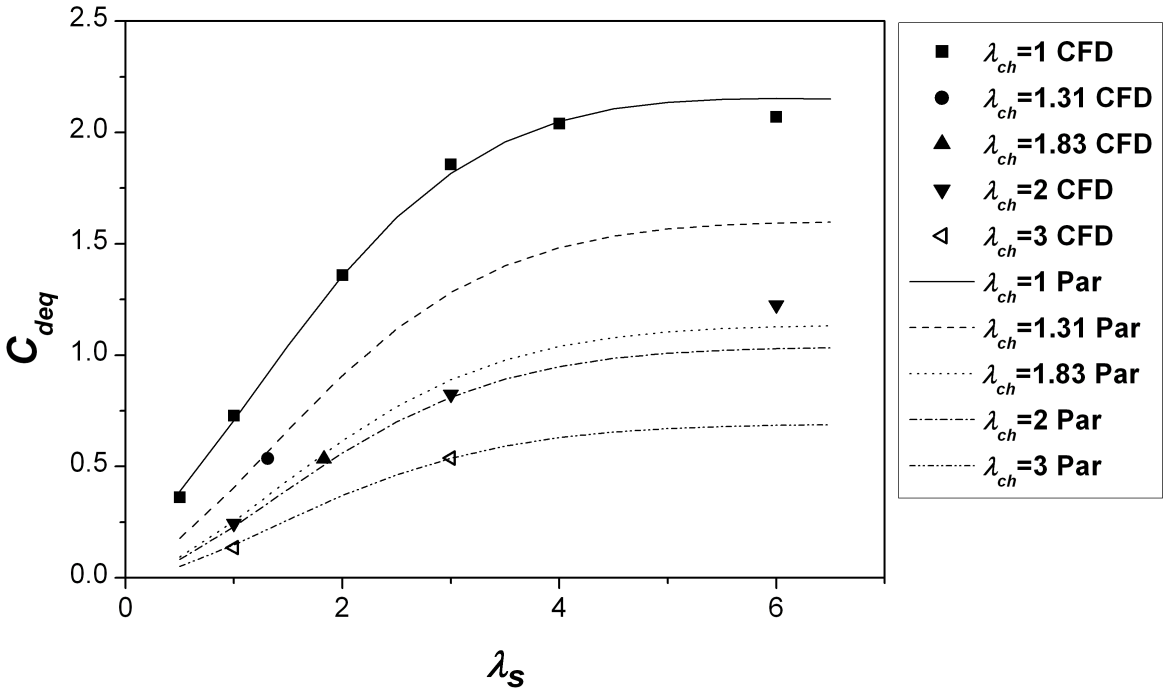

Figure 3.3: Comparison between C_{deq} from the RANS and the parameterization (Eq. 3.4) for different λ_{ch} and λ_s.

The first factor on the right-hand side of Eq. 3.4 accounts for the distance between buildings in the wind direction (sheltering). This effect is related to the penetration of air into the canyon, the more penetration the more effectively does the face of the downwind building exert a drag on the mean flow. When the streamwise distance between buildings approaches zero (maximum sheltering), there is no penetration and $C_{deq} \rightarrow 0$ (Fig. 3.4a). The opposite case is that of an isolated building, which exhibits maximum drag because the obstacle is completely unsheltered. In other words, the closer the buildings, the larger is the sheltering and the smaller C_{deq} (for constant λ_{ch}).

The second term in Eq. 3.4 represents the channelling of the flow within the streets, related with the distance between the buildings in the direction perpendicular to the flow. The larger the distance, the stronger the spatially-averaged wind field, because the section not affected by the presence of obstacles is larger. This implies a smaller C_{deq}, since it is inversely proportional to the square of the spatially-averaged x-wind component, see Eq. 2.31. When the channelling factor tends to zero the value of C_{deq} tends to infinity (Fig. 3.4b), meaning that this approach does not work if the channel disappears. In fact, in such a scenario, the flow cannot penetrate through the array of buildings, which implies that the array behaves as a barrier and not as a porous medium.

The third term modulates the two first factors in the equation. Its value is close to one when the channelling and sheltering factors are sufficiently high, and its importance increases when both geometrical factors decrease.

This new parameterization for C_{deq} is defined for aligned configurations of cubes and is not appropriate for non-cubical buildings. It differentiates between aligned configurations with the same λ_p (and λ_f) allowing for the discrimination between different distributions of buildings with similar building packing density per unit area, in terms of their impacts on the flow. However, it is formulated for aligned layouts, and modifications will likely be required to extend the scheme to staggered layouts, for example, although close to road level, the presence of the streets makes the aligned configuration more likely than the staggered.

3.3. Parameterization $l_\varepsilon/C_\varepsilon$

Turbulent length scales involved in turbulent transport and turbulence dissipation (see Eqs. 2.10 and 2.12, respectively) are also dependent on the obstacle configuration. The evolution of the turbulence dissipation length scale can be investigated by computing,

$$C_k l_k = C_\mu \frac{l_\varepsilon}{C_\varepsilon} \qquad (3.5)$$

where $\langle k \rangle$ and $\langle \varepsilon \rangle$ are calculated from the RANS results. Three zones are considered for the length scales: (i) inside the canopy ($z/H < 1$), where it is defined as a constant value; (ii) the transition zone ($1 < z/H < 1.5$), with linear behaviour; and (iii) well above the canopy ($z/H > 1.5$), also with linear behaviour, but with a different slope than for zone (ii):

$$l_\varepsilon / C_\varepsilon = \alpha_1 (H - d) \; for \; z/H < 1 \qquad (3.6a)$$

$$l_\varepsilon / C_\varepsilon = \alpha_1 (z - d) \; for \; 1 \leqslant z/H < 1.5 \qquad (3.6b)$$

$$l_\varepsilon / C_\varepsilon = \alpha_2 (z - d_2) \; for \; z/H \geqslant 1.5 \qquad (3.6c)$$

As in Santiago and Martilli (2010), in the lowest region the value of $l_\varepsilon/C_\varepsilon$ is approximated as a constant and defined as proportional to $(H - d)$, where d is the zero-plane displacement, obtained by a best fit method (see Eq. 3.7), and α_1 is a constant. The value of α_1 ranges from 1.91 to 2.46 for the different configurations. For simplicity, an average value of 2.19 is proposed. For the second and third zones, α_1 and α_2 are the slopes of the straight lines as a function of z, and α_2 is calculated using the linear dependency of $l_\varepsilon/C_\varepsilon$ with z above the canopy (region iii) from the RANS model. The constant α_2 ranges from 1.14 to 1.27 for the different configurations, thus an average value of α_2 =

1.2 is used for the parameterization. Both α_1 and α_2, as obtained for these aligned arrays, are similar to those calculated in Santiago and Martilli (2010) for staggered cases; d_2 is a constant defined in order to maintain the continuity at z/H = 1.5. A comparison between the RANS spatially-averaged results and the parameterization is shown in Fig. 3.5 for several configurations.

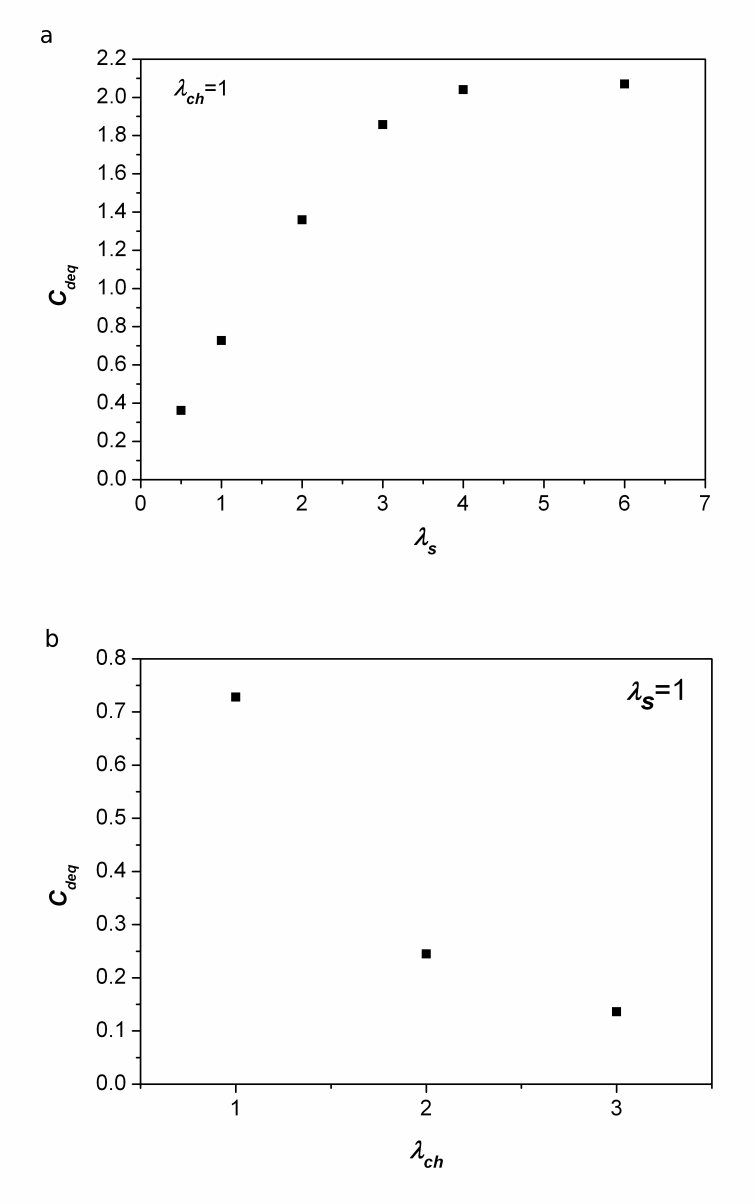

Figure 3.4: Variation of C_{deq} with a) λ_s and b) λ_{ch}

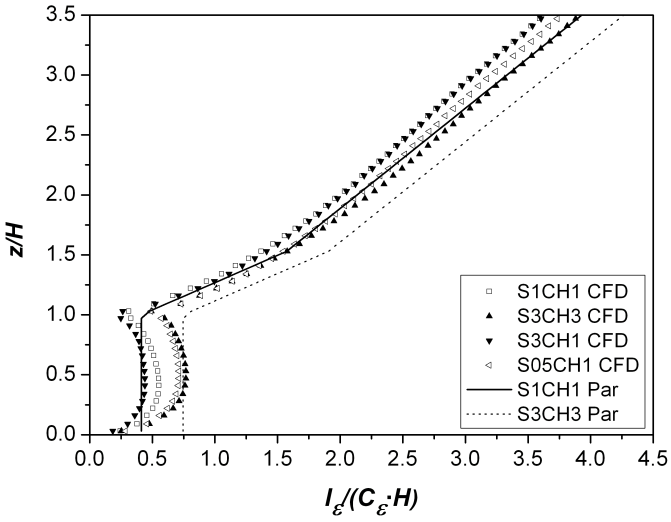

Figure 3.5: Comparison of vertical profiles of $l_\varepsilon/(C_\varepsilon H)$ calculated from spatially-averaged results from the RANS simulations and from the parameterization.

For each configuration the displacement height is deduced from the RANS results using a best fit method by adjusting the wind speed to a logarithmic profile. A simple parameterization of d/H as a function of λ_p is proposed (Eq. 3.6). This dependency is similar for staggered arrays (Santiago and Martilli 2010) (Fig. 3.6), suggesting that the displacement height is quite insensitive to the obstacle configuration (aligned or staggered), and that it can be represented as a function of λ_p only (in contrast to C_{deq}). A best-fit value of n = 0.15 is derived considering both aligned and staggered results:

$$d/H = \lambda_p^n \qquad (3.7)$$

The length scale for the turbulent transport is then calculated as:

$$C_k l_k = C_\mu \frac{l_\varepsilon}{C_\varepsilon} \qquad (3.8)$$

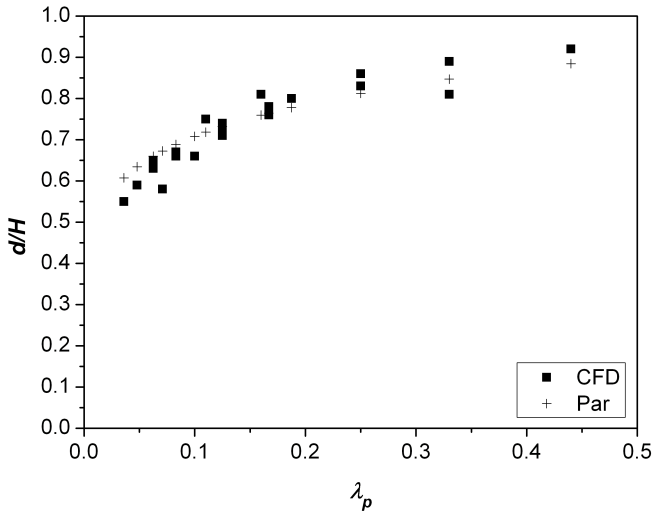

Figure 3.6: Variation of the displacement height with λ_p for the results from the RANS simulations (for staggered and aligned arrays) and from the parameterization.

3.4. Implementation of the Parameterization in a Column Model

The parameterizations described in Sects. 3.2 and 3.3 are introduced into the column model described in Sect. 2.2 and the results are compared against the horizontally-averaged values from the RANS model. First, the capacity of the new parameterization to reproduce the differences between different configurations with the same λ_p, is tested. Vertical profiles of $\langle \overline{u} \rangle$, $\langle \overline{k} \rangle$, $\langle \overline{u'w'} \rangle$ and K_m for the different configurations are compared, where wind speed is normalized by u_τ, the turbulent kinetic energy and fluxes by $u_\tau^{\,2}$, and K_m by $u_\tau H$. Then K_m is calculated from the RANS results following Eq. 2.9.

The analysis of the results for the three configurations with $\lambda_p = 0.125$ (Fig. 3.7) shows that the new parameterization distinguishes between the configurations. Hence, it is able to distinguish between configurations with identical λ_p but different λ_{ch} and λ_s. Clearly the best agreement is found for the mean wind speed, for which the relative differences between the configurations are reproduced with some underestimation. Nevertheless, in the S1CH3 case, although the shape of the profile is mostly reproduced, an underestimation is found with a maximum error of 17 % in the canopy. The shape of the *k* profile within the canopy produced by the 1-D model is different than the RANS averaged results, although the magnitude is in close agreement. The shear stress is underestimated in the canopy, as is K_m. However, the column model correctly orders the canopy magnitudes of all variables between the three scenarios with lower values for S3CH1 and higher values for S1CH3 in the same way as does the RANS simulations.

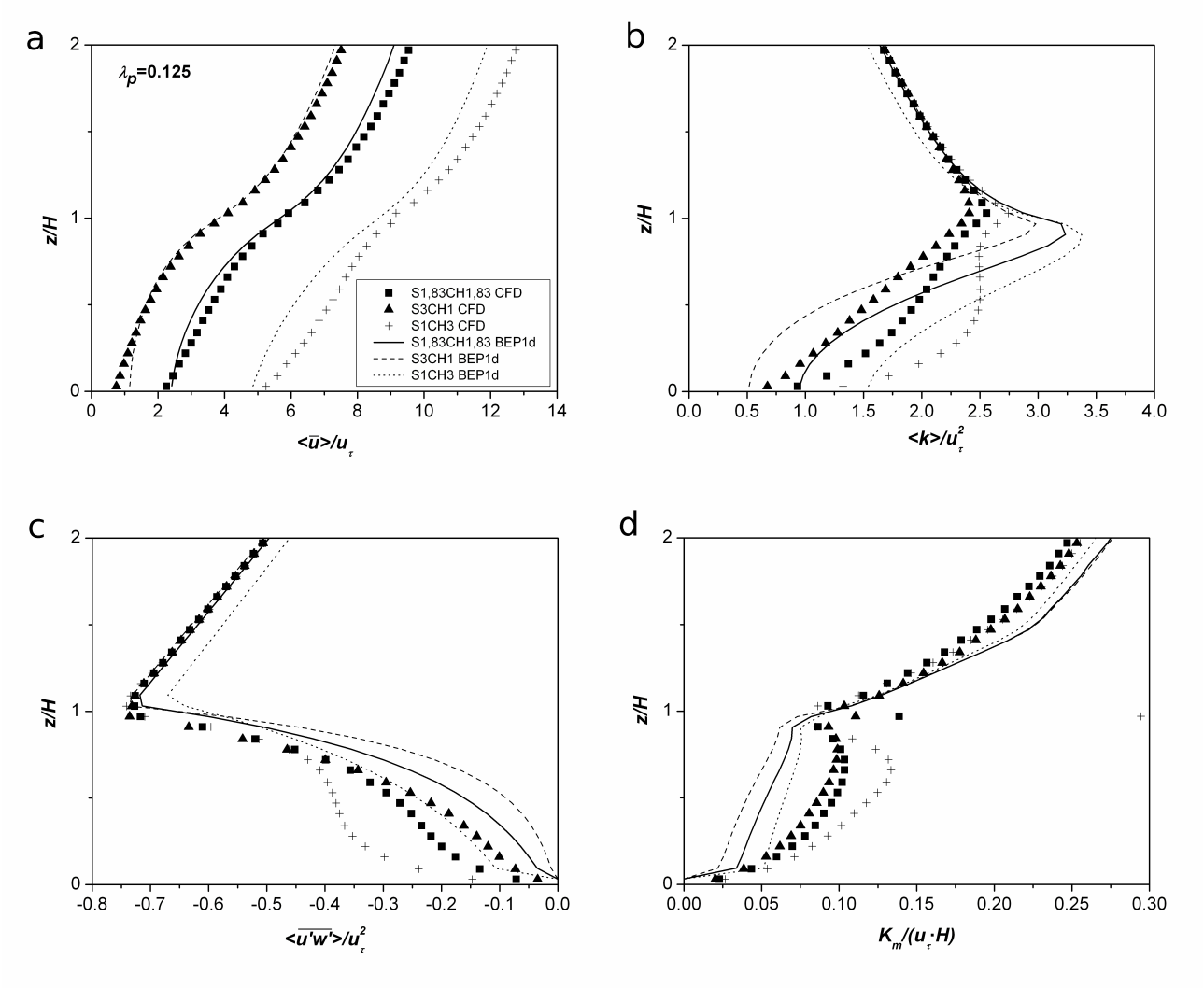

Figure 3.7: Comparison of vertical profiles of spatially-averaged results from the RANS simulations and from the UC parameterization results for configurations with λ_p = 0.125. a) Mean streamwise wind velocity; b) turbulent kinetic energy; c) Reynolds shear stress; d) diffusion coefficient

These results suggest that the most important factor for the mean wind is the drag force. That is, a good estimate of the drag force due to a good estimate of the drag coefficient results in a good estimate of the mean wind speed. For *k*, mechanisms other than the removal of momentum by drag play an important role (e.g., dispersive transport), meaning that a good estimate of C_{deq} is not enough to ensure a good match between the column model and the RANS averaged results. For example, the shear production term is assumed to be proportional to the square of the vertical gradient of the spatially-averaged mean components of the velocity. While this is a correct assumption for boundary-layer flows over flat surfaces, it is not for strongly three-dimensional heterogeneous flows such as those present in an urban canopy. To carefully reproduce *k*, a deeper

analysis of each term of the *k* equation, and of the way they are parameterized, is necessary, but this is beyond the scope of the present study that primarily focuses on the mean wind. For this reason, in the following the analysis centres on the horizontal components of the mean velocity.

The configurations S1CH1, S3CH1 and S05CH1 are compared in Fig. 3.8, all of them with λ_{ch} = 1 but different λ_p (0.25, 0.125, 0.33) and λ_s (1, 3, 0.5). In this case, although the results are very close, the parameterization is also capable of distinguishing between the different configurations, reproducing the relative differences between them. Accounting for configurations with the same λ_s but different λ_p and λ_{ch}, those with λ_s = 1 (S1CH2, S1CH3 and S1CH1) are compared in Fig. 3.9. As in the previous cases, the parameterization reproduces the differences between the different configurations. From the results presented, it is possible to observe that the wind speed inside the canopy is roughly proportional to $\frac{1}{\sqrt{\alpha C_{deq}}}$, where α is the density of vertical surfaces (see Eq. 2.7).

To quantify the differences between the RANS results and those from the column model, the root-mean-square error (*RMSE*) and the mean bias (*MB*) are computed for each configuration. These values are defined as:

$$RMSE = \sqrt{\frac{\sum_{K=1,M} \left(\langle \overline{U_{RANS,K}} \rangle - \langle \overline{U_{UCP,K}} \rangle \right)^2}{M}} \qquad (3.8a)$$

$$MB = 2 \frac{\sum_{K=1,M} \langle \overline{U_{UCP,K}} \rangle - \sum_{K=1,M} \langle \overline{U_{RANS,K}} \rangle}{\sum_{K=1,M} \langle \overline{U_{UCP,K}} \rangle + \sum_{K=1,M} \langle \overline{U_{RANS,K}} \rangle} \qquad (3.8b)$$

where the subscript RANS accounts for the RANS spatially-averaged results, UCP for the urban canopy parameterization, *K* refers to each vertical level and *M* is the number of vertical levels of the zone studied (within the canopy, over the canopy or in both zones). The results for *U* are presented in Table 3.2.

Figure 3.8: Comparison of the vertical profile of the spatially-averaged streamwise wind velocity for configurations with λ_{ch} = 1

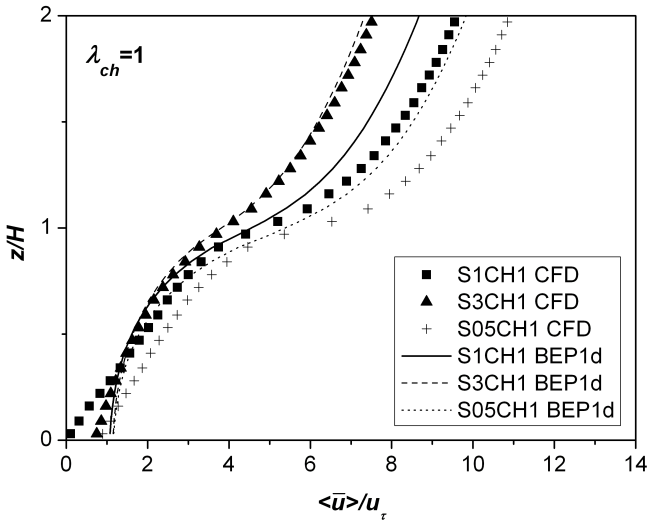

Figure 3.9: Comparison of vertical profile of spatially-averaged streamwise wind velocity for configurations with λ_s = 1

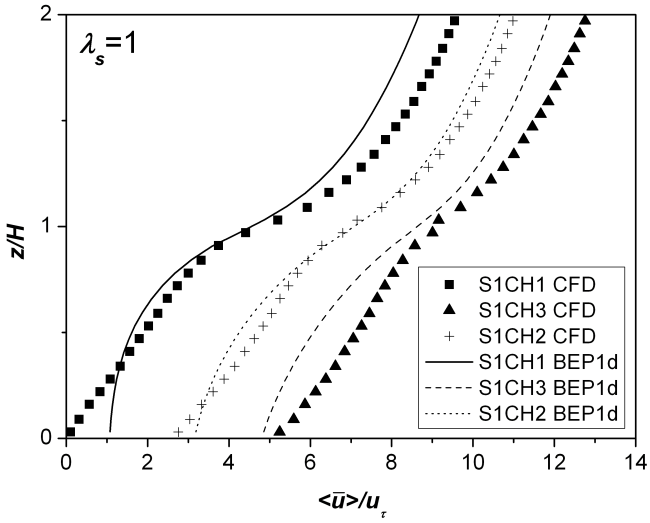

In the λ_p = 0.25 case (S1CH1), shown in Figs. 3.8, 3.9 and 3.10, the *RMSE* for the wind field is 0.42 within the canopy and 0.97 above, which implies that the results are better within the canopy. These values are of the same order of magnitude as those in Santiago and Martilli (2010) for the λ_p = 0.25 staggered case, although slightly smaller inside the canopy. As shown in Fig. 3.10, the column model value differs by <20 % from the RANS results, except in the lowest third of the canyon. These differences in the lowest part of the canopy are related to the neglect of the vertical variability of C_d. In fact, it is in the lowest part of the canopy where the differences between C_{deq} and the actual

relation between the drag and the square of the wind speed, computed as $\frac{\frac{-1}{\rho}\Delta\langle\overline{P(z)}\rangle}{\langle\overline{u(z)}\rangle\left|\langle\overline{u(z)}\rangle\right|}$ are the largest. Since wind speed is usually small at this level, the absolute errors obtained are also small. Related with this, a difference of slope in the wind profile is found. For the other configurations, the *RMSE* of the wind speed ranges from 0.16 to 0.86 inside the canopy and from 0.08 to 0.97 above, and is generally larger above. Inside the canopy, when λ_s is constant, the *RMSE* error increases with λ_{ch}, with larger increases for lower λ_s. On the other hand, with constant λ_{ch}, except for the case with $\lambda_{ch} = 1$, *RMSE* increases as λ_s decreases.

Conf	RMSE(can)	MB(can)	RMSE(ab)	MB(ab)	RMSE(tot)	MB(tot)
S6CH2	0.19	-0.012	0.21	-0.010	0.20	-0.009
S3CH3	0.31	-0.027	0.49	-0.02	0.45	-0.023
S6CH1	0.16	-0.02	0.08	0.005	0.11	0.003
S3CH2	0.16	-0.01	0.26	-0.01	0.24	-0.01
S4CH1	0.16	-0.006	0.1	-0.005	0.12	-0.005
S1.83CH1.83	0.29	-0.03	0.55	-0.03	0.5	-0.03
S3CH1	0.18	-0.002	0.28	-0.02	0.26	-0.01
S1CH3	0.86	-0.06	0.95	-0.04	0.93	-0.04
S2CH1	0.22	-0.002	0.62	-0.04	0.55	-0.03
S1CH2	0.31	-0.02	0.41	-0.02	0.39	-0.02
S1.31CH1.31	0.35	-0.04	0.8	-0.04	0.71	-0.04
S1CH1	0.42	0.001	0.97	-0.05	0.86	-0.047
S05CH1	0.43	-0.07	1.1	-0.05	0.98	-0.05

Table 3.2: RMSE and MB for U inside the canopy, above it and for the whole vertical column

Figure 3.10: Comparison of the streamwise wind velocity calculated by the column model with the RANS results for the S1CH1 case. A range of ±20 % from the RANS spatially-averaged streamwise wind profile is also indicated

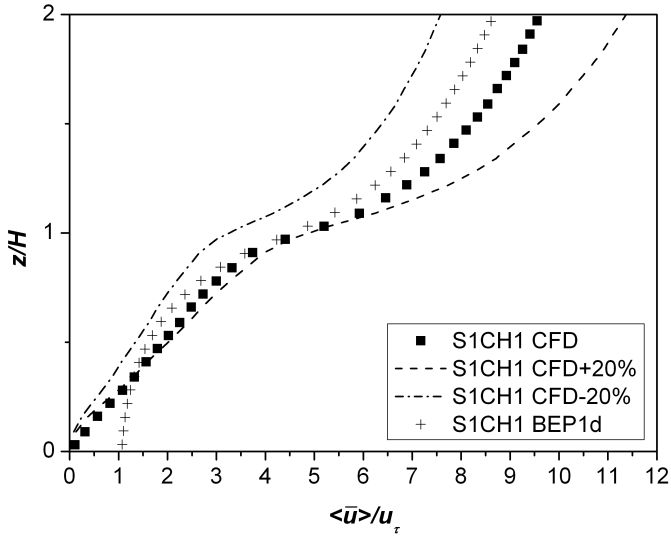

3.5. Summary and conclusions

In this chapter the methodology of Martilli and Santiago (2007), Santiago et al. (2008) and Santiago and Martilli (2010) is followed. RANS simulation results are used to generate data with which the variation of the sectional drag coefficient and turbulent length scales of an array of aligned cubical obstacles are explored as a function of its geometrical layout. This information is then used for the development of a parameterization of urban drag and turbulence that has been tested in an urban parameterization implemented in a column model. The main results can be summarized as follows:

- λ_p and/or λ_f do not unequivocally determine the sectional drag coefficient of an aligned array of cubes. In fact, two arrays with identical obstacle density may exert very different magnitudes of drag. Hence two additional geometrical parameters are introduced here, the sheltering factor λ_s, and the channelling factor λ_{ch}, and a relation is proposed to estimate the sectional drag coefficient (C_{deq}) as a function of these new parameters.
- The turbulent length scales for an aligned array of cubes behave similarly to those of a staggered array. This suggests that length scales are less sensitive to building arrangements than drag coefficients. The relationship proposed in Santiago and Martilli (2010) has been generalized by adapting the coefficients.
- The 1-D tests performed with a column model show that this methodology is a good compromise between accuracy and simplicity for the simulation of the spatially-averaged mean flow.
- The parameterization proposed is able to distinguish between different configurations with the same λ_p. This is a step towards better representation of the airflow in real-world neighbourhoods using mesoscale meteorological models.

In recent years, more detailed geometrical parameters have become available for an increasing number of cities (e. g. ‘National Urban Database and Access Portal Tool’, NUDAPT, Ching et al. 2009). An open question is how to best use these data to characterize, from a spatially- averaged dynamical point of view, the different neighbourhoods within the city. The current work contributes to the search for geometrical parameters that best determine the dynamic influence of an urban neighbourhood. To date, λ_p and/or λ_f are the parameters most frequently used, and our study indicates that other information may also be important, such as the degree of “sheltering” and ”channelling”. Indeed, for future work, this study should be extended to account for non-cubic buildings, by either varying their height or their plan area.

4. Effects of unstable thermal stratification on heat and momentum fluxes in urban areas[2]

The dynamical parameters determining the flow inside the cities as the drag coefficient or the turbulent length scales have been widely studied in the literature (Uno et al. 1989; Coceal and Belcher 2004; Santiago et al. 2008; Santiago and Martilli 2010; Simón-Moral et al. 2014). In previous chapters, these parameters have been parameterized by means of urban morphological parameters, showing the dependence of the flow structure with the configuration of the buildings and its density within the domain. Most of the studies have focused on neutral thermal conditions, not taking into account the effect of the thermal stratification, but *are the drag coefficient and the turbulent length scales affected by thermal stratification?* Considering that the purpose of the urban canopy parameterizations is to simulate real cities where heat fluxes from city surfaces are present, this effect must be studied and parameterized.

Recently, Santiago et al. (2014) has investigated the effect of a realistic unstable thermal stratification on the microscale flux within an idealized urban-like layout, demonstrating the modification of the flow properties with the solar angle and the incoming radiation. The spatially averaged properties have also been studied, showing how the variation of the flow structure due to the presence of the buoyancy force modifies the drag coefficient.

In this chapter, the effect of unstable thermal stratification on the evolution of the drag coefficient and the vertical fluxes (e. g. turbulent and dispersive) of heat and momentum are investigated and a its parameterization is presented. The expected result, in addition to a deeper understanding of the physical mechanism responsible of the exchanges of heat and momentum between buildings and atmosphere, is an extension of the range of applicability of the scheme and an increase of its reliability. The tool used for this study is the RANS model used in chapter 2, in which the thermal stratification is introduced by applying realistic thermal fluxes from the urban surfaces as boundary conditions.

In the following sections, the modeling set-up is presented, the results are analysed and analytical formulae for the drag coefficient and the turbulent length scales as function of the thermal forcing are presented. In addition, an alternative parameterization for the vertical diffusion fluxes is proposed, considering the dispersive fluxes by means of an extension of *K*-theory.

2 This chapter is mainly based on Simon-Moral et al. (2015) (in preparation)

4.1. Set up of the simulations

In this study, the results presented in Santiago et al. (2014) are used as starting point for the study of the influence of unstable thermal stratification on the evolution of the drag coefficient, the turbulent length scales and the vertical diffusion fluxes.

The RANS model (STARCCM+, a commercial code from CD-Adapco, 2012) (see Sect. 2.3) is used to simulate an aligned array of cubes with $\lambda_p = \lambda_f = 0.25$, which is in the range of the typical packing density of real urban areas (Grimmond and Oke, 1999). In order to simulate the unstable thermal stratification, realistic heat fluxes from the urban surfaces resulting from solar heating have been calculated by the TUF3D model (Krayenhoff and Voogt, 2007) and imposed as boundary conditions in each urban surface in the RANS model.

The array is defined parallel to the cardinal directions and the flow is imposed in the direction of the x – coordinate (Fig. 2.3). Periodic conditions are considered at the four lateral boundaries in order to simulate an infinite array. The domain top is defined at $4H$, being H the height of each cube, which is appropriate to simulate the flow within and above the canopy (Coceal et al. 2006).

As top boundary condition, a downward flux of momentum (ρu_τ) is imposed in order to maintain the flow, being u_τ the friction velocity, related with the pressure gradient from the momentum equation (Eqs. 2.22 and 3.3). This mechanical forcing is applied at the top of the domain and not in the whole vertical as the cases analyzed in chapter 2. This approach ensure that the vertical flux of momentum is constant with height above the canopy, a typical behaviour often observed in the inertial sub layer. Since the simulations are for steady state, ρu_τ^2 can be seen also as the total flux of momentum lost by the flow because of the drag induced by the buildings. For the thermal boundary condition a θ_{ref} is fixed on the top, inducing an upward heat flux out of the domain equal to $k_{eff}(\theta_{ref} - \theta)/\Delta z$ being k_{eff} the eddy conductivity for heat at the top of the domain and Δz is the depth of the top cells.

The surface heat fluxes are distributed with a resolution of $H/16$ in each direction of the cube, thus having 16x16 points in each building surface.

Several scenarios with different solar positions and ratios of buoyant to inertial imposed forces have been simulated as explained in Santiago et al. (2014). The seven solar positions considered are for solar zenith angles of ±60º, ±45º, ±30º and 0º which, during a solar equinox at the Equator, correspond to 0800 (1600), 0900 (1500), 1000 (1400), 1200 h local solar time (LST). The different ratios of buoyant to inertial imposed forces simulated for each solar position are characterized by an adimensional number H/L_{urb}, being L_{urb} a stability length scale, defined, in analogy to the Obukhov

length, as:

$$L_{urb} = \frac{u_\tau^3}{\left(\frac{g}{T_{ref}} \frac{Q_h}{\rho C_p} \right)} \qquad (4.1)$$

where Q_h is the total heat flux (W m^{-2}) from all urban surfaces divided by the plan area and C_p is the specific heat of the air.

The different ratios of buoyant to mechanical forces simulated (H/L_{urb}) are 0, which represents the neutral case, 0.4, 0.75, 1.13, 1.5, 2.25 and 3. For the analysis of the results, the wind velocity is normalized with u_τ, $\langle k \rangle$ with u_τ^2 and the difference between the temperature at the top of the domain and the temperature in the domain is normalized by:

$$\frac{Q_h / \rho C_p}{u_\tau} \qquad (4.2)$$

With this normalization, the results for a given H/L_{urb} but different u_τ and Q_h, produce equivalent results, thus, this adimensional number is appropriate to characterize the same configuration with different ratios of buoyant to inertial forces (Santiago et al. 2014).

The neutral case compares satisfactorily with a direct numerical simulation (Santiago et al. 2013; not shown here).

4.2. Mechanisms for vertical transport

In this section the mechanisms responsible for the vertical transport of heat and momentum are analyzed based on the results of the RANS model. As shown in Section 2.2 (Eq. 2.4), the vertical transport can be split in three components: the mean, the turbulent and the dispersive transport, although in our assumption of zero mean vertical velocity, only the turbulent and dispersive fluxes are considered.

For a flow over an homogeneous terrain the vertical transport is mainly driven by turbulent transport, which, as shown in Eq. 2.9, can be parameterized by the *K*-theory. Nevertheless, when dealing with a flow over heterogeneous terrain, as is the case of an urban area, both the turbulent and the dispersive fluxes can be important for vertical transport. Despite this, the dispersive flux has been neglected in many studies.

The dispersive fluxes for heat and momentum are averaged over all solar zenith angles, analyzed and compared with the turbulent fluxes for the different values of H/L_{urb}. The reason for the use of

the solar averaged values is that the flow averaged properties have low dependency on solar zenith angle (Santiago et al. 2014) and because we prefer to keep the parameterization as simple as possible. In Fig. 4.1 the “solar position averaged” vertical fluxes of heat and momentum for the H/L_{urb} 1.5 case are shown. The reason for the election of this case is that the intensity of the heating is high enough to significantly modify the thermal stratification of the flow. As shown in the figure, the dispersive fluxes for both variables are comparable to the turbulent fluxes. At the same time, the profile of the vertical gradient of both fluxes is also plotted as these are the relevant terms in the Eqs. 2.5 and 2.15, showing, also, comparable values and demonstrating the necessity of taking both fluxes into account. Focusing on the vertical derivatives of the heat fluxes, it is interesting to note that the sign of the derivatives of the turbulent and dispersive have opposite sign in the whole canopy layer. In particular, the derivative of the dispersive is positive (meaning a negative contribution in the temperature equation) in the lower part, and negative in the upper part. These results suggest that the dispersive mechanisms may be quite relevant for the redistribution of the heat exchanged with the walls in the urban canopy – probably more than for the momentum, as in the latter, the total flux is closer to the Reynolds flux than in the case of heat.

Following Eq. 2.3 and taking into account the zero mean vertical velocity, the dispersive flux for a generic variable ψ can be expressed as:

$$\langle \tilde{w}\,\tilde{\psi}\rangle = \langle |\bar{w}-\langle \bar{w}\rangle|\,|\bar{\psi}-\langle \bar{\psi}\rangle|\rangle = \langle \bar{w}\,\bar{\psi}\rangle - \langle \bar{w}\langle \bar{\psi}\rangle\rangle = \langle \bar{w}\,\bar{\psi}\rangle - \langle \bar{w}\rangle\langle \bar{\psi}\rangle = \langle \bar{w}\,\bar{\psi}\rangle \qquad (4.3)$$

Therefore, the fluxes for both momentum and heat depend on the spatially averaged value of the product of the time mean value for vertical velocity and the time mean value of the momentum or temperature, respectively.

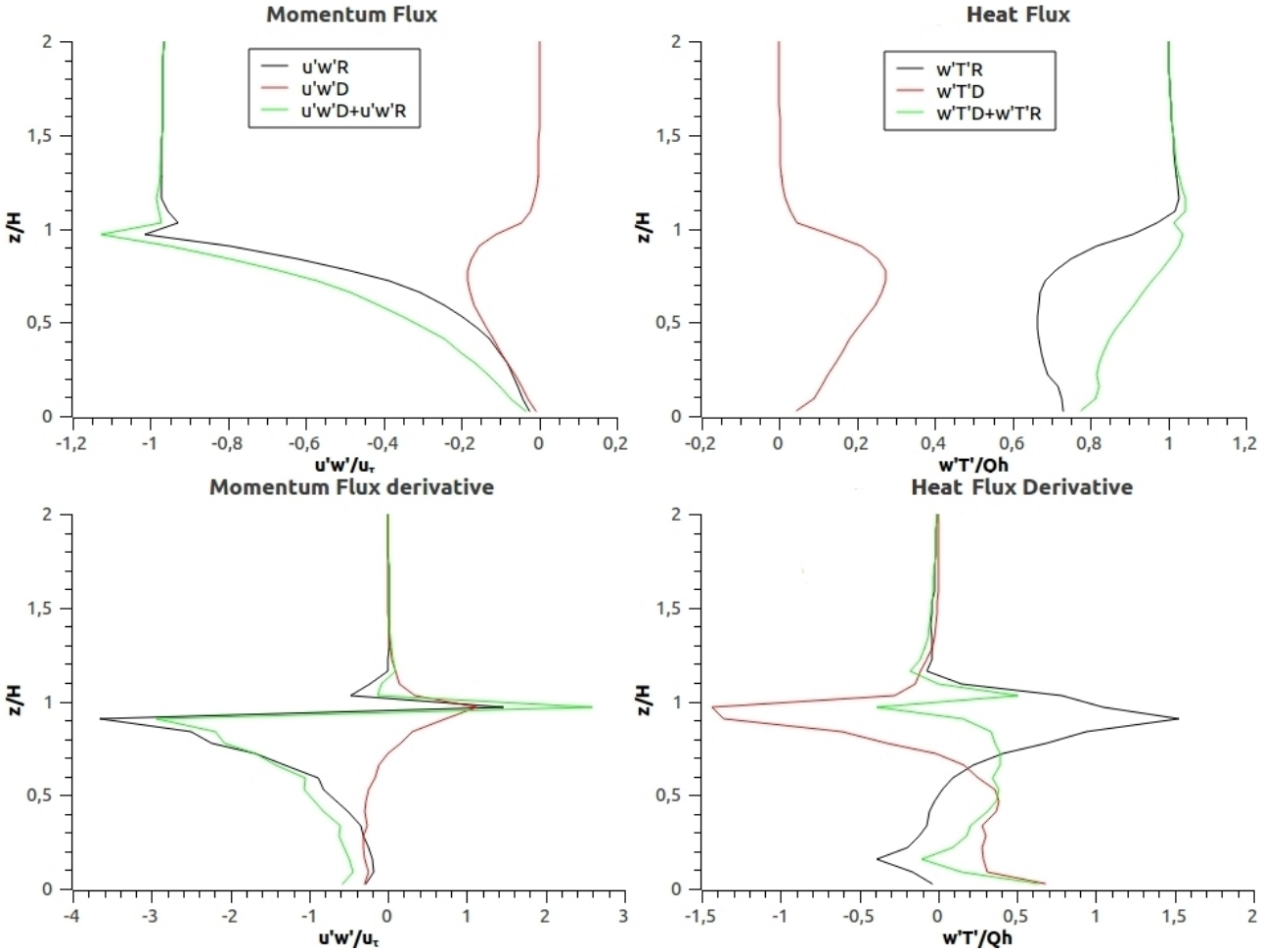

Figure 4.1: Solar position averaged values of the dispersive and turbulent fluxes and its derivatives of the vertical fluxes of momentum and heat for the H/L_{urb} = 1.5 case. R represents the turbulent flux and D the dispersive flux.

In Fig. 4.2, the vertical profiles of the dispersive fluxes of heat and momentum for each H/L_{urb} are plotted. As shown for the momentum dispersive flux (Fig. 4.2a), a displacement towards negative values is observed when the heat flux is increased (H/L_{urb}>0). This negative values are understood as a downward transport of fast air and an upward transport of slower air, increasing the vertical mixing inside the canopy. This effect is not linear, as the maximum transport is observed for H/L_{urb} = 1.13, decreasing towards lower absolute values for higher heat fluxes.

The dispersive flux of heat (Fig. 4.2b) shows positive values for every H/L_{urb}. Taking into account that the heat flux comes from the heated solid surfaces, a positive dispersive flux represents an upward flux of heat, which, as in the momentum case, also enhances vertical mixing. As before, the absolute value of the flux is not linear with the heat flux from the urban surfaces, showing a relation with the maximum absolute value of the momentum flux.

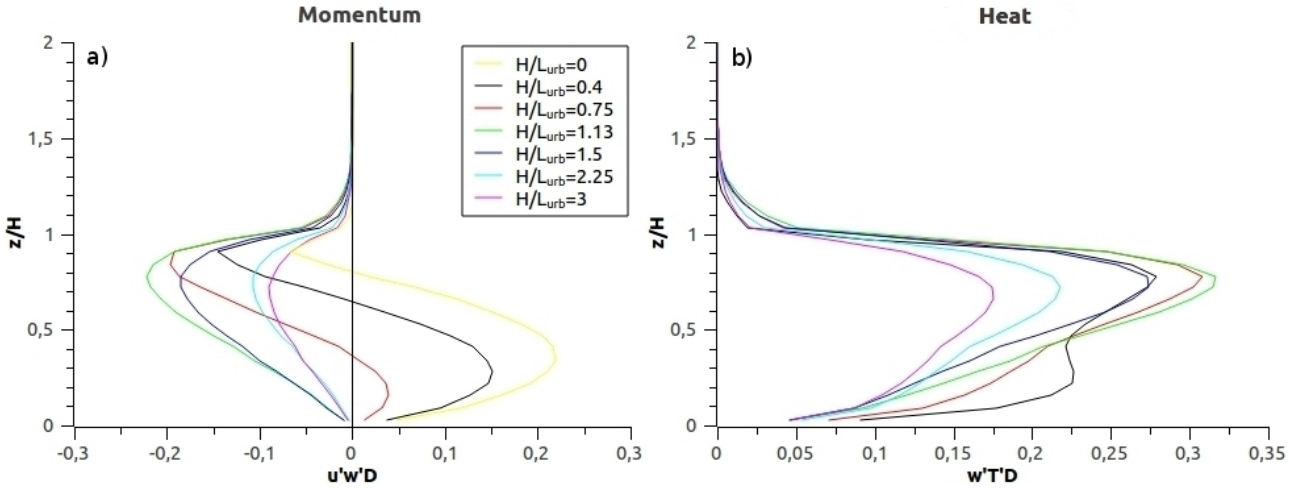

Figure 4.2: Solar position averaged values of the dispersive fluxes of momentum and heat for each H/L_{urb} case

From the point of view of a mesoscale model (e. g. with resolution much coarser than building dimensions) the subgrid vertical fluxes are parameterized with the *K*-theory. This method calculates the vertical flux as the product of the gradient of the transported variable multiplied by a diffusion coefficient (Eq. 2.9). Since the diffusion coefficient, defined in Eq. 2.10, is positive, in order to apply this method, the flux must be downgradient.

As shown in Fig. 4.2a, in the case of momentum, the dispersive flux can be either positive or negative so it is not possible to apply the *K*-theory for its representation. Nevertheless, the total flux (Fig. 4.3) (sum of the dispersive and the turbulent fluxes) is downgradient for all the cases, allowing its parameterization by means of the *K*-theory. In the case of the heat, both the turbulent and the dispersive flux are downgradient. The following equation is suggested for the subgrid fluxes:

$$\langle uw\rangle_{total}=\langle\overline{u'w'}\rangle+\langle\tilde{u}\tilde{w}\rangle=-K_M\frac{\partial\langle\bar{u}\rangle}{\partial z}$$
$$\langle w\theta\rangle_{total}=\langle\overline{\theta'w'}\rangle+\langle\tilde{\theta}\tilde{w}\rangle=-K_H\frac{\partial\langle\bar{\theta}\rangle}{\partial z} \qquad (4.4)$$

The diffusion coefficients K_M and K_H are parameterized within a *k-l* closure scheme by Eq. 2.10, where, as it will be described in the next section, we hypothesize that the length scale is the same for all the variables, being the differences between the diffusion coefficients driven by the differences in the C_k coefficients. Therefore, in this study the dispersive flux is introduced in the *K*-theory by a variation of the coefficient C_k in Eq. 2.10, which depends on the variable corresponding to transport equation. The unique length scale is estimated from the RANS results as:

$$l = C_\varepsilon \frac{\langle k \rangle^{3/2}}{\langle \varepsilon \rangle} \qquad (4.5)$$

Following the equations 2.10 and 4.5, the C_k coefficients are calculated from the RANS results as follows:

$$C_{k_m} = \frac{-\langle uw \rangle_{total}}{\frac{\partial \langle \bar{u} \rangle}{\partial z} \cdot C_\varepsilon \cdot \frac{\langle k^2 \rangle}{\varepsilon}}$$
$$C_{k_h} = \frac{-\langle w\theta \rangle_{total}}{\frac{\partial \langle \bar{\theta} \rangle}{\partial z} \cdot C_\varepsilon \cdot \frac{\langle k^2 \rangle}{\varepsilon}} \qquad (4.6)$$

In order to calculate the values for C_{km} and C_{kh}, as before, the results averaged over all solar zenith angles are used.

For every ratio of buoyant to inertial forces, a mean value for the coefficients inside the canopy and another over the canopy are computed. As shown in Table 1, while inside the canopy there is some variation with H/L_{urb}, over the top of the buildings the coefficients are mainly constant and show nearly the same value. For simplicity, inside the canopy, mean values equal to 0.15 and 0.2 for the momentum and heat diffusion, respectively, are chosen, while, over the canopy, a constant value of 0.13 for both variables is considered rewriting Eq. 2.10 as:

$$K_M = C_{k_m} l \langle k \rangle^{1/2} = 0.15 \cdot l \langle k \rangle^{1/2}$$
$$K_H = C_{k_h} l \langle k \rangle^{1/2} = 0.2 \cdot l \langle k \rangle^{1/2} \qquad (4.7a)$$

$$K_M = K_H = 0.13 \cdot l \langle k \rangle^{1/2} \quad (z/H > 1) \qquad (4.7b)$$

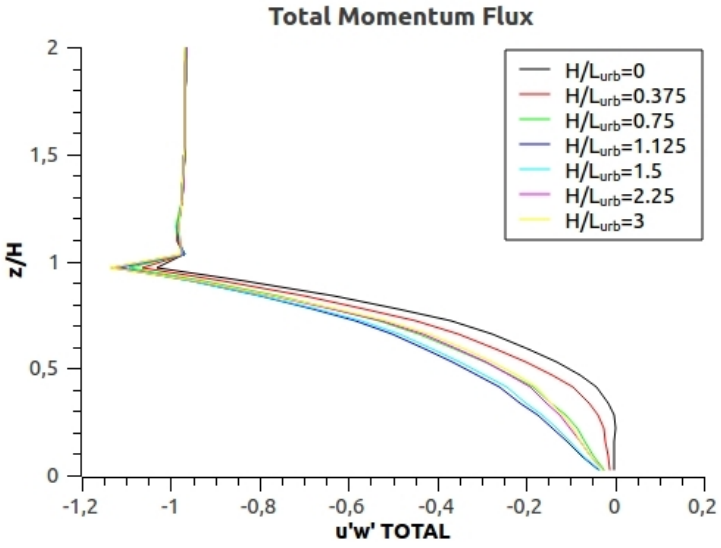

Figure 4.3: Solar angle averaged value of the total vertical flux of momentum

Table 4.1: Values for the coefficients C_{km} and C_{kh} inside and above the canopy

	Inside Canopy			Above canopy		
H/L_{urb}	C_{km}	C_{kh}	C_{km}/C_{kh}	C_{km}	C_{kh}	C_{km}/C_{kh}
0.38	0.097	0.210	0.480	0.131	0.115	1.14
0.75	0.145	0.233	0.626	0.131	0.128	1.02
1.125	0.226	0.198	0.887	0.131	0.130	1.01
1.5	0.180	0.177	1.02	0.131	0.133	0.98
2.25	0.135	0.207	0.661	0.130	0.132	0.99
3	0.126	0.199	0.642	0.130	0.130	1

4.3. Length Scales

Several parameterizations are found in the literature for the calculation of the length scales involved in turbulent transport and turbulence dissipation for neutral cases within urban areas (Santiago and Martilli 2010; Simón-Moral et al. 2014). Nevertheless, after the analysis of the results presented in Santiago et al. (2014), some changes are found in the values of the length scales, when a unstable stratification is investigated. In order to account for the variation due to thermal stratification, as introduced before, we hypothesize a unique length scale to be multiplied by a different coefficient for each of the process where it is involved. This unique length scale is estimated with Eq. 4.5, by using the averaged results from the RANS model.

The analysis of the length scale shows a positive dependency inside and above the street canyon with the variation of the value of the H/L_{urb} parameter (Fig. 4.4). This result is related with the increase of the buoyancy force, which increases the vertical transport of the meteorological variables.

In order to extract a simple parameterization, and following the idea of Santiago and Martilli (2010) or Simón-Moral et al. (2014), the values of l are divided in two vertical zones, according to its behaviour, where we hypothesize the relation:

$$\begin{aligned} l &= \alpha_1 (H - d); z/H \leqslant 1 \\ l &= \alpha_1 (z - d); z/H > 1 \end{aligned} \qquad (4.8)$$

where α_1 is a function of the H/L_{urb} parameter, defined as:

$$\alpha_1 = \alpha_{1_0} \cdot f\left(H/L_{urb}\right) \quad (4.9)$$

being α_{1_0} the value for the neutral case simulation (H/L_{urb} = 0) and d, the displacement height from the neutral case, equal to 0.81 (= $\lambda_p^{0.15}$) (Simón-Moral et al. 2014).

The values of α_1 are calculated for each H/L_{urb}, considering the averaged value of l inside the canopy from the spatially-averaged results from the RANS model calculated with Eq. 4.5 (note that l is considered constant inside the canopy). With this results, the function f(H/L_{urb}) is defined by the use of linear regression techniques, resulting in:

$$\begin{aligned} l &= \left(0.391 \cdot \left(H/L_{urb}\right)+1\right) \cdot \alpha_{1_0} \cdot \left(H-d\right), for\ z/H \leqslant 1 \\ l &= \left(0.391 \cdot \left(H/L_{urb}\right)+1\right) \cdot \alpha_{1_0} \cdot \left(z-d\right), for\ z/H > 1 \end{aligned} \quad (4.10)$$

In Fig. 4.5 a comparison of the RANS model and the parameterized values for the length scale is shown.

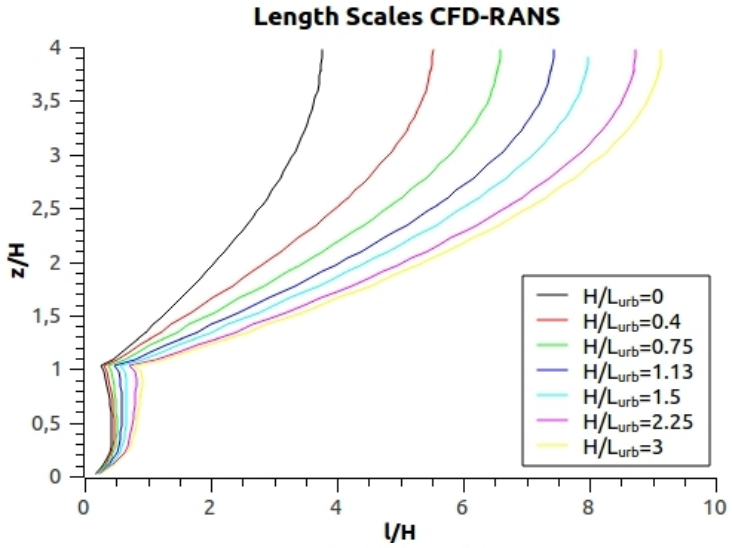

Figure 4.4: Solar position averaged vertical profile of the length scale

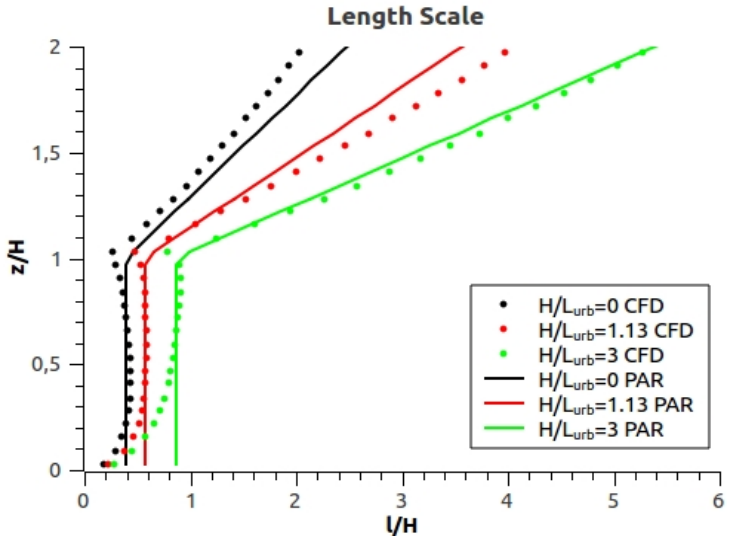

Figure 4.5: Comparison between the solar position averaged length scale and its parameterization. CFD represents the profiles calculated from the RANS model and PAR the parameterizations

4.4. Drag coefficient

In previous studies, parameterizations for the sectional drag coefficient used in Eqs 2.7 and 2.14 by means of the configuration and height of the obstacles within the domain have been presented (Santiago and Martilli 2010; Simón-Moral et al. 2014). In addition, in Santiago et al. (2013a) the influence of wind direction over C_{deq} has been shown. These parameterizations have been deduced from neutral cases, but, when the solar radiation is introduced, a dependency with the heat intensity and the solar angle is found (Fig. 4.6) (Santiago et al. 2014). In this study, a modification of the sectional drag coefficient as a function of H/L_{urb} is proposed. Although the solar angle also contributes to the sectional drag coefficient variation, its effect over the spatially averaged meteorological variables is lower than the effect due to the variation of H/L_{urb} (Santiago et al, 2014), and hence neglected in this study.

Following Santiago and Martilli (2010) the sectional drag coefficient is computed for all the simulations with Eq. 2.31 from the RANS averaged results, calculating, for each H/L_{urb}, the solar angle-averaged value. As seen in Fig. 4.6 the solar angle averaged C_{deq} is relatively constant up to H/L_{urb} approximately equal to 0.7-0.8 and increases almost linearly up to 3.5 for H/L_{urb} = 3. With this behaviour in mind, the following parameterization is proposed:

$$\begin{aligned} C_{deq} &= C_{deq0}\,; for\ H/L_{urb} \leqslant 0.838 \\ C_{deq} &= \left(A \cdot H/L_{urb} + B\right) \cdot C_{deq0}\,; for\ H/L_{urb} > 0.838 \end{aligned} \qquad (4.11)$$

where C_{deq0} refers to the neutral case (= 0.7849), the values for A and B, equal to 1.67 and -0.4, respectively, are calculated by a linear regression. The limit between the different vertical behaviours of C_{deq} has been calculated also by linear regression techniques. A comparison of the RANS and the parameterized results is showed in Fig. 4.7.

Note that these results have been deduced from a configuration with λ_p equal to 0.25. The dependency with H/L_{urb} and the relation with the neutral case should be investigated for different packing densities and obstacle arrangements.

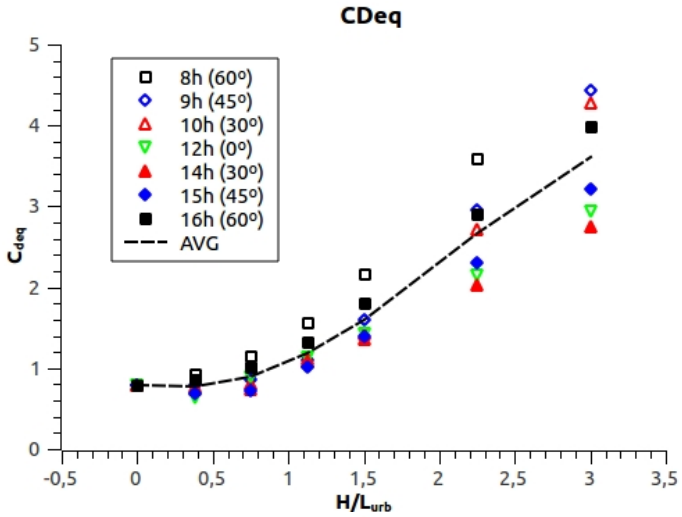

Figure 4.6: C_{deq} calculated for each H/L_{urb} and solar angle and the solar position averaged value.

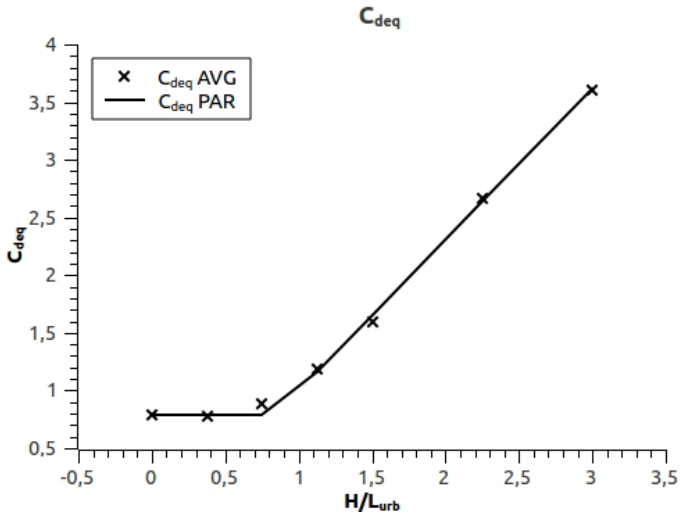

Figure 4.7: Solar position averaged value of the C_{deq} and its parameterization

4.5. Implementation of the parameterizations in the column model

The developed parameterizations presented for the total flux (dispersive plus turbulent), the length scales and the drag coefficient are implemented in the column model presented in Sect. 2.2. The effect of the heat fluxes is represented in the column by adding a source term in the temperature equation at each level derived from the TUF3D heat fluxes imposed in the RANS simulation, averaged over all the sun directions and over all the RANS grid cells in each vertical layer. The changes are implemented one-by-one and compared in order to evaluate the relative importance of each feature and the sensibility of the model.

Four versions of the parameterization are compared: The old one (OLD), where the drag coefficient and the length scales are those of the neutral case (e. g. there is no dependency with H/L_{urb}), a

version where only the drag coefficient variation with H/L_{urb} is taken into account (CDnew), a third one, where only the length scale and diffusion coefficients are affected by the change in H/L_{urb} (LengthNEW), and a version in which the changes on the drag coefficient, the length scales and the diffusion coefficients are taken into account (NEW).

The vertical profiles of the wind speed, the turbulent kinetic energy and the temperature are plotted in Figs. 4.8 to 4.10, respectively, for H/L_{urb} equal to 1.125, 1.5, 2.25 and 3 and compared with the RANS results averaged in all solar zenith angles. Results for H/L_{urb} lower than 0.75 are not plotted because, as the drag coefficient is not affected by the buoyancy force (Eq. 4.11), they give less information about the parameterization improvements.

Concerning the wind speed, the main differences inside the street canyon are driven by the differences in the drag coefficient, although its connection with higher levels by the vertical transport of momentum is also important. As can be observed in Fig. 4.8, CDnew simulation, with the same drag coefficient than NEW simulation, has lower values for the wind speed inside the canyon because of the lower vertical mixing of momentum, mainly determined by the lower length scales (Eq. 2.10), which in this case are not affected by the H/L_{urb} parameter, taking into account that the only source of momentum is at the top. In addition, this lower wind speed produces lower TKE values, which generates lower vertical mixing. Over the top of the buildings, the magnitude of the wind speed is mainly determined by the vertical transport of momentum. Higher length scales enhance vertical mixing, decreasing the wind speed in higher levels due to the mixing with the lower wind speed within the urban canopy. When comparing simulations with same length scale as NEW and LengthNEW, the same profile shape is observed. In this case, a constant difference, depending on the magnitude of the drag coefficient, is showed for the whole profile. This difference increases with H/L_{urb} due to the increase of the difference in the C_{deq} values.

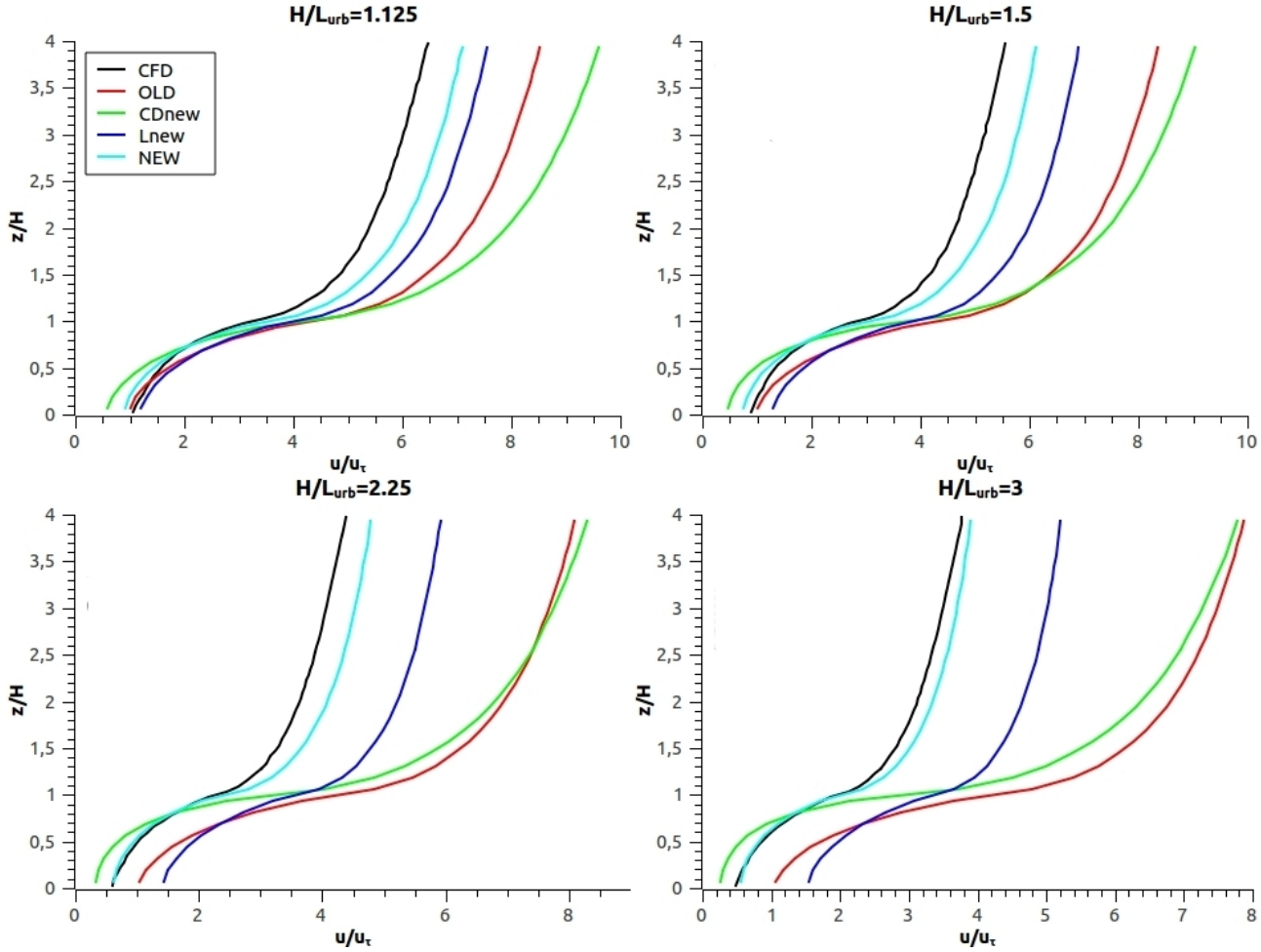

Figure 4.8: Verical profiles of the solar position averaged value of the wind speed for H/L_{urb} = 1.125, 1.5, 2.25 and 3

The turbulent kinetic energy is plotted in Fig. 4.9. The production term due to interactions with the buildings is proportional to the cube of the wind speed and the drag coefficient. An increase of the latter increases the turbulent production, but, at the same time, decreases the wind speed, with the opposite effect. As shown in the figure, in all the cases the higher values correspond to the LengthNEW simulation, which also has the higher values for the wind speed. The lowest values correspond to the CdNEW case, that, although has higher values of C_{deq}, has the lowest values of the wind speed.

In Fig. 4.10 the vertical profile of the temperature is presented, which mainly depends on the vertical mixing. As explained, the vertical transport of any variable is determined by the magnitude of the length scales and the $<k>$. For all the values of H/L_{urb}, inside the canopy, the lower the length scale and the $<k>$, the higher the temperature.

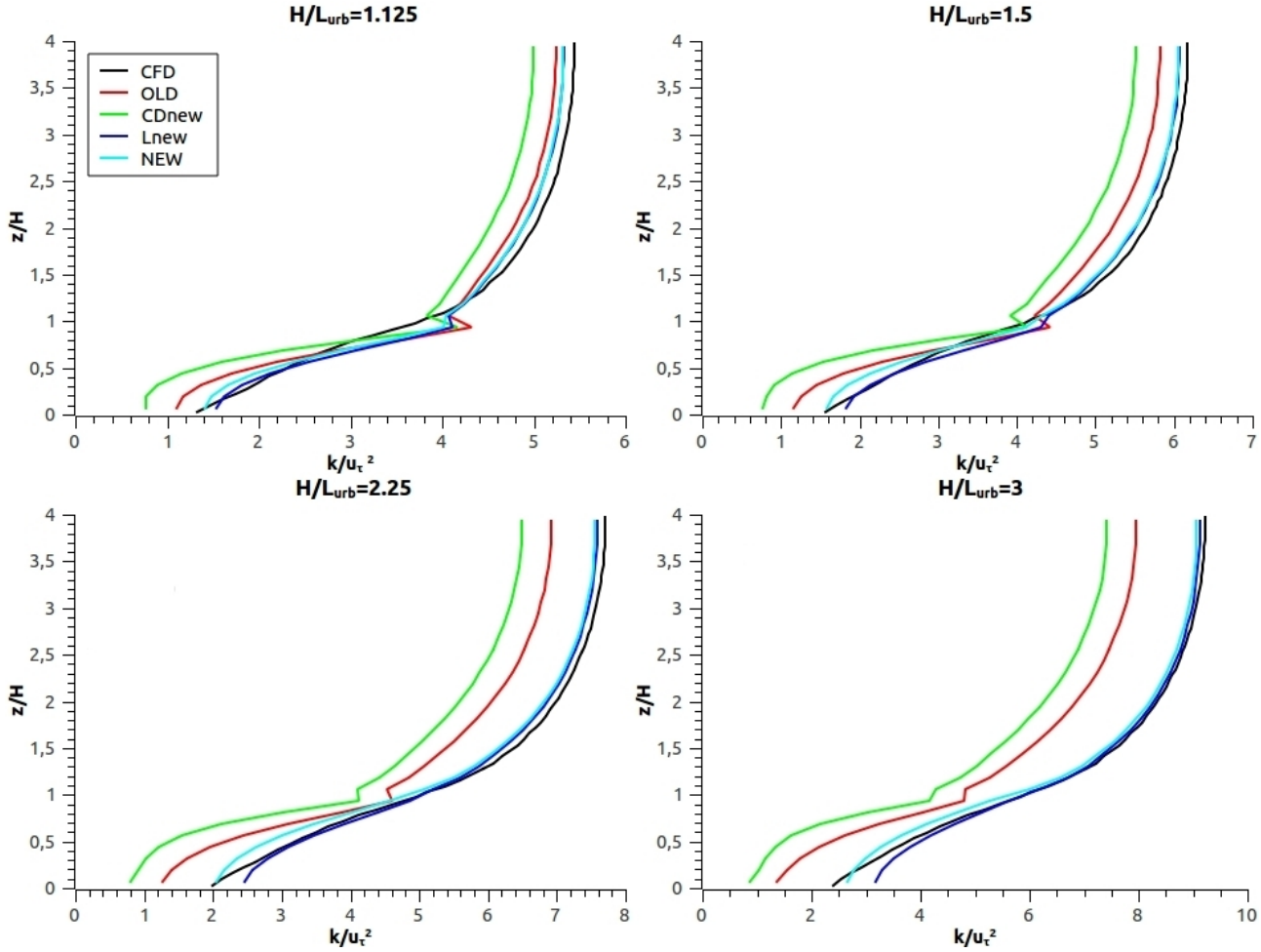

Figure 4.9: Verical profiles of the solar position averaged value of the turbulent kinetic energy for H/L_{urb} = 1.125, 1.5, 2.25 and 3

In order to detect the main processes in the evolution of the meteorological variables, the *RMSE* is calculated for the wind speed, the temperature and the turbulent kinetic energy, by the use of Eq. 3.8a. The *RMSE* is calculated inside and above the street canyon and the results are averaged for all the values of H/L_{urb}, in order to capture the general skill of each model. The results are presented in Fig. 4.11.

Inside the canyon (Fig. 4.11a) the wind speed results show larger errors for the LengthNEW and OLD simulations, indicating that the main process affecting the wind inside the canyon is the drag force caused by the buildings, for which a good estimation of the drag coefficient is needed. Concerning the temperature, vertical mixing with the air above the canopy seems to be the most important mechanism, as the larger errors are found for the models not considering the modification of the length scales by H/L_{urb}. The turbulent kinetic energy, although depends on both drag coefficient and length scale, shows better skills for the simulations with improved length scales,

thus vertical mixing appears to be more important than the drag force on the turbulence calculation. Following the same analysis for the results above the canyon, we can conclude that the main mechanism driving the three variables studied is the vertical mixing, as the simulations with improved length scales show better results than the ones not taking into account the H/L_{urb} modification. This is coherent with the fact that the perturbations to the flow are produced inside the canopy and transported upwards. In the case of the wind speed, as expected, the drag force affects the profile above the canyon, showing lower values of the *RMSE* in the case of the NEW simulation.

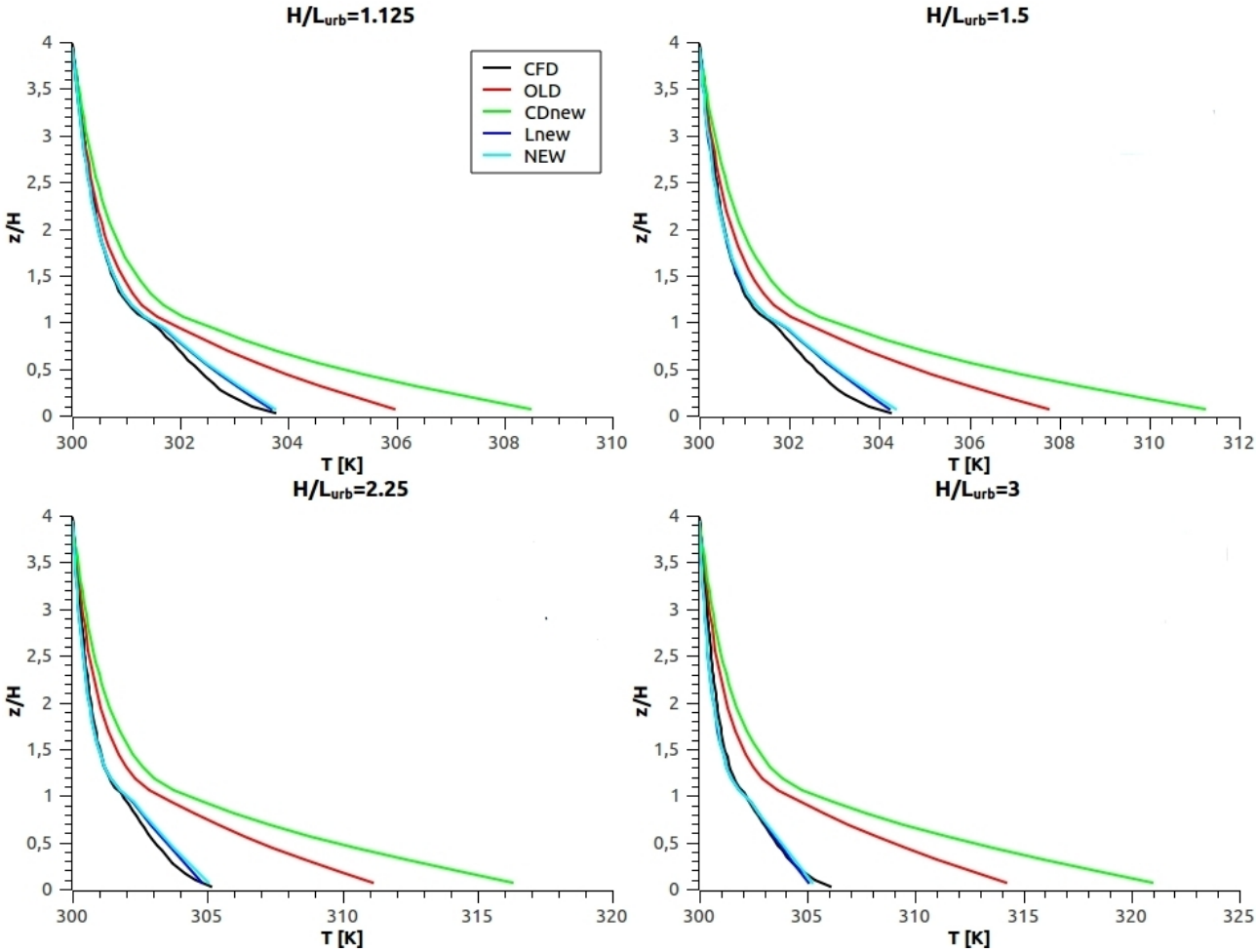

Figure 4.10: Verical profiles of the solar position averaged value of the temperature for H/L_{urb} = 1.125, 1.5, 2.25 and 3

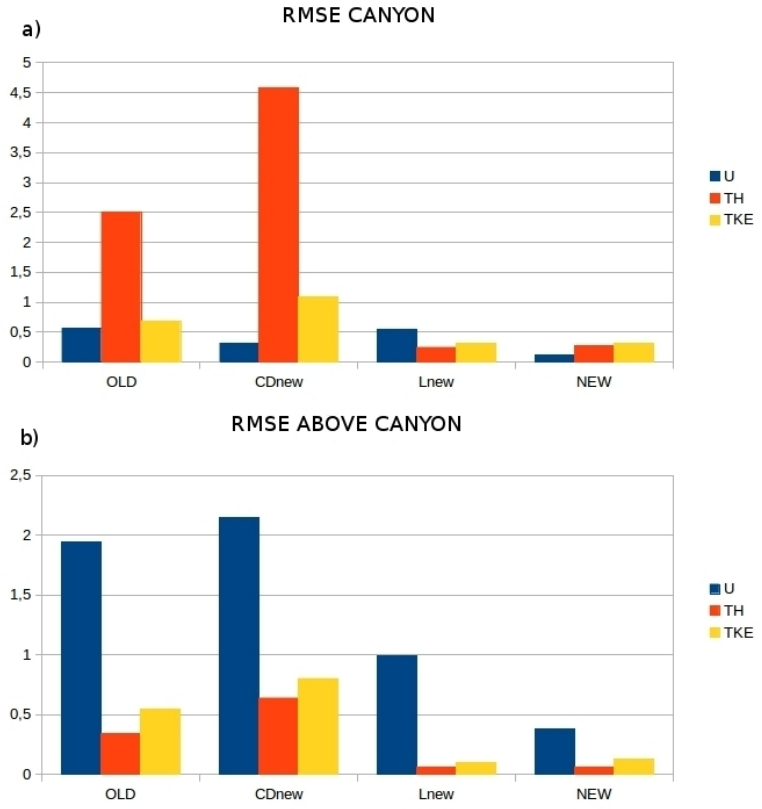

Figure 4.11: *RMSE* for *U*, *T* and *k*, inside and over the urban cayon, for the 4 different models

4.6. Summary and conclusions

In this chapter the effects of unstable thermal stratification on the evolution of the drag coefficient, the turbulent length scales and the vertical transport fluxes have been studied from RANS simulation. The main results can be summarized as follows:

- The increase of the dispersive fluxes have shown the need to take them into account within mesoscale models. Therefore, they have been parameterized by an extension of the *K*–theory, accounting simultaneously for both the turbulent and the dispersive fluxes.
- The increase of the turbulent length scales related with the presence of a buoyancy force has also been parameterized. An approach has been derived, considering a unique length scale.
- Different values for the vertical diffusion coefficient, depending on the variable vertically transported have been observed. These differences have been calculated by defining different coefficients for each variable in the diffusion coefficient calculation.
- An increase of the drag coefficient due to the increase of the buoyancy force have been

shown and parameterized.

- The previous results have been implemented in an urban canopy parameterization and compared between each other and with the RANS model results
- Within the canopy, the drag coefficient have appeared to be more important in the wind speed modification while the turbulent length scales show more importance for the temperature and turbulent kinetic energy calculation.
- Over the canopy, the length scales seem to be more important in every variable calculation.

It is important to note that these results are obtained for aligned arrays with λ_p = 0.25. More experiments have to be done in order to extend these conclusions for different building arrangements. On the other hand, this is the first attempt of parameterization of the effect of stability on drag coefficient and length scale, and of the representation of the dispersive fluxes. Results are very promising, and they already represent an advance compared to previous approaches and can constitute the starting point for future refinements and generalizations.

5. New technique for UCP and mesoscale coupling

The parameterizations developed in chapters 3 and 4 are implemented in the BEP (Martilli et al. 2002) based column model presented in Sect. 2.2 and coupled within the full 3D mesoscale model WRF. In addition, a new technique of coupling the column model within the three dimensional model is introduced. This technique allows an increase of vertical resolution within the urban canopy without increasing the computational time.

As it has been described in chapters 3 and 4, microscale models have been used for the definition of averaged properties for mesoscale modeling. These improvements increase the degree of detail of the characterization of the urban morphology effects on the atmosphere. While the microscale and the column models used for these studies use a vertical resolution of 1 m, a typical mesoscale vertical grid has a resolution of 40 – 50 m near the ground, thus, in order to take advantage of the high resolution improvements, the vertical resolution of the mesoscale model should be increased. This problem drives us to the research question of this chapter, *how can we properly simulate the vertical profiles of the the averaged microscale properties within a mesoscale model without increasing the computational time?*

This question is particularly relevant, because typical high resolution mesoscale simulations over urban areas may have a ratio between CPU time and simulated time of 1:2-1:3 (it means that to simulate 2-3 days, you need 1 day of CPU[3]), depending on the cluster used. With this set-up, the simulation of long periods, needed for climate studies, or air quality assessment, becomes very time consuming and in many cases impossible without reducing the resolution.

The aim of this chapter is to present a new technique to couple a UCP within a mesoscale model which allows an increase of the resolution in the canopy, without increasing the number of mesoscale levels. The advantage of this technique is twofold. First, it allows a better representation of the city morphology, accounting for its effects on the atmosphere, and taking full advantage of the detailed improvements presented in the previous chapters and, on the other hand, it allows a decrease of the number of mesoscale vertical levels (decrease of the resolution), with a consequent decrease of the computational time both through a decrease of the number of points and an increase of the time step (reduce the constrain on the CFL condition).

3 These times are estimated based on a spatial resolution of less than 1km, vertcial resolution of 5m close to ground, and 240X270X50 grid points, for the Euler cluster of CIEMAT.

5.1. BEP scheme

The BEP urban canopy parameterization (Martilli et al. 2002) is based on a high resolution urban grid, coupled within a coarser resolution mesoscale model, which communicate between each other in every time step. A scheme of the calculation process is presented in Fig. 5.1.

First, at each time step, the meteorological variables are interpolated from the coarse resolution grid to the high resolution urban grid (Point 2 in Fig. 5.1). With the new meteorological values, the momentum, heat and turbulent fluxes produced by the urban obstacles are calculated within the high resolution urban grid with the equations presented in Sect. 2.2 (Point 2 in Fig. 5.1). These fluxes are interpolated to the grid of the mesoscale model, where the new meteorological values are calculated by the resolution of a diffusion equation (Points 3 and 4 in Fig. 5.1).

One important feature to consider is that the high resolution urban grid has no memory, this is, is not able to memorize the values of the meteorological variables between time steps. In addition, the urban high resolution signal is diffused within the coarser resolution model, loosing the increase of urban physics detail obtained by techniques as the one presented in Chapter 2.

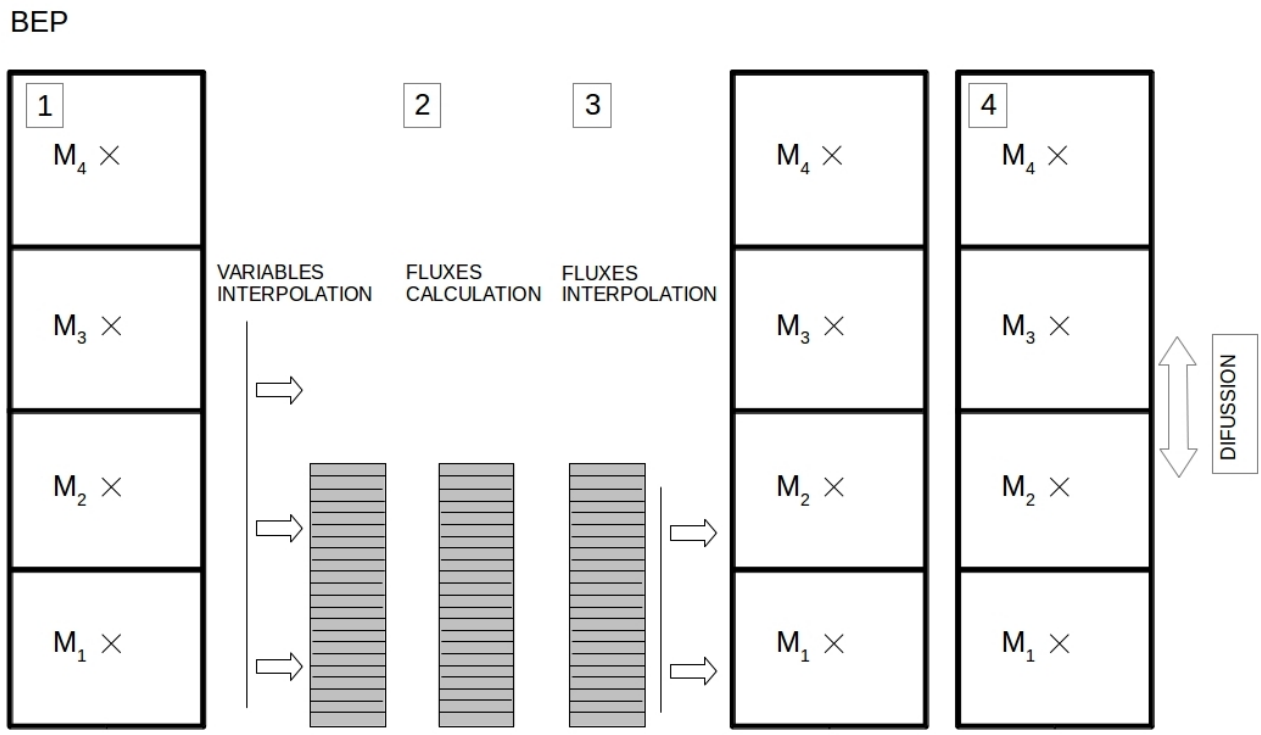

Figure 5.1: Calculation scheme for the BEP model

5.2. BEPCOL scheme

In order to increase the accuracy and resolution of the BEP urban canopy parameterization, without increasing the computational cost, some changes are introduced in the calculation process of the meteorological variables and the coupling of the urban and the mesoscale models. As the BEP scheme, BEPCOL is based on a high resolution urban grid coupled within a coarser resolution mesoscale model, communicating in every time step between each other. In this case, both the forcing and the calculating method are changed from the previous version of the scheme. The calculation process is presented in Fig. 5.2.

5.2.1. Forcing

In the new version of the scheme, the set of metereological variables (wind, temperature, and k) are computed in the urban grid by solving the equations described in Sect. 2.2, with a forcing at the top of the urban grid, which is set at two times the height of the buildings (Point 1 in Fig. 5.2). In each time step, the temperature, the wind speed, and the humidity are forced by an interpolation from the two closest levels of the mesoscale grid and the turbulent kinetic energy is forced by an inverse weighted average. The air density and the pressure are interpolated in the whole urban grid, as in BEP scheme, because no perturbations to these variables are calculated inside the urban canopy. The forcing signal is transmitted downward by vertical diffusion, modifying the urban variables, which are memorized from the previous time step.

This technique to force the scheme increases the accuracy of the urban results because the urban information is retained in every time step instead of being replaced from the mesoscale low resolution grid.

5.2.2. Calculation process of the urban meteorological variables

In the BEPCOL scheme, the new values of the meteorological variables are calculated in the high resolution urban grid by solving a diffusion equation with the heat, momentum and turbulent kinetic energy fluxes calculated from the interaction with the urban surfaces (Point 2 in Fig. 5.2). These fluxes are calculated by the equations presented in Sect. 2.2 in which the improvements on the drag

coefficient (Eqs. 2.7 and 2.14), the length scales (Eqs. 2.10 and 2.12) and the vertical fluxes of momentum and heat (dispersive and turbulent fluxes in Eqs. 2.5 and 2.15) parameterizations presented in chapters 3 and 4 are introduced

The new urban values are then interpolated into the mesoscale grid, where a diffusion equation is calculated from the top of the urban grid upwards, in order to compute the mesoscale meteorological fields. In addition, heat, momentum and turbulent kinetic energy fluxes calculated in the urban model are introduced from the top of the urban grid as lower boundary conditions for the mesoscale calculations (Points 2 and 3 in Fig. 5.2).

Calculating both the fluxes and its diffusion in the high resolution mesh, increases the accuracy of the model, as less information is lost during the interpolation and calculation process, capturing more efficiently the vertical variability of the urban areas. In addition, as the variables are retained within the urban grid, they can be extracted as output from the model, providing accurate results inside the canopy regardless of the mesoscale resolution. This is an important feature, as it allows a decrease of the mesoscale resolution and the number of vertical levels and thus a decrease of the computational time.

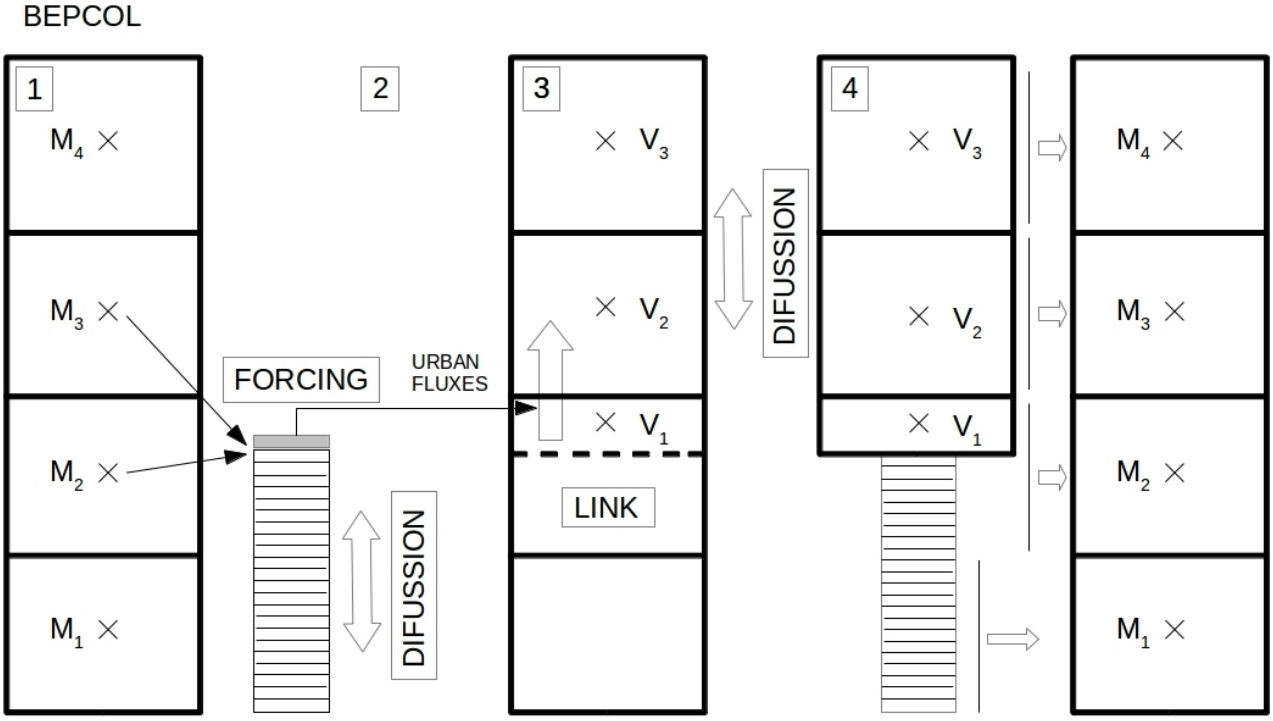

Figure 5.2: Calculation scheme for the BEPCOL model

5.2.3. Mesoscale calculation

In order to introduce the urban signal into the calculation of the mesoscale variables, the mesoscale grid is divided in three parts (Fig. 5.2):

- Urban canopy: The mesoscale cells with vertical limit equal or lower than the top of the urban high resolution grid.
- Link cell: The below portion of the mesoscale cell cut by the urban grid top.
- Virtual grid: A grid defined from the top of the urban grid to the top of the mesoscale grid. The lower cell is the above portion of the mesoscale cell cut by the urban grid top.

The results from the urban high resolution grid are interpolated into the urban canopy part of the mesoscale grid and the link cell. In addition, the urban fluxes of heat, momentum and turbulent kinetic energy at the top cell of the urban grid are introduced as lower boundary conditions in the virtual grid in order to compute a diffusion equation. The new values of the mesoscale meteorological variables are then assigned as follows:

- On the urban canopy part of the mesoscale grid, the variables are interpolated/averaged from the urban grid.
- The value in the mesoscale cell cut by the urban grid top limit is calculated by a weighted average between the link cell value and the value in the first cell of the virtual grid.
- Over the cut cell, the values are those of the virtual grid.

5.3. Urban morphology

In order to calculate the urban fluxes of heat, momentum and turbulent kinetic energy, the urban morphology must be simplified. Attending on the buildings distribution and characteristics, the urban areas are represented by different urban classes, each of them defined by buildings with the same thermal properties and the same size and distribution inside the domain, that is, with the same buildings and streets morphological parameters. As a typical mesoscale horizontal grid is not able to distinguish where and how the individual buildings are distributed or its height, for each urban class, these parameters are simplified. In this model, the distribution and heights are calculated by means of four morphological parameters; the frontal area density, λ_f, the packing area density, λ_p

(defined in Grimmond and Oke, 1999), the mean height and the ratio between the distance between buildings in the directions of the buildings axes W_x and W_y, gamma, defined as:

$$\lambda_p = A_p / A_T \qquad (5.1)$$

$$\lambda_f = A_f / A_T \qquad (5.2)$$

$$\gamma = W_x / W_y \qquad (5.3)$$

where A_p is the plan area of the buildings in a grid cell, A_f is the sum of the areas of all the vertical surfaces and A_T is the total area of the grid cell. Note that λ_f is defined differently from the one used previously.

The urban canyon geometry taken into account when calculating the momentum and the turbulent kinetic energy is a regular array of cubes. As showed in Fig. 5.3a, for these cases, aligned configurations of buildings are considered. However, for the calculation of the temperature and the heat exchange, the classical bidimensional analysis, with quasi infinite urban canyons is considered (Fig. 5.3b). This choice is done mainly to avoid the complex calculation of view factors in 3D, and also because for many urban types, a 2D approach for radiation is a good approximation of reality (Martilli, 2009) . In both cases the same λ_p and λ_f are considered.

For the calculation of the radiation trapping and shadowing, in which a 2D approach is considered, the width of the street, with the assumption that the frontal area density in x and y directions is the same, can be calculated as:

$$W_y = \frac{1-\lambda_p}{1+\gamma}\frac{4h_{mean}}{\lambda_f} \qquad (5.8)$$

$$W_x = \gamma W_y \qquad (5.9)$$

The width of the streets and buildings, needed for the estimation of the λ_s, and λ_{ch} parameters, are calculated considering a 3 dimensional approach:

$$B_x = \frac{4h_{mean}\lambda_p}{\lambda_f} \qquad (5.10)$$

$$B_y = B_x \qquad (5.11)$$

$$W_y = \frac{\left(-\beta-\sqrt{\delta}\right)}{2\gamma} \qquad (5.12)$$

$$W_x = \gamma W_y \qquad (5.13)$$

where

$$\beta = B_x(\gamma + 1) \qquad (5.14)$$

$$\omega = B_x^2 - \frac{4 B_x h_{mean}}{\lambda_f} \qquad (5.15)$$

$$\delta = \beta^2 - 4\gamma\omega \qquad (5.16)$$

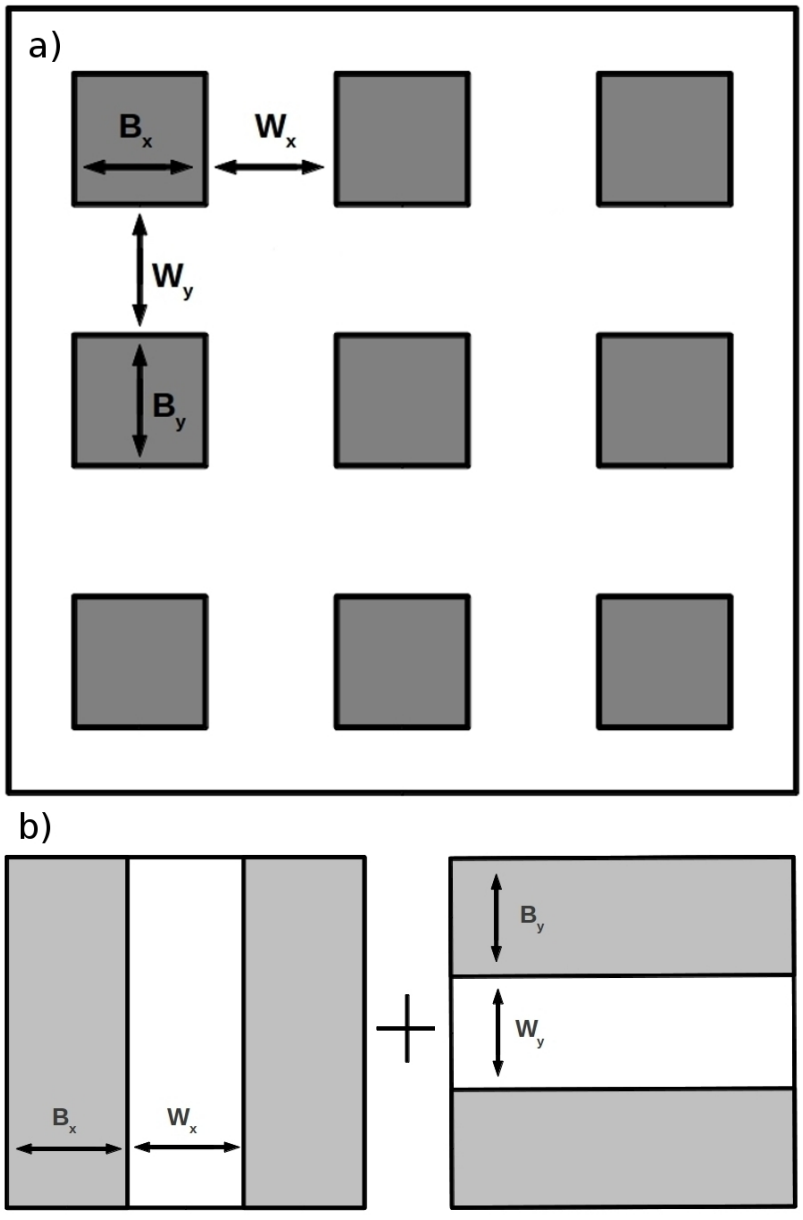

Figure 5.3: Simplification of the urban morphology for the a) 3D analysis and the b) 2D analysis

Note that the dimensions of the buildings and the streets are different for the 2D and 3D analysis. This is an improvement from BEP scheme because it adds the possibility to differentiate between *x* and *y* direction (two directions perpendicular between each other) and to use the approach described in chapter 3 to estimate the drag coefficients.

5.4. Simulation set-up.

In order to test and compare the new version of the urban canopy parameterization, an idealized city is simulated with both versions of the model (BEPCOL and BEP). The domain, presented in Fig. 5.4, consists of a rectangular surface of 200 x 4 cells in the *x* and *y* direction, respectively, with a rectangular city located in the middle of the domain (from the cells 91 to 110 in *x* – direction), surrounded by vegetation both up and downwind. The urban area is characterized by values of λ_p = 0.25, λ_f = 1, γ = 1. All the buildings have an height of 16m.

Different mesoscale vertical grids are used with each version of the model in order to test the sensibility of the results and the computational time required in each case. The mesoscale vertical grids used are defined by a first level at 10, 20, 30, 40 and 50 meters, and 48, 26, 24, 22 and 21 vertical levels, respectively. For the urban mesh, the same grid with 16 vertical levels with a constant resolution of 2 m is used in every simulation.

The idealized city is located at 45º N and 0º W and the simulated period goes from the 21st March 2007 at 06:00 am to the 22nd March of 2007 at 12:00 pm. An initial value for the wind speed of 3 m/s in the *x* direction is considered.

Figure 5.4: Domain for the UCP simulations. The grey area represents the idealized city and the green area, the sourrounding vegetation

5.5. Results

5.5.1. Vertical sections

The vertical sections of temperature and wind speed at 12h and 00h from the results of BEP and BEPCOL are presented in Figs. 5.5-5.8.

As shown, during the day (Fig. 5.5), an increase of temperature compared to the rural sourounding area is observed in both schemes, being slightly higher for BEPCOL. At the same time, an increase of temperature is also observed downwind the city, due to the advection effect. This increase is the same for both schemes.

At night (Fig. 5.6) the same effect is observed. An increase of the temperature inside the city and downwind. In this case, the temperature inside the city increases in the flow direction, also due to the advection effect. As inthe previous case, the temperature is higher in the BEPCOL scheme.

Concerning the wind, during the day (Fig. 5.7), a decrease of the speed is observed in both versions of the scheme, being higher in BEPCOL. A little wake is also observed just behind the city in both cases. At night (Fig. 5.8), the same behaviour is observed, with lower wind speed inside the city and higher above, probably due to the lower vertical mixing existing at this time of the day. A wake is also generated behind the city, althoug farther than in the 12h case.

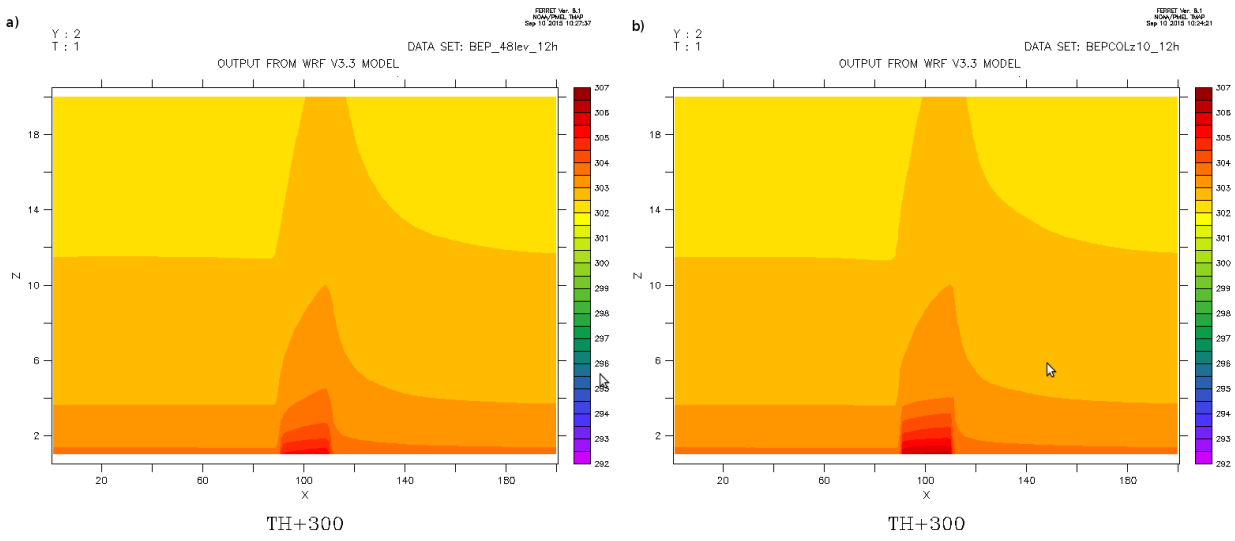

Figure 5.5: Vertical section of temperature [K] at 12h from a) BEP results and b) BEPCOL results

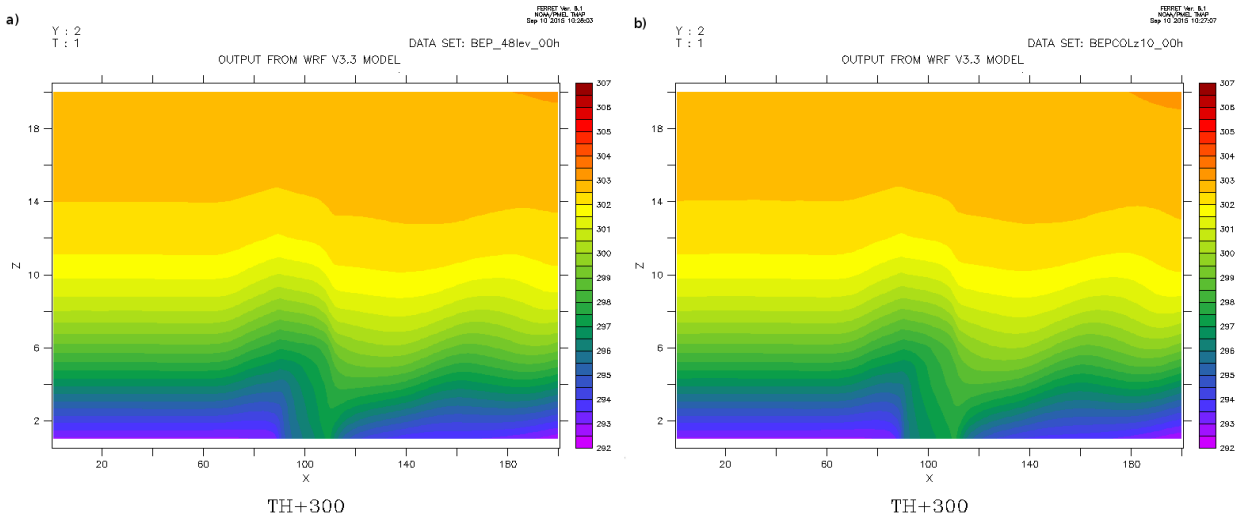

Figure 5.6: Vertical section of temperature [K] at 00h from a) BEP results and b) BEPCOL results

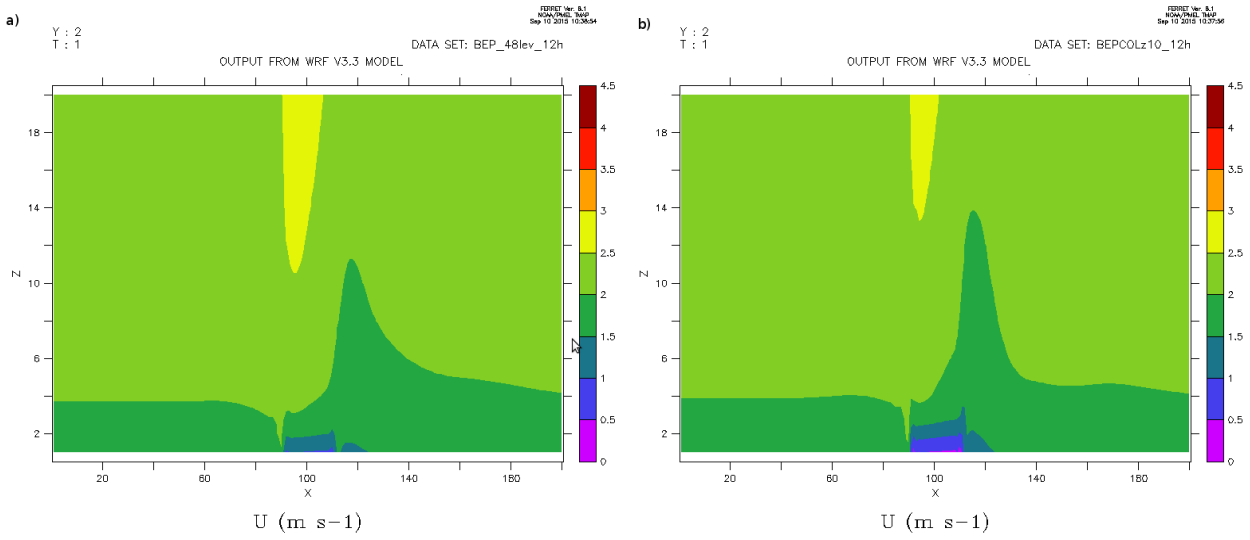

Figure 5.7: Vertical section of wind speed [m/s] at 12h from a) BEP results and b) BEPCOL results

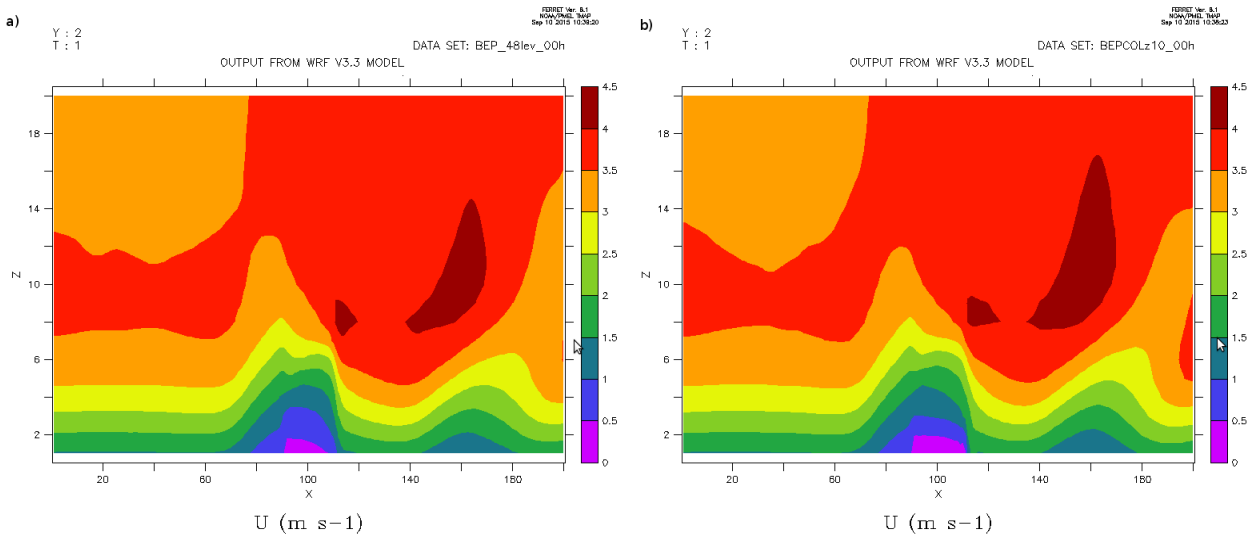

Figure 5.8: Vertical section of wind speed [m/s] at 00h from a) BEP results and b) BEPCOL results

5.5.2. High resolution urban results

As presented before, the BEPCOL scheme is able to produce high resolution results without having high resolution in the mesoscale vertical grid. As shown in Fig. 5.9, with this version of the urban scheme, it is possible to have the vertical profile of the meteorological variables up to two times the height of the obstacles, which is approximately the height of the roughness sublayer, regardless of the mesoscale vertical grid. This feature allows to decrease the resolution of the mesoscale model, providing more resolution than the BEP scheme. This increase of the urban resolution allows to take advantage of the improvements of the UCP developed with the high resolution RANS results.

In Fig. 5.10 the vertical profiles from the z_1 = 10 m and the z_1 = 50 m simulations of the urban grid results for the temperature, the wind speed and the turbulent kinetic energy are shown for 12h, 18h and 00h. Small differences are observed inside and above the canopy.

Concerning the temperature, the same profiles shape is observed regardless of the mesoscale vertical resolution grid. This result is very important considering the buoyancy force for the turbulent kinetic energy production and the stability of the first layers of the atmosphere.

As in the case of the temperature, the wind speed also shows the same profiles inside the canopy, although small differences are observed above the height of the buildings at 00h.

The turbulent kinetic energy shows larger differences than the previous variables, however, the profiles are conserved between simulations. The largest differences are observed over the canopy, especially in the 00h case, although at this time of the day the values are very small.

These results can be very useful for the study of the thermal confort and the air quality inside the city, allowing a microscale study inside the street canyons coupled with the regional meteorological variability.

Figure 5.9: Vertical profiles of temperature at 12h for BEP and BEPCOL, for the $z_1 = 10$ and $z_1 = 50$ simulations. COL represents the high resolution results from the urban grid.

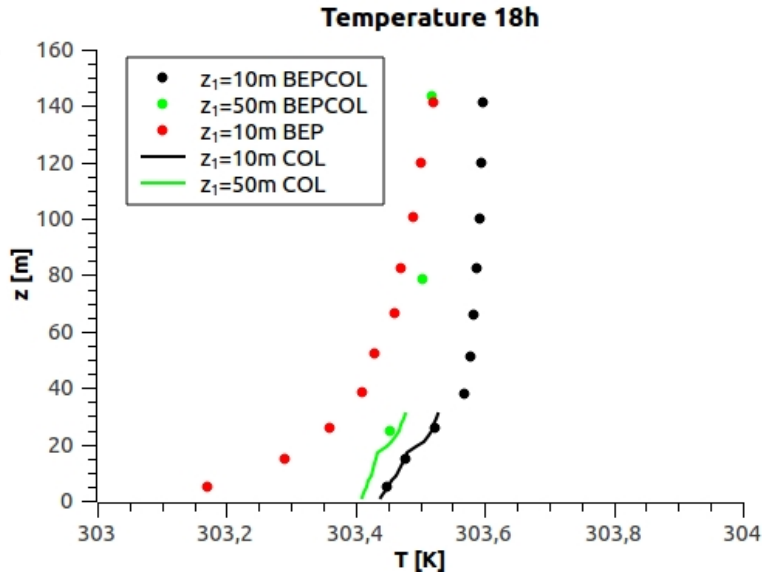

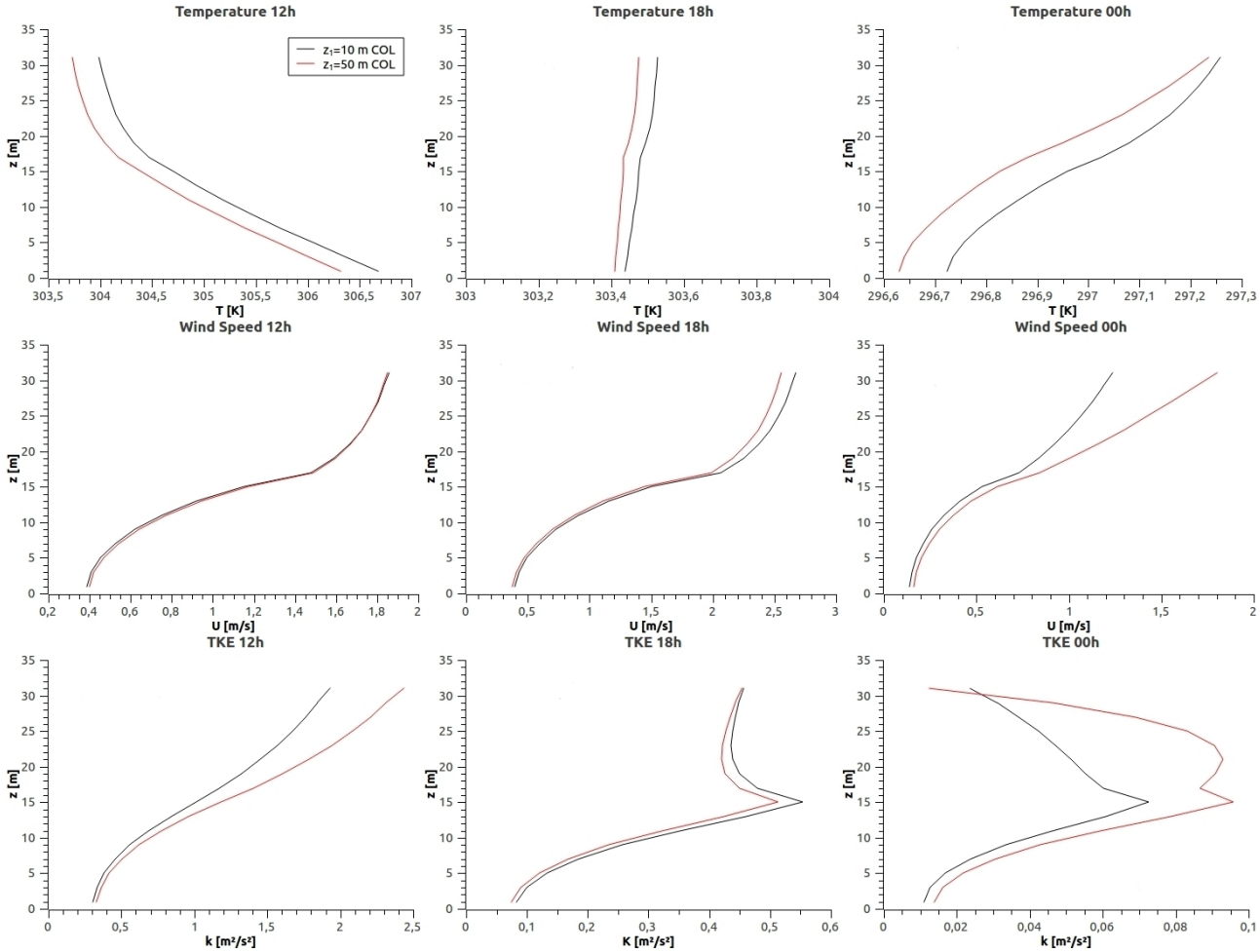

Figure 5.10: Comparison of the urban vertical profiles of temperature, wind speed and turbulent kinetic energy at 12h, 18h and 00h for the $z_1 = 10$ m (black) and $z_1 = 50$ m (red) simulations

5.5.3. Computational time

In this section, the time taken by the z_1 = 10 m and z_1 = 50 m simulations by both BEP and BEPCOL is compared (Table 5.1). As observed, BEPCOL simulations are slower than the ones performed by BEP, However, as shown in previous sections, the small sensitivity of the results with the variation of the vertical mesoscale grid and the possibility of having high resolution results in the roughness sublayer, allows to decrease the number of mesoscale levels and thus decrease the computational time.

Therefore, as we can obtain mostly the same roughness sublayer results with the z_1 = 50 m simulation, taking the time values from Table 5.1, the computational time can be decreased by a 38%. Furthermore, even if not tested in this case, the use of a lower vertical resolution may allow an increase of the timestep, due to a less stringent CFL condition.

Table 5.1: Time taken for 1 hour of simulation by BEP and BEPCOL schemes

	BEP	**BEPCOL**
z_1 = 10 m	12'02”	13'26”
z_1 = 50 m	5'18”	7'32”

5.5.4. BEP vs BEPCOL comparison.

The results for the temperature, wind speed and turbulet kinetic energy of both versions of the urban scheme are compared in this section for 12h, 18h and 00h. The vertical profiles of the meteorological variables for the z_1 = 10 m simulation, as well as the diffusion coefficient are presented. Two main differences exist between both versions of the model. The mesoscale and urban models coupling technique which can produce differences in the highest levels of the urban grid and the physics of the urban canopy parameterization that can produce differences in the shape of the profiles. The high resolution results from the urban grid are refered as urban values, and as COL in the figures.

As observed Fig. 5.11, at 12h the temperature shows higher values in the case of the BEPCOL scheme in the first 35 m. This feature is related with a lower vertical mixing, process related with the dffusion coefficients. As explained, in the urban region, the meteorological variables are calculated by the urban scheme, by use of the urban diffusion coefficients. As observed in Fig. 5.12,

where the results of the high resolution urban grid (COL in the figure) are compared with the lower resolution BEP and BEPCOL grids, in the first 7 m, the urban diffusion coefficient (COL) is larger than the one calculated by BEP. From this height to 23 m, the opposite case is observed, and from 23 to 30m, again the urban coefficients are larger. The urban temperature (Fig. 5.12) profile is in close agreement with the relation between the urban diffusion coefficient and the one calculated by BEP, showing larger vertical mixing at the top of the urban grid (larger slope of the profile) and lower in the bottom part. The difference at the top of the urban grid between the BEPCOL profile and the urban one comes from the averaging process done for the link cell calculation, which average the urban results and the ones from the mesoscale grid (Sect. 5.2.3). It is interesting to note that in previous studies over real areas (Salamanca et al. 2011 over Madrid) the model BEP has shown a slight tendency to underestimate temperatures (positive mean bias). This technique can likely help to reduce this bias.

Concerning the wind speed, as observed in Fig. 5.11, the profile calculated by the BEPCOL scheme shows lower values than the one calculated by BEP. In this case, the drag coefficient used by BEPCOL is larger than the one used by BEP (C_{deq}(BEPCOL) = 0.785·f(H/Lurb) while C_{deq} (BEP) = 0.4), producing lower wind speed inside the canopy. The larger perturbation generated by drag effect is transmitted upwards, producing a gap between both profiles. Similarly to what mentioned above, previous tests have shown a tendency of WRF + BEP to overestimate wind speeds in urban areas, compared to measurements. These results may idicate a reduction of this effect with the new approach.

The analysis of the turbulent kinetic energy is not straightforward, as this variable depends on the wind speed magintude and its vertical shear, the buoyancy force and the drag coefficient. As seen in Fig. 5.11, the BEPCOL profile shows slightly lower values in the first 30 m. Although the drag coefficient is higher in BEPCOL scheme (positive contribution), the wind speed shows lower values (negative contribution), which in addition to the lower vertical diffusion, can produce lower values of *k*.

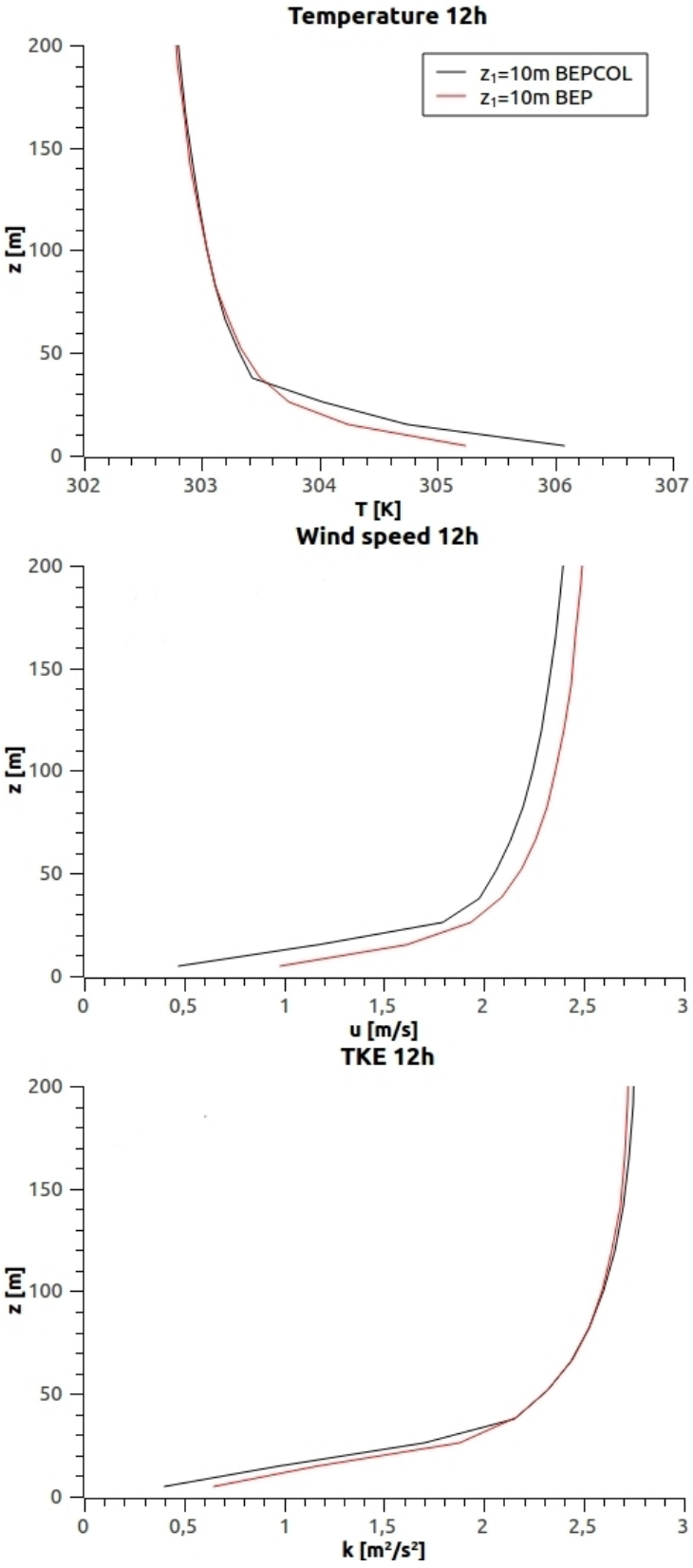

Figure 5.11: Vertical profiles of temperature, wind speed and turbulent kinetic energy at 12h, for BEPCOL (black) and BEP (red)

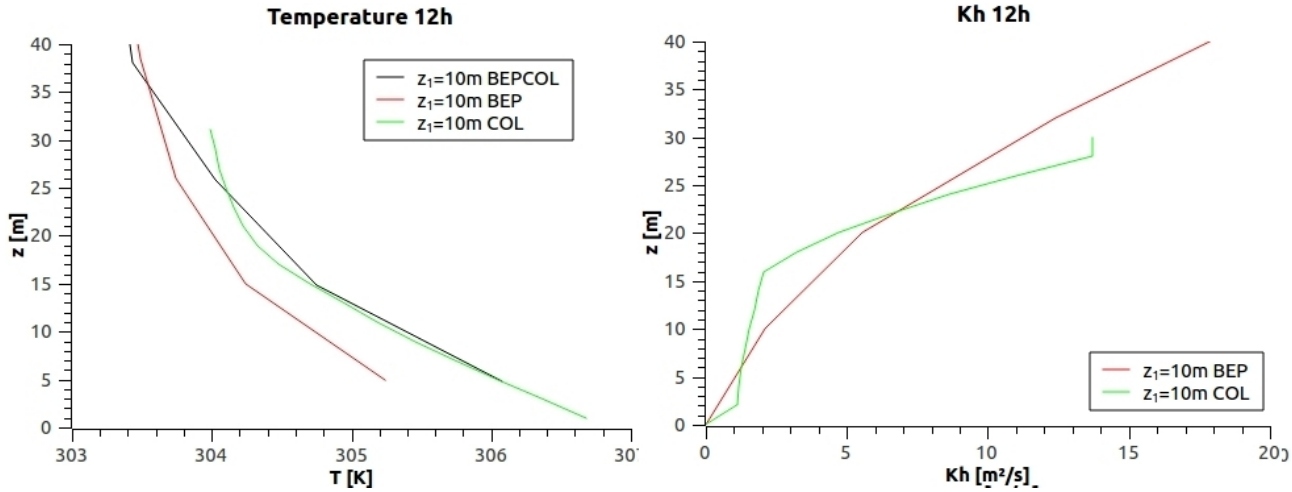

Figure 5.12: Vertical profile of temperature (left) and the diffusion coefficient (right) for BEPCOL (black), BEP (red) and COL (green), which represents the results within the urban high resolution grid, at 12h

Concerning the 18h profiles (Fig. 5.13), the differences in the diffusion coefficients observed at high levels of the atmosphere (Fig. 5.14), are in correspondance with the ones observed for temperature, which clearly determine the differences between BEP and BEPCOL, producing higher values in the latter. The wind speed, on the other side, shows lower values inside the canopy due to higher values of the drag coefficient and higher values from the top of the canopy region upwards. The turbulent kinetic energy shows lower values on the surface due to the lower values of the wind speed. On the other side, at higher levels, the higher temperature observed from 200 to 1400 m in BEPCOL produces higher turbulence production which can lead to higher values of the turbulent kinetic energy.

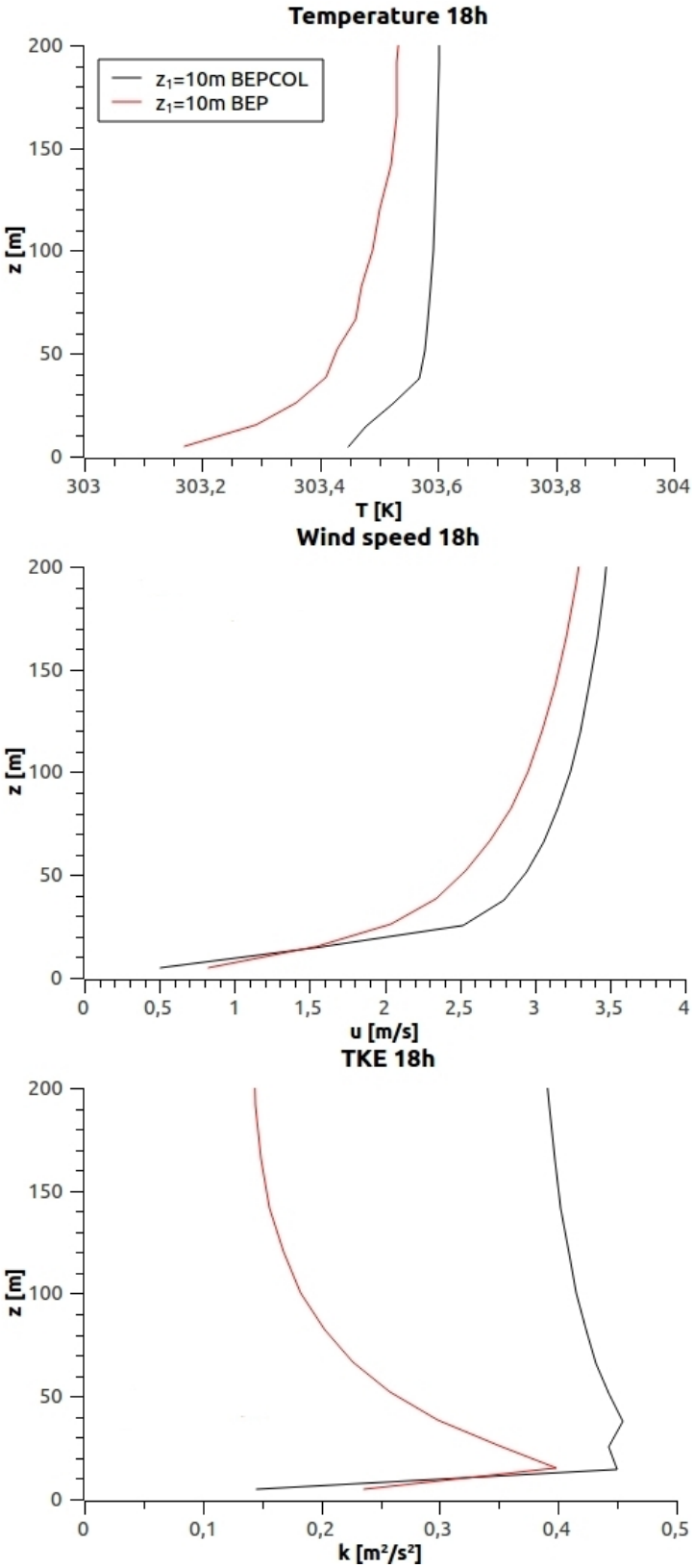

Figure 5.13: Vertical profiles of temperature, wind speed and turbulent kinetic energy at 18h, for BEPCOL (black) and BEP (red).

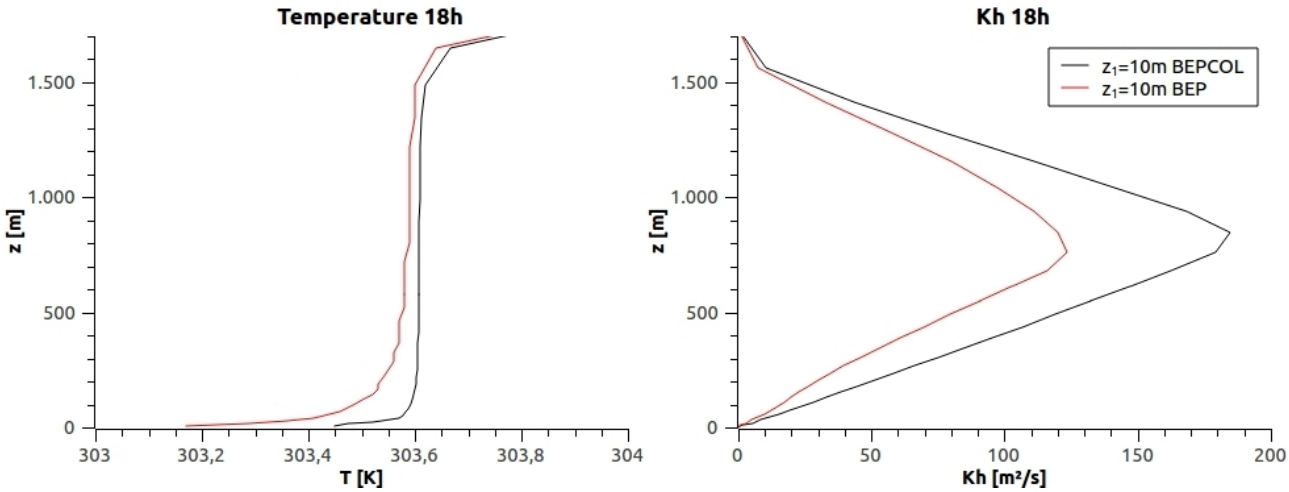

Figure 5.14: Vertical profiles of the temperature and the diffusion coefficient for BEPCOL (black) and BEP (red) at 18h

In the case of 00h (Fig. 5.15) although the BEPCOL scheme shows lower urban diffussion coefficients (Fig. 5.16) from the ground to the first 25 m, the ones calculated from this height to 70 m are much larger, thus producing higher vertical mixing and higher temperature values. The wind speed, although slightly lower near the ground, shows mainly the same values than the BEP ones, this is coehrent with the fact that the modifcation of the drag coefficients is larger during daytime (unstable conditons), than during night. Concerning the turbulent kinetic energy, both models produce very similar values, although a bit lower in the BEPCOL case, probably due to the slightly lower values of wind speed found.

The comparison of these results show that BEPCOL, in this case, produces higher values of temperature and lower values of wind speed and the turbulent kinbetic energy. The lower values of wind speed and the higher values of temperature could help to decrease the bias of the BEP results found in Salamanca et al. (2011). In the case of the wind speed, the results depend strongly on the drag coefficient value, which depends on the configuration of buildins. These results, at the same time, influence the values of turbulent kinetic energy inside the urban canopy.

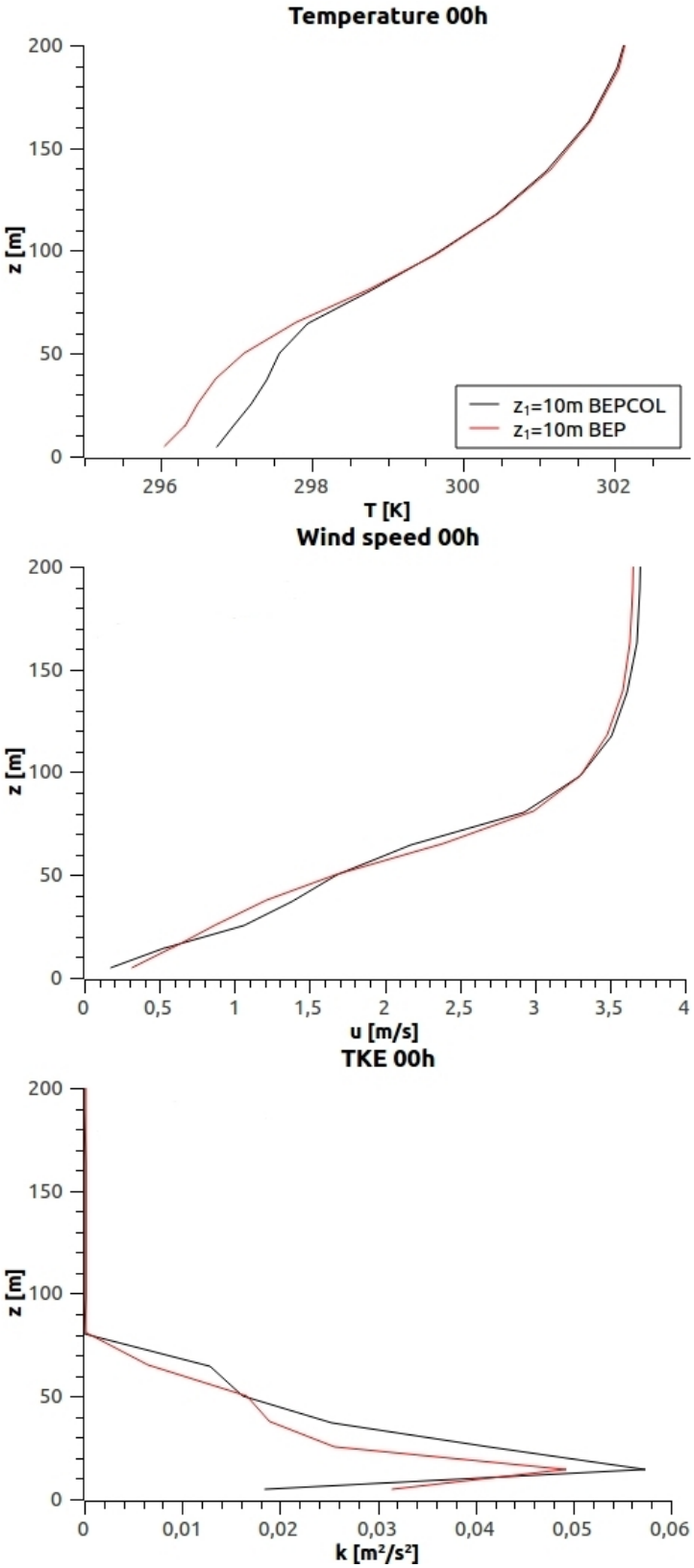

Figure 5.15: Vertical profiles of temperature, wind speed and turbulent kinetic energy at 00h, for BEPCOL (black) and BEP (red).

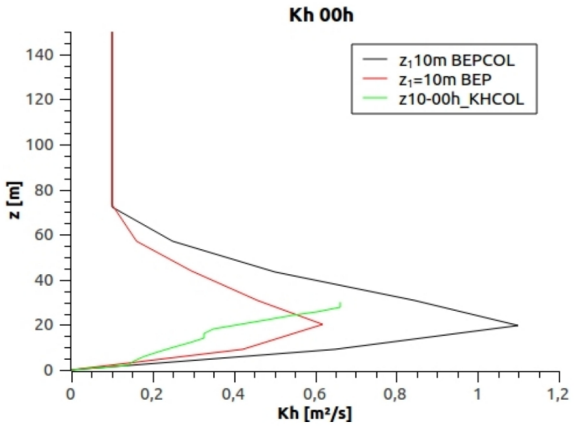

Figure 5.16: Verical profile of the diffusion coefficient for BEPCOL (black) BEP (red) and COL (green) at 00h

5.6. Summary and conclusions

In this chapter, the parameterizations developed in chapters 3 and 4 are implemented in a BEP based UCP, coupled with the full 3 dimensional mesoscale model WRF. In addition, a new technique to couple the UCP within the mesoscale model is presented, changing the forcing method and the urban variables calculation. The main results are summarized as follows:

- The new version of the model is forced at the top of the urban grid (roughly twice the mean building height) and calculates the urban meteorological variables within the urban grid, retaining the microscale properties of the city (as the developments presented in previous chapters) and increasing the accuracy of the UCP.
- The values of the meteorological variables are transmitted from one timestep to the other in each time step, allowing the microscale study of the city (accounting for the in-canyon variability), regardless of the mesoscale resolution. This result can be very useful for the study of the pollutants concentration, as having a detailed temperature, wind and turbulent kinetic energy profile inside the canopy can provide detailed calculations of the dispersion of the traffic emitted pollutants.
- Although the computational time is slightly increased, the increase of the urban resolution allows a decrease of the mesoscale resolution without loosing accuracy, and thus a decrease of the computational time up to 38%, when comparing a vertical grid with the first level at 10 m and 48 vertical levels with a vertical grid with the first level at 50 m and 21 vertical levels.

- The implementation of the drag coefficient developments allows a variation of the drag effect with the buildings configuration and the relation between the radiation and momentum forcing. This produces more realistic results and allows a differentiation between neighborhoods within the same city and different times of the day. In the case studied, the drag coefficient is increased respect to the BEP scheme, resulting in a decrease of the wind speed inside the urban canyon.
- The lenght scales parameterizations developed in previous chapters are also implemented in the UCP, producing a modification of the vertical diffusion of the meteorological variables. This development also allows a differentiation of neighborhoods and times of the day.

The model has been tested for an alligned building configuration, with λ_p= 0.25. More experiments have to be done in order to extend the results for different configurations. In addition, a comparison with real results would be desirable in the future.

6. Summary and conclusions

The structure and composition of the urban boundary layer have a direct impact on citizens' quality of life. A good understanding of the mechanisms involved is necessary to proper manage those impacts. In this context, numerical modeling plays a crucial role: from one side it is a powerful scientific tool to deepen our understanding of very complex and often non-linear phenomena, and from the other side it allows to explore possible future scenarios, and, in this sense, it can be used to support urban planning. A reliable model can, then, help to strengthen the link between scientists and policy makers.

One of the biggest challenges in modeling the urban atmosphere is in the wide range of spatial scales involved – from the scale of a single building, to the scale of the whole city and its surroundings. With today's computer it is impossible to perform simulations with resolution high enough to resolve the building scale, and at the same time a domain large enough to resolve the whole city and the surroundings. For this reason, in order to simulate the effect of the cities over the meteorological fields, in mesoscale models (that have typically a horizontal spatial resolution of the order of one kilometer), the so called urban canopy parameterizations are developed. These parameterizations average the microscale processes occurring inside the urban areas to represent their effect in a coarser scale model. From the 90's several urban schemes have been developed; while the first ones simply change the thermal and dynamical properties of the surface, modern ones use one or more vertical layers in order to account for the spatial heterogeneity of the cities. Nowadays, most of the urban canopy parameterizations consider the different surfaces existing within the city and take into account the radiation trapping and shadowing effect produced by the street canyons. The effect on the wind field is estimated by means of a drag force, parameterized by a drag coefficient multiplied by the square of the wind speed. The vertical transport is taken into account only as turbulent transport, estimated with the *K*-theory, considering a modification of the length scales produced by the presence of buildings. The same drag coefficient is considered for every neighborhood and only the height of the buildings is used for the estimation of the length scales modification. The dispersive fluxes are not taken into account and only the turbulent fluxes are considered for vertical mixing. Another of the limitations of the urban canopy parameterizations is the time required for a simulation, directly related to the vertical resolution of the model. Due to computational limitations, both the simulation of long term scenarios and the use of high resolution vertical grids are impossible to deal with.

This thesis is structured in two parts:

The first part (chapters 3 and 4) is focused on the improvement of the UCP (BEP, Martilli et al. 2002) itself, by exploring the dependency of the drag coefficient, and the length scales involved in the vertical transport, with the building arrangements and the intensity of the heat fluxes exchanged between the building and the atmosphere (only daytime conditions are considered). This task is performed with the aid of a RANS microscale model.
The second part of the study (Chapter 5) deals with a new technique for the coupling between the atmospheric model and the urban scheme. This new technique allows an increase of the urban resolution regardless of the mesoscale vertical resolution. This is a necessary step in order to be able to use the improvements of the UCP obtained in the first part, and, at the same time, to allow a decrease of the computational time. The new urban canopy parameterization version presented has been tested and compared against the previous version of the BEP scheme in order to examine its sensitivity with the change of vertical mesoscale resolution and the effect of the new parameterization of the dynamical parameters.
Below is a short description of the most original and relevant points of the work.

Part 1

Methodology

This methodology consists in the use of Reynolds Averaged Navier - Stokes microscale computational fluid dynamics (RANS-CFD) models, able to solve the flow between the obstacles, in order to obtain data for the development of the parameterizations. The results from the microscale models are spatially and temporally averaged in order to extract averaged properties for a coarser resolution model. The averaged properties are parameterized and implemented within the UCP and tested against the results of the RANS. The advantage of this approach, that was first proposed by Santiago and Martilli (2010), is that spatial averages – the variables that are simulated in the mesoscale model - can be computed, something that is impossible to do using only measurements due to the limited spatial representativeness of point measurements in such heterogeneous environment.
To use this methodology, it is important to be confident in the results of the RANS model, and for this reason a validation against Direct Numerical Simulations (DNS) and wind tunnel measurements

was done (Chapter 2).

Arrangement matters

As mentioned, previous urban schemes used drag coefficients independent of the building density and arrangement. Other works (see a review in Grimmond and Oke 1999) used different combinations of plan areal fraction (λ_p), frontal area fraction (λ_f) and mean building height to characterize the aerodynamic behaviour of an urban surface (and define the roughness lengths). Santiago and Martilli (2010) proposed a formulation for the drag coefficient as a function of the packing density (λ_p) for a staggered array of cubes. Results of this thesis, based on a set of RANS simulations, show that the flow behaves in a different way depending if the array of obstacles is staggered or aligned, and that for this last case (aligned) the packing density is not the appropriate parameter that characterizes the drag coefficient. Instead, a sheltering factor, depending on the distance between buildings in the flow direction and a channeling factor, depending on the distance between buildings in the direction orthogonal to the flow are defined in order to parameterize the drag coefficient. This new way to parameterize the drag effect shows better results for the wind field when comparing with the RANS results and adds the possibility to distinguish between different neighborhoods by its effect over the wind.

On the other hand, the modification of the length scales involved in turbulent transport and turbulence dissipation can be parameterized by means of the density of the buildings. This is an extension for aligned configuration of buildings of the parameterization presented in Santiago and Martilli (2010) for staggered arrays. This result shows the dependency of the turbulent length scales with the density of obstacles, regardless of its configuration.

The results presented in this part of the study have been published in Simón-Moral et al. (2014).

Heat fluxes are important even in the canopy.

It has been quite common in the last decades to assume that the heat fluxes exchanged between the buildings and the atmosphere have little impact on the dispersion and the flow dynamics in the canopy, given that the atmosphere in urban areas is often measured to be close to neutral (Britter and Hanna 2003). To test this, the TUF3D model (Krayenhoff and Voogt 2007) has been used to calculate realistic heat fluxes from the urban surfaces, resulting from solar heating, that were imposed as boundary conditions for the RANS simulations. A set of simulations for an aligned configuration of buildings with λ_p = 0.25 has been performed, with different ratios of buoyant to

inertial forces.

An increase of the drag coefficient and of the length scales with the increase of the ratio of buoyant to inertial forces is observed, in particular when $H/L_{urb}>1$ (see in chapter 4 the definition of the symbols). A parameterization for the drag coefficient increase as a function of H/L_{urb} is presented. Considering the length scales, a modification of its calculation is proposed, by supposing a unique length scale to be multiplied by a different factor, function of H/L_{urb}, depending on the process involved, in order to calculate the diffusion coefficients. Moreover, results show that the dispersive fluxes, the non turbulent fluxes smaller than the mesoscale grid that are induced by the presence of the buildings, significantly contribute to the vertical transport of heat and momentum. They can be considered by parameterizing the total vertical flux (dispersive + turbulent) within the *K*-theory. The extension of the *K*-theory results in a modification of the diffusion coefficients, providing different values for each transported variable.

Part 2

A new version of the BEP urban canopy is developed, called BEPCOL, where two kinds of modifications are introduced. From one side, the physics of the urban scheme are improved by improving the representation of the drag effect produced by the buildings over the wind speed and the modification of the mechanisms involved in vertical transport, including the dispersive fluxes. From the other side, the coupling technique used for the connection between the urban and the mesoscale models is modified, allowing an increase of the urban resolution, regardless of the mesoscale resolution.

Two main aspects have been modified for the coupling technique of the urban and mesoscale models, the forcing of the urban scheme and the technique used for the meteorological variables calculation.

Forcing at the top:

In BEPCOL, the forcing is made at the top of the urban grid and the forcing signal is transmitted downward by vertical diffusion. This method allows an independence of the urban meteorological variables, as previously they were interpolated in the whole vertical from the coarser mesoscale grid in each time step.

Meteorological variables computed and saved on the urban grid.

On the other side, the meteorological variables are now calculated within the high resolution urban grid and interpolated into the mesoscale grid. Taking into account that also the urban fluxes calculation is made within the high resolution urban grid, more accuracy is retained and, thus, more advantage of the parameterization improvements obtained from microscale simulations can be taken. This new technique memorize the value of the meteorological variables every time step, keeping the urban entity, instead of loosing part of it in the interpolation process. Another important consequence of this technique is the possibility of having high resolution results of the model within the urban grid, instead of only having averaged values in some mesoscale vertical grid points. This possibility allows the decrease of the mesoscale vertical grid, without loosing accuracy within the urban canopy, and allowing a decrease of the computational time.

The results have shown that the new technique can significantly save CPU time, without losing in resolution.

Limitations and future work

In this section, some limitations of the parameterizations and the model presented in this thesis are summarized. In addition, future work focused on the improvements of the urban canopy parameterizations and the simulations of urban areas within regional models are presented.

First, the drag coefficient and length scales parameterizations proposed in the third chapter of the thesis have been developed for aligned configurations of cubic shaped buildings, all of them with the same size. More studies should be done in order to extend the parameterization to different configurations or to heterogeneous neighborhoods (e. g. Non-cubical buildings, height varying arrays of buildings, etc). However, the results presented represent an improvement comparing to the previous version, where no distinction was made between neighborhoods, except by the influence of the height of the buildings over the length scales.

Concerning the results of chapter 4, where the influence of urban heat fluxes on the drag force and the vertical transport of the meteorological variables is analyzed, the results are limited to an aligned configuration of buildings, with packing density equal to 0.25. As before, more experiments should be done in the future in order to extend these results to different types of neighborhoods. As before, it represents an improvement from the previous scheme, as it allows a distinction of the moment of the day.

The new version of the urban scheme presented takes into account the advection of the meteorological variables only at the top, as it is taken into account by the mesoscale model and thus in the forcing. Nevertheless, the advection is not taken into account inside the urban high resolution grid. This is a limitation that should be solved in the future, as the urban advection can be very important, especially when dealing with the air pollution from traffic or the thermal comfort, in particular just above the canopy.

To a certain extent, the work presented in the first part of this thesis is a contribution towards finding an answer to a the still open question: *which is the simplification of the real urban morphology more consistent with reality in terms of the meteorological variables results?*.

As future work it will be interesting to implement the BEP-BEM building energy model (Salamanca et al. 2010) in the column model presented here. At the same time, the effect of the trees within the street canyon have been parameterized by Krayenhoff et al. (2014). Putting together the parameterization improvements presented here, with the buildings energetics and the trees influences on the urban climate can provide us with more accurate results when simulating urban climate. In addition, the improvement in urban resolution presented in the last part of this thesis can help taking advantage of all these physics improvements.

7. References

Allwine KJ, Shinn JH, Streit GE, Clawson KL, Brown M (2002) Overview of URBAN 2000: a multiscale field study of dispersion through an urban environment. Bulletin of the AMS 83:521–536.

Allwine KJ, Leach MJ, Stockham LW, Shinn JS, Hosker RP, Bowers JF, Pace JC (2004) Overview of Joint Urban 2003—an atmospheric dispersion study in Oklahoma City. In: AMS Planning, Nowcasting, and Forecasting in the Urban Zone Symposium, Seattle, WA, Preprints, CD-ROM, J7.1.

Best MJ (1998) Representing urban areas in numerical weather prediction models. In: AMS 2nd urban environment symposium, Alburquerque, NM, USA; 148-151

Bougeault P, Lacarrere P (1989) Parameterization of orography-induced turbulence in a mesoscale model. Mon Wea Rev 117:1872-1890

Britter RE, Hanna SR (2003) Flow and dispersion in urban areas. Annu Rev Fluid Mech 35: 469-496.

Brown M, Williams M (1998) An urban canopy parameterization for mesoscale meteorological models. In: AMS 2nd urban environment symposium, Albuquerque, NM, 144–147

CD-adapco (2012) User Guide STAR-CCM+ Version 7.04.011. Cd-adapco, p 11448

Cheng H, Castro IP (2002) Near wall flow over urban-like roughness. Boundary-Layer Meteorol 104:229–259

Cheng H, Hayden P, Robins AG, Castro IP (2007) Flow over cube array of different packing densities. J Wind. Eng. Ind. Aerodyn. 95:715–740

Chin HNS, Leach MJ, Sugiyama A, Leone JM, Walker H, Nasstrom JS, Brown MJ Jr. (2005) Evaluation of an urban canopy parameterization in a mesoscale model using VTMX and URBAN 2000 data. Mon Wea Rev 133:2043-2068

Ching J, Brown M, Burian S, Chen F, Cionco R, Hanna A, Hultgren T, McPherson T, Sailor D, Taha H, Williams D (2009) National Urban Database and Access Portal Tool (NUDAPT). Bulletin of the AMS 90(08):1157–1168

Clarke JA (1985) Energy simulation in building design, Adam Hilger, Bristol, 362 pp.

Claus J, Coceal O, Thomas TG, Branford S, Belcher SE, Castro IP (2012a) Wind-direction effects on urban-type flows. Boundary-Layer Meteorol 142:265–287

Claus J, Krogstad PA, Castro IP (2012b) Some measurements of surface drag in urban-type boundary layers at various angles. Boundary-Layer Meteorol 145:407–422

Coceal O, Belcher SE (2004) A canopy model of mean winds through urban areas. Q J R Meteorol Soc 130:1349–1372

Coceal O, Thomas TG, Castro IP, Belcher SE (2006) Mean flow and turbulence statistics over groups of urban-like cubical obstacles. Boundary-Layer Meteorol 121:491–519

Di Sabatino S, Solazzo E, Paradisi P, Britter R (2008) A simple model for spatially-averaged wind profiles within and above an urban canopy. Boundary-Layer Meteorol 127:131–151

Finnigan J (2000) Turbulence in plant canopies. Annu Rev Fluid Mech 32: 519-571

Galmarini S, Thunis P (1999) On the validity of the Reynolds assumptions for running-mean filters in the absence of a spectral gap. J Atmos Sci 56:1785-1796

Grimmond CSB, Oke TR (1999) Aerodynamic properties of urban areas derived from analysis of surface form. J Appl Meteorol 38:1262–1292

Grimmond CSB, Oke TR (2002) Turbulent heat fluxes in urban areas: observations and a local-scale urban meteorological parameterisation scheme (LUMPS). J Appl Meteorol, 41:792–810.

Hagishima A, Tanimoto J, Nagayama K, Meno S (2009) Aerodynamic parameters of regular arrays of rectangular blocks with various geometries. Boundary-Layer Meteorol 132:315–337

Hamdi R, Masson V (2008) Inclusion of a drag approach in the Town Energy Balance (TEB) scheme: offline 1D evaluation in a street canyon. J Appl Meteorol Clim 47:2627–2644

Kanda M, Moriwaki R, Kasamatsu F (2004) Large eddy simulation of turbulent organized structure within and above explicitly resolved cube arrays. Boundary-Layer Meteorol 112:343–368

Kanda M, Kawai T, Kanega M, Moriwaki R, Narita K, Hagishima A (2005b) A simple energy balance model for regular building arrays. Boundary-Layer Meteorol 116:423–443.

Kanda M, Inagaki A, Miyamoto T, Gryschka M, Raasch S (2013) A new aerodynamic parametrization for real urban surfaces. Boundary-Layer Meteorol 148:357–377

Kondo H, Genchi Y, Kikegawa Y, Ohashi Y, Yoshikado H, Komiyama H (2005) Development of a multi-layer urban canopy model for the analysis of the energy consumption in a Big City: structure of the urban canopy model and its basic performance. Boundary-Layer Meteorol 116:395–421

Krayenhoff, E. S., and J. A. Voogt, 2007: A microscale three-dimensional urban energy balance model for studying surface temperatures. Boundary-Layer Meteorol 123:433-461.

Krayenhoff ES, Christen A, Martilli A, Oke TR (2014) A multi-layer radiation model for urban neighbourhoods with trees. Boundary-Layer Meteorol 151:139-178.

Kusaka H,Kondo H, Kikegawa Y, Kimura F (2001) A simple single-layer urban canopy model for atmospheric models: Comparison with multi-layer and slab models. Boundary- Layer Meteorol 101: 329-358.

Louis JF (1979) A parametric model of vertical eddies fluxes in the atmosphere. Boundary-Layer Meteorol. 17:187-202

Lemonsu A, Masson V (2005) Simulation of a summer urban breeze over Paris. Boundary-Layer Meteorol. 104:463-490

Liu Y, Chen F, Warner T, Basara J (2006) Verification of a mesoscale data assimilation and forecasting system for the Oklahoma City area during the joint urban 2003 field project. J Appl Meteorol Clim 45:912-929.

Macdonald RW (2000) Modelling the mean velocity profile in the urban canopy layer. Boundary-Layer Meteorol. 97:25–45

Martilli A, Clappier A, Rotach MW (2002) An urban surface exchange parameterization for mesoscale models. Boundary-Layer Meteorol 104:261–304

Martilli A (2007) Current research and future challenges in urban mesoscale modeling. Int. J. Climatol., 27:1909-1918.

Martilli A, Santiago JL (2007) CFD simulation of airflow over a regular array of cubes. Part II: analysis of spatial average properties. Boundary-Layer Meteorol 122:635–654

Martilli A, 2009 On the derivation of input parameters for urban canopy models from urban morphological datasets. Boundary Layer Meteorol 130: 301-306.

Masson V (2000) A physically-based scheme for the urban energy budget in atmospheric models. Boundary-Layer Meteorol 94:357-397.

Masson V, Seity Y (2009) Including atmospheric layers in vegetation and urban offline surface schemes. J Appl Meteorol Clim 48:1377–1397

Mestayer PG, Durand P, Augustin P, Bastin S, Bonnefond J-M, Bénech B, Campistron B, Coppalle A, Delbarre H, Dousset B, Drobinski P, Druilhet A, Fréjafon E, Grimmond CSB, Groleau D, Irvine M, Kergomard C, Kermadi S, Lagouarde J-P, Lemonsu A, Lohou F, Long N, Masson V, Moppert C, Noilhan J, Offerle B, Oke TR, Pigeon G, Puygrenier V, Roberts S, Rosant M, Sanïd F, Salmond J, Talbaut M, Voogt J (2005) The urban boundary-layer field campaign in Marseille (UBL/CLU-ESCOMPTE): Set-up and first results. Boundary-Layer Meteorol 114:315–365.

Pal Arya S (1998) Introduction to micrometeorology. Academic Press Inc, 420 pp.

Pigeon G, Durand P, Masson V (2006) Evaluating parameterization of anthropogenic heat release in urban land surface scheme from field measurements and energy consumption inventory over Toulouse during CAPITOUL. In: AMS Sixth Urban Environment Symposium, Atlanta, 29th of Jan-2nd of Feb 2006 (extended abstract available from the AMS web site www.ametsoc.org).

Raupach MR, Shaw RH (1982) Averaging procedure for flow within vegetation canopies. Boundary-Layer Meteorol 22:79-90

Rotach MWL, Vogt R, Bernhofer C, Batchvarova E, Christen A, Clappier A, Feddersen B, Gryning SE, Martucci G, Mayer H, Mitev V, Oke TR, Parlow E, Richner H, Roth M, Roulet YA, Ruffieux D, Salmond JA, Schatzmann M, Voogt JA (2005) BUBBLE—an urban boundary layer meteorology project. Theor Appl Climatol 81:231–261.

Salamanca F, Krpo A, Martilli A, Clappier A (2010) A new building energy model coupled with an urban canopy parameterization for urban climate simulations-part I. Formulation, verification, and sensitivity analysis of the model. Theor Appl Climatol 99:331-344.

Salamanca F, Martilli A,Tewari M, Chen F (2011) A study of the urban boundary layer using different urban parameterizations and high-resolution urban canopy parameters with WRF. J. Appl Meteorol 50:1107–1128.

Santiago JL, Martilli A, Martín F (2007) CFD simulation of airflow over a regular array of cubes. Part I: three- dimensional simulation of the flow and validation with wind-tunnel measurements. Boundary-Layer Meteorol 122:609–634

Santiago JL, Coceal O, Martilli A, Belcher SE (2008) Variation of the sectional drag coefficient of a group of buildings with packing density. Boundary-Layer Meteorol 128:445–457

Santiago JL, Martilli A (2010) A dynamic urban canopy parameterization for mesoscale models based on computational fluid dynamics Reynolds-averaged Navier–Stokes microscale simulations. Boundary-Layer Meteorol 137:417–439

Santiago JL, Coceal O, Martilli A (2013a) How to parameterize urban-canopy drag to reproduce wind-direction effects within the canopy. Boundary-Layer Meteorol 149:43-63.

Santiago JL, Krayenhoff ES, Martilli A (2014) Flow simulations for simplified urban configurations with microscale distributions of surface thermal forcing. Urb Clim DOI: 10.1016/j.uclim.2014.07.008

Simón-Moral A, Santiago JL, Krayenhoff ES, Martilli A (2014) Streamwise versus spanwise spacing of obstacle arrays: Parameterization of the effects on drag and turbulence. Boundary-Layer Meteorol 151:579-596.

Simón-Moral A, Santiago JL, Martilli A (2015) Effects of unstable stratification on heat and momentum fluxes in urban areas, manuscript in preparation.

Skamarock WC, Klemp JB, Dudhia J, Gill DO, Barker DM, Duda MG, Huang XY, Wang W, Powers JC (2008) A description of the advanced research wrf version 3. NCAR/TN-475+STR NCAR TECHNICAL NOTE, 125 pp.

Taha H (1999) Modifying a mesoscale meteorological model to better incorporate urban heat storage: a bulk-parameterization approach. J Appl Meteorol 38:466-473

United Nations, Department of Economic and Social Affairs, Population Division (2014) World Urbanization Prospects: The 2014 Revision, Highlights (ST/ESA/SER.A/352).

Uno I, Ueda H, Wakamatsu S (1989) Numerical modeling of the nocturnal urban boundary layer. Boundary-Layer Meteorol 49:77-98.

8. Appendices

8.1. Appendix 1: Calculation of the Drag Coefficient Parameterization

Here, the derivation of the relationship between the drag coefficient and the geometrical parameters (Eq. 3.4) is explained. First, λ_s is kept fixed at a value of 1.0, and λ_{ch} is varied. In this case, C_{deq} decreases as c/λ_{ch}, where c is a constant to be determined (Fig. 3.4b). On the other hand, for constant λ_{ch}, C_{deq} behaves as $(1 - \exp(-\lambda_s))$ (Fig. 3.4a), up to a maximum asymptotic value for large λ_s. Therefore, combining the two relations, as a first step, we hypothesize that C_{deq} follows a relation of type,

$$C_{deq} = \left[\left(1 - \exp\left(-a \cdot \left(\lambda_s\right)^b\right)\right)\right] \cdot \left(\frac{c}{\left(\lambda_{ch}\right)}\right) \quad \text{(A.1)}$$

where a, b and c are constants determined to minimize the differences between the relation and the values of C_{deq} derived from the whole set of simulations available (using a 'best fit' procedure). This gives a, b and c equal to 0.24, 1.67 and 2.07, respectively. However, the proposed relation underestimates the value of the drag coefficient as λ_{ch} and λ_s decrease (not shown). This has been interpreted as an interaction between λ_{ch} and λ_s that becomes more important as the buildings become closer. An analysis of the differences between the values predicted by a Eq. 3.4, and those obtained from the RANS simulations, suggests that this interaction can be represented by adding a factor $\left(\frac{f}{\left(\lambda_s^i \cdot \lambda_{ch}^j\right)} + 1\right)$ to the expression, where f, i and j are again determined by a best fit procedure. The final equation then reads,

$$C_{deq} = \left[\left(1 - \exp\left(-a \cdot \left(\lambda_s\right)^b\right)\right)\right] \cdot \left(\frac{c}{\left(\lambda_{ch}\right)}\right) \cdot \left(\frac{f}{\left(\lambda_s^i \cdot \lambda_{ch}^j\right)} + 1\right) \quad \text{(A.2)}$$

with a = 0.24, b = 1.67, c = 2.07, f = 0.6, i = 1.4 and j = 4.

8.2. Appendix 2: Publications and conference participations

Boundary-Layer Meteorol (2014) 151:579–596
DOI 10.1007/s10546-013-9901-3

ARTICLE

Streamwise Versus Spanwise Spacing of Obstacle Arrays: Parametrization of the Effects on Drag and Turbulence

Andres Simón-Moral · Jose Luis Santiago · E. Scott Krayenhoff · Alberto Martilli

Received: 7 January 2013 / Accepted: 23 December 2013 / Published online: 6 February 2014

Abstract A Reynolds-averaged Navier–Stokes model is used to investigate the evolution of the sectional drag coefficient and turbulent length scales with the layouts of aligned arrays of cubes. Results show that the sectional drag coefficient is determined by the non-dimensional streamwise distance (sheltering parameter), and the non-dimensional spanwise distance (channelling parameter) between obstacles. This is different than previous approaches that consider only plan area density (λ_p). On the other hand, turbulent length scales behave similarly to the staggered case (e. g. they are function of λ_p only). Analytical formulae are proposed for the length scales and for the sectional drag coefficient as a function of sheltering and channelling parameters, and implemented in a column model. This approach demonstrates good skill in the prediction of vertical profiles of the spatially-averaged horizontal wind speed.

Keywords Building packing densities · Drag coefficients · Length scales · Obstacle array · Reynolds-averaged Navier–Stokes · Urban canopy parametrization

1 Introduction

Cities strongly influence local meteorological fields. The presence of obstacles reduces wind speeds and enhances turbulence, affecting the dispersion of the pollutants released inside the urban canopy. Considering that half of the world's population lives in the urban canopy where high levels of air pollutant emissions from traffic are often found, this can cause serious health issues. Furthermore, radiation trapping due to the structure of the urban canyons, and increased energy absorption and release due to the high thermal admittance of typical building

A. Simón-Moral (✉) · J. L. Santiago · A. Martilli
Atmospheric Pollution Division, Environmental Department, CIEMAT,
Avda. Complutense 40, Ed. 70, 28040 Madrid, Spain
e-mail: andres.simon1982@gmail.com

E. S. Krayenhoff
Department of Geography, University of British Columbia,
1984 West Mall, Vancouver, BC V6T 1Z2, Canada

ICUC8 – 8th International Conference on Urban Climates, 6th-10th August, 2012, UCD, Dublin Ireland.

Implementation and Testing of a Drag Parameterization in Mesoscale Modelling.

A. Simón-Moral[1]*, A. Martilli [2], J. L. Santiago [2], S. Krayenhoff [3]

Tecnalia Research and Innovation, City, Spain[1]*
Andres.simon@tecnalia.com
Environment dept, Research Centre for Energy, Environment and Technology (CIEMAT), Madrid, Spain[2]
Department of Geography, University of British Columbia, Vancouver, Canada[3]

Abstract

The parameterization of the urban canopy is necessary in mesoscale modelling to take into account the urban canyon microscale effects on wind and turbulence. Therefore the drag force and the length scales modification generated by buildings must be parameterized. Results from Reynolds Averaged Navier Stokes (RANS) simulations over arrays of obstacles show a variation of the drag coefficient with building densities and heights, which must be taken into account for a good representation of the heterogeneity of the city. Based on RANS simulations, this study proposes an extension of the formulation explained by Santiago et al. (2010) to represent this feature. The parameterization is implemented in a BEP based column model and validated against RANS simulations.

Keywords: Urban canopy parameterization, numerical modelling.

1. Introduction

Mesoscale models do not have resolution high enough to solve explicitly the effect of the buildings on the meteorological fields. For this reason these effects are parameterized and implemented in an Urban Canopy Parameterization (UCP).
This tool allows the calculation of the wind field inside the city and over it, which can be applied to urban air quality or thermal comfort studies.
In this study the technique presented in Santiago and Martilli (2007) is applied for the improvement of the parameterization. This technique is based on the use of microscale models to make detailed simulations inside a domain of cubes arranged in different configurations. These data will be averaged in time and space in order to extract averaged properties of the flow to introduce in the UCP.
The advantage of this kind of technique is that it is possible to have data with high resolution in the whole domain instead of having some point measurements, which could not be representative of the whole domain.

2. Model and Methodology

2.1 Model description

In this study the Urban Canopy Parameterization BEP [2] has been used. The dynamic effect of the buildings on the wind field is computed in terms of a sink of momentum and a sink/source of turbulent kinetic energy (TKE). Both are calculated by terms of a Drag force, calculated by a Drag coefficient.

$$D_u = S(z) C_d \left\langle \overline{u(z)} \right\rangle \left| \left\langle \overline{u(z)} \right\rangle \right| \qquad (1)$$

$$D_k = S(z) C_d \left| \left\langle \overline{u(z)} \right\rangle \right|^3$$

Where D_i are the Drag forces for the streamwise velocity (U) and the TKE, S(z) the vertical surface facing the wind and $\left\langle \overline{u(z)} \right\rangle$ is the time and space average of the streamwise wind.
Also, the turbulent transport of this and other variables is affected by the presence of obstacles inside the city, so the length scales involved in this transport and in the dissipation of the TKE should also be parameterized.
A CFD-RANS model (StarCCM+) has been used to simulate a set of microscale configurations. Following [1] and [5] (BLM2010), these results of have been averaged both in time and space to obtain mean properties of a group of cubes, acting as a group of buildings. These ones are used to develop a parameterization for the Drag coefficient and the length scales used in the parameterization.

2.2 Simulations set-ups

Aligned configurations of cubes have been simulated with the CFD-RANS model, with different packing densities, λ_p, and distances between building rows (W_x and W_y). A list of the parameters used is presented in Table 1, where H is the building height (H=16m).
The variable λ_p is defined as:

$$\lambda_p = \frac{A_p}{A_t} = \frac{B_x \cdot B_y}{(B_x + W_y) \cdot (B_y + W_y)} \qquad (2)$$

Where A_p and A_t are the plan area of each building and the total area, respectively, and B_x and B_y are the building widths in both directions.
A representation of the general set-up is presented in Figure 1.

ICUC8 – 8th International Conference on Urban Climates, 6th-10th August, 2012, UCD, Dublin Ireland.

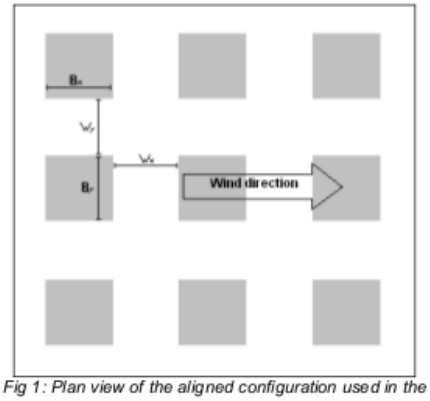

Fig 1: Plan view of the aligned configuration used in the CFD-RANS simulations.

3. Parameterization description

3.1 Drag parameterization

To solve the equation for the drag force, the UCP uses a value of the C_d coefficient. This is parameterized by means of a, C_{deq}, (BLM2010) with constant value in the whole canopy. This parameter is calculated from the spatially averaged CFD-RANS results as:

$$C_{deq} = \frac{\frac{-1}{\rho h}\int_0^h \Delta\left\langle \overline{p(z)}\right\rangle dz}{\frac{1}{h}\int_0^h \left\langle \overline{u(z)}\right\rangle \left|\left\langle \overline{u(z)}\right\rangle\right| dz} \qquad (3)$$

Different values of this coefficient for different configurations with the same building density are obtained, showing that C_{deq} depends both on the packing density and the distribution of the buildings in the area of study.

An equation relating this parameter with the spacing between buildings in the stream wise direction, W_x, and in the perpendicular one, W_y, is found (a sheltering parameter $\lambda_s=W_x/H$ and a channelling parameter $\lambda_c=W_y/B_y$ are defined). The relation is the following:

$$C_{deq} = \left[\left(1-\exp\left(-a\cdot(\lambda_s)^b\right)\right)\right]\cdot\left(\frac{c}{(\lambda_c)}\right)\cdot\left(\frac{d}{(\lambda_s\cdot\lambda_c)}+1\right) \qquad (4)$$

Where a=-0.24, b=1.67, c=2.07 and d=0.6643. In the Fig 2 a comparison between the values calculated from the CFD-RANS and the parameterized values of C_{deq} is shown.

The first factor in the right hand side of the C_{deq} equation accounts for the effect generated by the distance between buildings in the wind direction (sheltering). This effect is related with the penetration of the air into the canyon - the more penetration the more the effective drag of each building is. When λ_s goes to zero, there is no penetration and the C_{deq} goes to zero. It can be understood as if the effective ground gets displaced to the roof height. The opposite case represents an isolated building, which makes the maximum drag. In other words, the closer the buildings are, the larger the sheltering is, and the smaller the C_d is.

Table 1: Aligned configurations used for the CFD simulations

conf	λ_s	λ_c	λ_p	C_{deq}
Wx6Wy2	6	2	0.043	1.225
0.0625	3	3	0.0625	0.538
Wx6Wy1	6	1	0.071	2.070
Wx3Wy2	3	2	0.083	0.820
Wx4Wy1	4	1	0.1	2.040
0.125c1	1.83	1.83	0.125	0.535
0.125c2	3	1	0.125	1.857
0.125c3	1	3	0.125	0.136
Wx2Wy1	2	1	0.167	1.357
Wx1Wy2	1	2	0.167	0.250
0.1875	1.31	1.31	0.1875	0.536
0.25	1	1	0.25	0.728
Wx05Wy1	0.5	1	0.33	0.360

The second term represents the effect of the distance between each row of buildings. The larger the distance is, the stronger the wind is because it is less affected by the friction from the buildings, which implies a smaller C_{deq} (see Eq. 2). This term is related to the channelling of the flow within the streets. The third term represents an interaction term between sheltering and channelling.

3.2 Parameterization Le/Ce Aligned Cubes.

From the spatial average of the equation of the dissipation we define the dissipation length scale as:

$$\frac{l_\varepsilon}{C_\varepsilon} = \frac{\langle k\rangle^{3/2}}{\langle\varepsilon\rangle} \qquad (5)$$

Being <k> and <ε> the spatially averaged kinetic energy and dissipation, both calculated from the CFD-RANS results.

Following BLM2010 three zones are supposed, (i) inside the canopy (z/H<1), where we define the length scale as a constant value; (ii) transition zone (1<z/H<1.5), with a linear behaviour; and (iii) well above the canopy (z/H>1.5), also with a linear behaviour, with a different slope than the previous zone.

In the lowest region we define the value of $L_\varepsilon/C_\varepsilon$ as proportional to the thickness of the shear layer (H-d), where d is calculated from the CFD results as:

$$d/H = \lambda_p^{\,0.15} \qquad (6)$$

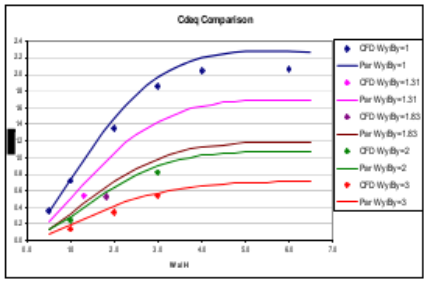

Fig 2: *Comparison between the CDeq values calculated from the CFD and following the parameterization for differents λ_c and λ_s.*

The value of the constant of proportionality is calculated with the mean value of $L_\varepsilon/C_\varepsilon$ inside the canopy as:

$$\alpha_1 = \frac{L_\varepsilon / C_\varepsilon)_{canopyAverage}}{(H-d)}$$

This value is calculated for all the configurations and an average value of 2.19 is obtained, similar to the value of 2.24 obtained in BLM2010.

For the second zone, we use the α_1 calculated for the canopy region to parameterize the $L_\varepsilon/C_\varepsilon$ as:

$$L_\varepsilon / C_\varepsilon = \alpha_1 \cdot (z-d) \qquad (7)$$

For the third zone we suppose that $L_\varepsilon/C_\varepsilon$ depends linearly on $(z-d_2)$, d_2 defined as a constant to maintain the continuity at z/H=1.5. We assume a relation like:

$$L_\varepsilon / C_\varepsilon = \alpha_2 \cdot (z-d_2) \qquad (8)$$

Where α_2 is calculated as the mean slope between the slopes of $L_\varepsilon/C_\varepsilon$ against z calculated for each configuration. A value of 1.2 is obtained, which, as in the case of α_1, is very similar to the value of 1.12 obtained in BLM2010. The parameterization for the length scale is then:

$$\begin{aligned} l_\varepsilon / C_\varepsilon &= \alpha_1 (h-d), z/h \le 1 \\ l_\varepsilon / C_\varepsilon &= \alpha_1 (z-d), 1 \le z/h \le 1.5 \\ l_\varepsilon / C_\varepsilon &= \alpha_2 (z-d_2), z \ge 1.5 \end{aligned} \qquad (9)$$

3. Results

The parameterizations previously described are implemented in a BEP based column model and tested comparing with average results from CFD-RANS.

3.1 Comparison with CFD-RANS data

The results obtained from the BEP based column model are compared with the time and space averaged results from the CFD-RANS model.

A comparison of the vertical profiles of U, tke, $\overline{u'w'}$ and K_m for the configurations is made. Wind speed is normalised by U_τ, the turbulent fluxes by U_τ^2 and Km, which is calculated by:

$$K_m = -\left\langle u'w' \right\rangle \Big/ \partial \left\langle u \right\rangle \Big/ \partial z$$

is normalised by $U_\tau \cdot H$.

In order to quantify the differences from the CFD-RANS results for each configuration the root-mean-square-error (RMSE) and the Mean Bias (MB) are computed as:

$$RMSE = \sqrt{\frac{\sum_{k=1,n} \left(\left\langle U_{RANS,k} \right\rangle - \left\langle U_{UCP,k} \right\rangle \right)}{n}}$$

$$MB = \frac{\sum_{k=1,n} \left\langle U_{UCP,k} \right\rangle - \sum_{k=1,n} \left\langle U_{RANS,k} \right\rangle}{\sum_{k=1,n} \left\langle U_{UCP,k} \right\rangle + \sum_{k=1,n} \left\langle U_{RANS,k} \right\rangle} \qquad (10)$$

Where the subtitle RANS accounts for the CFD-RANS spatially averaged results, UCP for the Urban Canopy Parameterization ones, k refers to each vertical level and n is the number of vertical levels. The results are presented in the Table 2.

The analysis of the results of the λ_p=0.125 configurations (Fig 2) shows that the new parameterization gives different results for each of the set-ups. This means that it is able to distinguish between configurations with same λ_p and different λ_c and λ_s. In addition, this figure also shows that the relative differences between these configurations are well reproduced with a little subestimation.

The configurations 0.25, 0.125c2 and Wx05Wy6 are then analysed showing the ability of the parameterization to distinguish between cases with different $\boldsymbol{\lambda_p}$ (0.25,0.125,0.33) and $\boldsymbol{\lambda_s}$ (1, 3, 0.5). (not shown here).

Taking into account configurations with the same $\boldsymbol{\lambda_s}$ but different $\boldsymbol{\lambda_p}$ and $\boldsymbol{\lambda_c}$ we analyse the ones with $\boldsymbol{\lambda_s}$=1 (Wx1Wy2, 0.125c3 and 0.25), we see that the differences between the different configurations are well reproduced (not shown here).

In order to get a general understanding of the parameterization skills the $\boldsymbol{\lambda_p}$=0.25 configuration is analysed, in figure 3. Concerning the streamwise wind speed, the results show an overestimation in the bottom of the canopy due to the subestimation of the C_d value in this region. In the upper half of the canopy parameterization shows very good results. Above the canopy top, the wind speed is subestimated.

The RMSE is 0.42 within the canopy and 0.97 above, which means that the result is better inside the canopy. These values are in the same order of magnitude than the ones presented in BLM2010 for the λ_p=0.25 staggered case, although slightly smaller within the canopy.

The turbulent kinetic energy is underestimated in the first half of the canopy and overestimated in the second, showing a bigger peak on canopy top.

The RMSE value in this region is of the same order than the one presented BLM2010 for the C_d, but slightly higher. The negative result of the mean bias shows an underestimation tendency. Above the canopy the result converges to the one from the CFD-RANS simulation few levels above the canopy top.

Table 2: RMSE and ME for mean wind speed, k and <u'w'>.

conf	RMSE(can)	MB(can)
0.048_U	0.21	-0.013
0.048_k	0.42	0.076
0.048_uw	0.15	-0.208
0.0625_U	0.46	-0.043
0.0625_k	0.37	-0.054
0.0625_uw	0.14	-0.199
0.125c1_U	0.53	-0.07
0.125c1_k	0.47	0.003
0.125c1_uw	0.12	-0.228
0.125c2_U	0.2	-0.02
0.125c2_k	0.4	-0.04
0.125c2_uw	0.15	-0.32
0.125c3_U	1.32	-0.10
0.125c3_k	0.49	0.02
0.125c3_uw	0.15	-0.21
0.167(Wx1Wy2)_U	1.15	-0.03
0.167(Wx1Wy2)_k	0.11	-0.03
0.167(Wx1Wy2)_uw	0.02	-0.33
0.1875_U	0.55	-0.08
0.1875_k	0.6	-0.04
0.1875_uw	0.14	-0.30
0.25_U	0.42	0.0006
0.25_k	0.6	-0.089
0.25_uw	0.18	-0.415
0.33_U	0.33	-0.044
0.33_k	0.52	-0.079
0.33_uw	0.23	-0.491

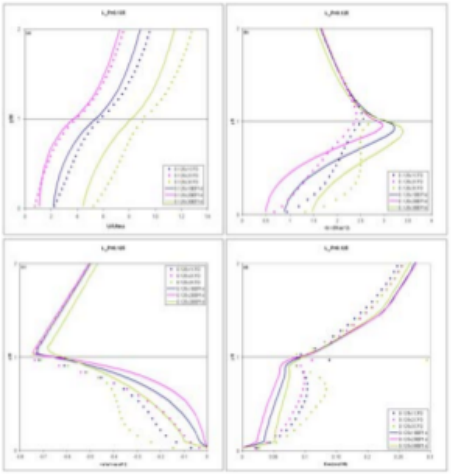

Fig 3: Comparison of vertical profiles of spatially averaged results of the CFD-RANS simulations and the UCP results for configurations with λ_p=0.125. a) Mean streamwise wind speed; b) turbulent kinetic energy; c) Reynolds shear stress; d) diffusion coefficient

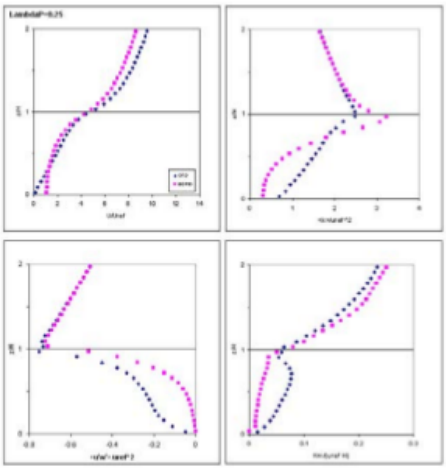

Fig 4: The same as figure 2, for the λ_p=0.25 configuration .

The shear stress is underestimated in the entire canopy, although it gives very good results over it. The values of the RMSE into the canopy are bigger than in the staggered case, but the difference is small.
The diffusion coefficient K_m shows good agreement with the ones from the CFD-RANS although it is underestimated into the canopy and overestimated above.

4. Conclusions and future work

An improved parameterization for the modification of the length scales involved in the turbulence scheme and for the drag force, both generated by aligned configurations of buildings, is presented.
The new parameterization for the C_{deq} allows to distinguish between different configurations with same λ_p. In other words, it is sensitive to the buildings arrangement, and different distributions of buildings in a neighbourhood can be differenciated.
The equation for the length scale has a similar form than the one presented in BLM2010, with a slight change in the coefficients. It is also based on a relation with the displacement height, which, in the same way, is calculated in a very similar way than the one in BLM2010, with staggered cases. That means this parameter is not sensitive to the arrangement of the buildings.
The results are similar to the CFD, showing a mean RMSE of 0.77 for the wind inside the canopy region for the configurations studied.

6. Acknowledgements

Financial support for this work is from one side acknowledged to TECNALIA and Iñaki Goenaga Technological Foundations. Also thanks to Dr. J. A. Acero and Iratxe Gutierrez for their daily support.
From the other it is acknowledged to the project Modelización de la Influencia de la Vegetación Urbana en la Calidad del Aire y Confort Climático a Microescala (2012-2014), funded by the Economy and Competitivity Ministry of the government of Spain.

7. References

1. Martilli A, Santiago JL (2007) CFD simulation of airflow over a regular array of cubes. Part II: analysis of spatial average properties. Boundary-Layer Meteorol 122:635–654.
2. Martilli A, Clappier A, RotachMW (2002) An urban surface exchange parameterization for mesoscale models. Boundary-Layer Meteorol 104:261–304.
3. Santiago JL, Martilli A, Martín F (2007) CFD simulation of airflow over a regular array of cubes. Part I: three-dimensional simulation of the flow and validation with wind-tunnel measurements. Boundary-Layer Meteorol 122:609–634.
3. Santiago JL, Coceal O, Martilli A, Belcher SE (2008) Variation of the sectional drag coefficient of a group of buildings with packing density. Boundary-Layer Meteorol 128:445–457.
4. Santiago JL, Martilli A, Martín F (2007) CFD simulation of airflow over a regular array of cubes. Part I: three-dimensional simulation of the flow and validation with wind-tunnel measurements. Boundary-Layer Meteorol 122:609–634.
5. Santiago JL, and Martilli, A (2010): A dynamic urban canopy parameterization for mesoscale models based on computational fluid dynamics Reynolds-averaged Navier–Stokes microscale simulations, Bound.-Lay. Meteorol., 137, 417–439, 2010. 1306

14th Annual WRF Users' Workshop: Short Abstracts *June 24-28, 2013*

3A.2 Implementation and evaluation of a new drag and length scale parameterization in the multilayer urban canopy parameterization of WRF

Simon-Moral, Andres, Jose-Luis Santiago, Alberto Martilli, *CIEMAT,* and Scott Krayenhoff, *University of British Columbia*

A new parameterization for the drag coefficient (Cd) and the length scales involved in the turbulence transport and dissipation is introduced in the multilayer urban canopy parameterization implemented in WRF. This parameterization has been derived from microscale CFD simulations over array of cubes with different layouts. These results show a dependence of the Cd on the sheltering (distance between buildings in the direction parallel to the wind), and channelling (distance between buildings in the direction orthogonal to the wind). The new scheme distinguishes between configurations with the same packing density, but different sheltering and channelling. Moreover, the turbulent length scales in the canopy and just above, are controlled by the building packing density. Different WRF 3D simulations over idealized cities with different morphological parameters are carried out in order to evaluate the impact of the microscale features parameterized by the new scheme. The results show different values for the wind and Turbulent Kinetic Energy inside the canopy depending on the value of the Cd. Also, the new scheme increases vertical diffusion and the height of the planetary boundary layer, compared to the old one, reducing the variability of the temperature in the urban canopy up to 0.5-1 K.

AMERICAN METEOROLOGICAL SOCIETY

J1.2
Development and implementation of a column version of an Urban Canopy Parameterization in WRF and testing over Madrid

- Indicates paper has been withdrawn from meeting
- Indicates an Award Winner

More

Thursday, 6 February 2014: 8:45 AM
Room C212 (The Georgia World Congress Center)

***Andres Simon-Moral**, Centro de Investigaciones Energéticas, Medioambientales y Tecnológicas, Madrid, Spain; and A. Martilli and J. L. Santiago*

Recorded Presentation

An improved version of the Urban Canopy Parametrization BEP, (Building Effect Parametrization Martilli et al., Boundary-layer Meteorology, 2002) has been developed and implemented in the WRF model. In this new version, conservation equations of momentum, heat and turbulent kinetic energy are solved in a vertical column up to 2-3 times the mean building height, with a high spatial resolution (few meters). In this column the exchanges of heat and momentum between the building surfaces and the atmosphere are considered. In this framework the mesoscale model forces the column model from the top, while the column provide the heat and momentum fluxes to the mesoscale model. Concerning the physics, a new parameterization for the drag coefficient and the length scales involved in turbulent transport and turbulence dissipation is also incorporated, allowing the distinguishing of different configurations of buildings. The advantage of this approach is to allow high resolution vertical profiles of the mean flow variables, like wind, temperature and turbulent kinetic energy, within the canopy and just above, without the need to have very fine vertical resolution in the mesoscale model. This will reduce the computational time, without reducing the accuracy, and allowing to run the code for longer periods. This new version of the urban scheme has been tested over the city of Madrid.

9. Curriculum Vitae

Andrés Simón Moral

PhD student in urban climate

C/Iturribide nº9, 2ºI, 48006 Bilbao (Spain)

Phone number: 00 34 655485461

E-mail: andres.simon1982@gmail.com

Education:

2010 - 2011: **Master's degree in Geophysics and Meteorology**, University of Granada (Spain)

2009 - 2010: **Master's degree in Climatic Sciences**, University of Vigo (Spain)

2007 - 2008: **Master´s degree in Climatic Risks and environmental impact** in the Complutense University of Madrid and The national Institute of Meteorology of Spain

2000-2007: **Graduate in Physical Sciences** at the Complutense University of Madrid, Spain (Speciality of Atmospheric Physics)

Training/Courses:

2007 **Stage in the Meteorological department** of the television channel “Tele 5” (Spain) making weather prediction (July-September)

2007 **Course of Software and applications development** (370 hours) (April – June), Spain

Professional experience:

April 2013 – December 2013: **Researcher** at the Atmospheric Pollution Modelling Unit of the Environmental Department of CIEMAT

October 2010 – October 2012: **Doctorate Scholarship** at the Environmental Department of TECNALIA R&I (Grant given by the Iñaki Goenaga Foundation)

June 2008 – September 2010: **Junior researcher** at the Urban and Industrial Environment Department of LABEIN Tecnalia

Teaching experience:

Formation on air quality issues to Bilbao environmental public servants. City council of Bilbao (Spain), 2009

Languages:

- **ENGLISH:** High level read, medium level written and spoken.
- **FRENCH:** High level spoken and read, medium level written.
- **SPANISH:** Mother tongue

IT Skills:

- Programming languages: **FORTRAN,C++, PYTHON 2.x, VBA, IDL**
- Operating Systems: **LINUX, WINDOWS**
- Basic Software: **MicroSoft Office 2003, XP (Word, Excell, PowerPoint, MsProyect)**
- Geographic information systems: **SAGA, arcGIS 9.x, Idrisi**
- Data Bases: **MICROSOFT SQL SERVER, Access**

Meteorological models:

- ENVImet (German microscale model focused on thermal confort)
- WinMISKAM (German microscale model focused on air quality)
- PROKAS (German gaussian-adaptated model focused on Air Quality)
- WRF model (International mesoscale model)
- SURFEX: (French Urban Canopy parameterization, actually implemented in MesoNH)

Publications:

A. Simon-Moral, J.L. Santiago, S. Krayenhoff, A. Martilli (2014) **Streamwise Versus Spanwise Spacing of Obstacle Arrays: Parametrization of the Effects on Drag and Turbulence** Boundary-Layer Meteorology: Volume 151, Issue 3 (2014), Page 579-596

Olazabal, M., Feliu, E., Herranz-Pascual, M. K., Abajo, B., González-Aparicio, I., Simón-Moral, A., and Alonso, A. (2012) **Climate Change Adaptation Plan of Vitoria-Gasteiz, Spain. Resilient Cities 2: Cities and Adaptation to Climate Change. Proceedings of the Global Forum 2011**, Local Sustainability, ed Otto-Zimmermann K (Springer), Vol 2, Part 4, pp 335-347.

J.A. Acero, A. Simon, A. Padro, O. Santa Coloma (2012), **Impact of local urban design and traffic restrictions on air quality in a medium sized town**, Environmental Technology. DOI:10.1080/09593330.2012.672472

J.A. Acero, J. Hidalgo, A. Simon, I. Gonzalez, Jon Arrizabalaga (2011), **Climate Change; Impact and adaptation in the Autonomous Community of the Basque Country: Urban areas.** Scientific report. Basque Government, ISBN: 978-84-457-3175-8 In Spanish

Conference Presentations:

A. Simon-Moral*, J. L. Santiago, A. Martilli "**Development and implementation of a column version of an Urban Canopy Parameterization in WRF and testing over Madrid**", (Oral presentation), 11th Symposium on the Urban Environment (AMS 94th Annual Meeting), 2-6 February 2014, Atlanta (USA).

A. Simon-Moral*, J. L. Santiago, A. Martilli, S. Krayenhoff "**Implementation and evaluation of a new drag and length scale parameterization in the multilayer urban canopy parameterization of WRF**", (Oral presentation), 14th Annual WRF Users' Workshop, 24-28 June 2013, Boulder (Colorado, USA).

A. Simon-Moral*, A. Martilli, J. L. Santiago, S. Krayenhoff "**Implementation and Testing of a Drag Parameterization in Mesoscale Modelling"**, (Oral presentation), 8th International Conference on Urban Climate – ICUC 8, 6th – 10th August 2012, Dublin (Ireland).

J.A. Acero, A. Simon, J. Arrizabalaga **"Influence of vegetation on air quality and urban climate"**, (Written comunication), CONAMA10: Spanish National Environment Conference, ISBN: 978-84-614-6112-7, Madrid, November 2010. In spanish

J.A. Acero, A. Simon **“Influence of vegetation scenarios on the local air quality of a city square”, (Poster presentation), International Conference on Local Air Quality and its Interactions with Vegetation** – CLIMAQS-project, Antwerp, (Belgium) January 2010.

J.A. Acero, A. Simon*, A. Padro, **“Evaluating air quality legislation with different street canyon models: Gaussian & CFD”**, (Oral presentation), 7th International Conference on Air Quality – Science and Application, Istanbul (Turkey), March 2009